

①

APPENDIX

**MANUFACTURING METHODS AND TECHNOLOGY
(MANTECH) PROGRAM: MANUFACTURING TECHNIQUES
FOR A COMPOSITE MAIN ROTOR BLADE FOR THE
ADVANCED ATTACK HELICOPTER - APPENDICES**

R. KIRALY
R.E. HEAD



Hughes Helicopters, Inc.

July 1982

FINAL REPORT

**Basic Ordering Number
DAAK50-78-G-0004
Delivery Order 003**

SDTIC
ELECTE
JUL 31 1989
@ B D

AD-A210 583



Approved for public release;
distribution unlimited

89 7 28 0 65

UNITED STATES ARMY AVIATION RESEARCH AND DEVELOPMENT
COMMAND, DRDAV-EGX, ST. LOUIS, MO

THE FINDINGS IN THIS REPORT ARE NOT TO BE CONSTRUED AS AN OFFICIAL DEPARTMENT OF THE ARMY POSITION, UNLESS SO DESIGNATED BY OTHER AUTHORIZED DOCUMENTS.

MENTION OF ANY TRADE NAMES OR MANUFACTURERS IN THIS REPORT SHALL NOT BE CONSTRUED AS ADVERTISING NOR AS AN OFFICIAL ENDORSEMENT OR APPROVAL OF SUCH PRODUCTS OR COMPANIES BY THE UNITED STATES GOVERNMENT.

Unclassified

SECURITY CLASSIFICATION OF THIS PAGE (When Data Entered)

REPORT DOCUMENTATION PAGE		READ INSTRUCTIONS BEFORE COMPLETING FORM															
1. REPORT NUMBER USAAVRADCOM TR-83-F-2	2. GOVT ACCESSION NO.	3. RECIPIENT'S CATALOG NUMBER															
4. TITLE (and Subtitle) Manufacturing Methods and Technology (MANTECH) Program: Manufacturing Techniques for a Composite Main Rotor Blade for the Advanced Attack Helicopter - Appendices		5. TYPE OF REPORT & PERIOD COVERED Final Report															
7. AUTHOR(s) R. Kiraly R. E. Head		6. PERFORMING ORG. REPORT NUMBER HHI 82-143															
9. PERFORMING ORGANIZATION NAME AND ADDRESS Hughes Helicopters, Inc. Cent nela and Teale Streets Culver City, CA 90230		8. CONTRACT OR GRANT NUMBER(s) DAAK50-78-G-0004 (D0-0003)															
11. CONTROLLING OFFICE NAME AND ADDRESS U. S. Army Aviation Research and Development Command, DRDAV-EGX 4300 Goodfellow Blvd, St. Louis, MO 63120		10. PROGRAM ELEMENT, PROJECT, TASK AREA & WORK UNIT NUMBERS 1827340															
14. MONITORING AGENCY NAME & ADDRESS (if different from Controlling Office)		12. REPORT DATE April 1982															
		13. NUMBER OF PAGES															
		15. SECURITY CLASS. (of this report) Unclassified															
		15a. DECLASSIFICATION/DOWNGRADING SCHEDULE															
16. DISTRIBUTION STATEMENT (of this Report) Approved for public release; distribution unlimited.																	
17. DISTRIBUTION STATEMENT (of the abstract entered in Block 20, if different from Report) Approved for public release; distribution unlimited.																	
18. SUPPLEMENTARY NOTES																	
19. KEY WORDS (Continue on reverse side if necessary and identify by block number)																	
<table border="0"> <tr> <td>Rotor</td> <td>Erosion Protection</td> <td>Resin</td> </tr> <tr> <td>Blade</td> <td>Lightning Protection</td> <td>Graphite</td> </tr> <tr> <td>Composite Structure</td> <td>Tooling</td> <td>Fiberglass</td> </tr> <tr> <td>Ballistic Survivability</td> <td>Fabrication</td> <td>Kevlar</td> </tr> <tr> <td></td> <td></td> <td>Nomex</td> </tr> </table>			Rotor	Erosion Protection	Resin	Blade	Lightning Protection	Graphite	Composite Structure	Tooling	Fiberglass	Ballistic Survivability	Fabrication	Kevlar			Nomex
Rotor	Erosion Protection	Resin															
Blade	Lightning Protection	Graphite															
Composite Structure	Tooling	Fiberglass															
Ballistic Survivability	Fabrication	Kevlar															
		Nomex															
20. ABSTRACT (Continue on reverse side if necessary and identify by block number) This manufacturing methods and technology program refined the design for a composite main rotor blade (CMRB) for the AH-64A advanced attack helicopter, perfected the fabrication technology for manufacturing it by wet filament winding process, and demonstrated it through laboratory tests and whirlstand tests. The CMRB replaces the equivalent metal main rotor blade with a weight saving of 24 pounds and a unit production cost saving of \$194,300 per shipset. Ballistic tolerance against 23mm HEI-T was																	

UNCLASSIFIED

SECURITY CLASSIFICATION OF THIS PAGE (When Data Entered)

demonstrated, and satisfactory erosion protection and lightning protection methods were incorporated. Flight test information will be added in a later revision of this report.

This volume contains Appendices that pertain to the basic final report.



Accession For	
NTIS GRA&I	<input checked="checked" type="checkbox"/>
DTIC TAB	<input type="checkbox"/>
Unannounced	<input type="checkbox"/>
Justification	
By	
Distribution/	
Availability Codes	
Dist	Avail and/or Special
A-1	

UNCLASSIFIED

SECURITY CLASSIFICATION OF THIS PAGE (When Data Entered)

TABLE OF CONTENTS

	<u>Page</u>
APPENDIX A - STATIC STRESS ANALYSIS	A-1
APPENDIX B - FATIGUE STRESS ANALYSIS	B-1
APPENDIX C - STRUCTURAL ANALYSIS OF A BALLISTICALLY DAMAGED BLADE	C-1
APPENDIX D - DYNAMIC ANALYSIS	D-1
APPENDIX E - ENGINEERING PROCESS MANUAL <i>missing pages not available</i>	E-1
APPENDIX F - NONDESTRUCTIVE EVALUATION PLAN	F-1
APPENDIX G - FAILURE, MODES, EFFECTS, AND CRITICALITY ANALYSIS	G-1
APPENDIX H - STRESS ANALYSIS	H-1
APPENDIX I - MASS PROPERTIES	I-1
APPENDIX J - AEROELASTICITY AND MECHANICAL STABILITY	J-1
APPENDIX K - RELIABILITY ASSESSMENT	K-1
APPENDIX L - MAINTAINABILITY ASSESSMENT	L-1
APPENDIX M - REFERENCES	M-1
APPENDIX N - DRAWING LIST FOR THE COMPOSITE MAIN ROTOR BLADE FOR THE AH-64A HELICOPTER	N-1

APPENDIX A

STATIC STRESS ANALYSIS OF THE COMPOSITE MAIN ROTOR
BLADE FOR THE AH-64A HELICOPTER

REPORT TITLE Static Stress Analysis for the YAH-64 CMRB		REPORT NO. CMRB 79-005
PREPARED BY APC	3/25/82	CHECKED BY
SUBJECT YAH-64 CMRB Static Analysis		MODEL NO YAH-64

TABLE OF CONTENTS

<u>Section</u>		<u>Page</u>
A10	References	A10.02
A10	Introduction	A10.03
A10	Summary of Test Results	A10.04
A15	Margins of Safety	A15.01
A20	CMRB Loads	A20.01
A30	Section Properties	A30.01
A40	Blade Root Attach Lugs	A40.01
A50	Basic Section	A50.01
A51	Trailing Edge Longos	A51.01
A60	Swept Tip and Tip Weights	A60.01

REPORT TITLE Static Stress Analysis for the YAH-64 CMRB		REPORT NO CMRB 79-005
PREPARED BY APC	3/25/82	CHECKED BY
SUBJECT YAH-64 CMRB		MODEL NO. YAH-64

REFERENCES

1. CMRB-79-004 Basic Loads Report for the Composite Main Rotor Blade for the YAH-64 Advanced Attack Helicopter
1 June 1979
Revised July 1979
Revised March 1982
2. Structural Test Report for the CMRB YAH-64/AAH
Feb. 1982.
3. CMRB 79-041 Safety of Flight Review Airworthiness Substantiation Document Composite Main Rotor Blade for the YAH-64/AAH May 1980, Vol. I and II

REPORT TITLE Static Analysis for the YAH-64 CMRB		REPORT NO CMRB-79-005
PREPARED BY APC 3-26-82	CHECKED BY	MODEL NO YAH-64
SUBJECT YAH-64 CMRB		

INTRODUCTION

This appendix contains the revised static and fail safe stress analysis of the YAH-64 CMRB.

Based on this analysis, there will be no failure at ultimate load (1.5x limit) and negligible permanent set under limit loads. In addition, with a critical structure element failed (i.e., one lug in four (4) lug joint) the CMRB will be capable of taking limit loads as ultimate without failure. Permanent set is allowed under these conditions.

The CMRB static loads are given in Section 20 starting on Pg. A20.01. Centrifugal Force vs. Blade station at various rotor speeds along with blade moments are listed. Loads are from Reference 1.

Revised section properties are given on Pg. A30.02 in Table 30-1. A plot of section properties is given on Pg. A30.03.

A summary of all testing done on the CMRB, both the original design and the re-designed blade is shown on pg. A10.04. See also References 2 and 3. Redesign consists of the following:

1. .048" graphite inner skin; was .010" Kevlar.
2. Honeycomb supporting the trailing edge skin and swept tip; was Kevlar tubes and Kevlar ribs respectively.
3. .075 graphite channel that runs the length of the blade; was .048" Kevlar web.
4. Double flange bushing (spool) at the attach lub; was a single flange bushing.

The above changes increased the blade strength, however all static testing was done with specimens which were of the original design.

REPORT TITLE <u>Static Analysis for the YAH-64 CMRB</u>		REPORT NO. <u>CMRB-79-005</u>
PREPARED BY <u>APC</u>	<u>3-26-82</u>	CHECKED BY <u>YAH-64</u>
SUBJECT <u>YAH-64 CMRB</u>		

INTRODUCTION - (Cont'd)

Pg. A40.01 shows the cross section of the lugs with double flange bushings (spools) now being used on the CMRB to contain the fibers because they tend to spread or flatten out when loaded. This design also allows the fibers to be wound tightly around the bushing resulting in 10% more fibers being used in the make-up of the lug versus the single flange design. This results in a lug of greater strength.

Pg. A40.02 shows the maximum lug load reach during test (specimen had single flange lug bushings). The lug did not fail (specimen club end failed, Ref. 2) and calculations show the lug can withstand a load 40% higher than ultimate. The test substantiated the attach lugs and root portion of the blade. Analysis for the blade's constant section is shown on Pgs. A50.01 and A50.02.

The tip section of the blade has been structurally substantiated by static test (see Ref. 2). Loading of the tip is shown on Pg. A60.01. The blade tip withstood 356% of limit load.

Structural integrity has been established by analysis and test. For analysis before test see the main body of the report.



Hughes Helicopters, Inc.

A10.04
CMRB 79-005

SUMMARY OF TESTS RESULTS

This page presents the results of tests conducted on the Composite Main Rotor Blade for the YAH-64 Advanced Attack Helicopter. The tests were conducted at the Hughes Helicopters Inc. Structures Test Laboratory, Culver City, CA., between January 1980 and August 1981.

One each, Swept Tip specimens were subjected to Static, Ground-Air-Ground, and Fatigue loading. One each, Root-Midspan specimens were subjected to Static and Ground-Air-Ground loading. Five Root specimens were tested under fatigue loading.

Significant test results are as follows:

1. Swept Tip Static, GAG and Fatigue tests.
 - a. 100% radial limit load achieved on swept tip section without failure or permanent set.
 - b. 100% vertical limit load and ultimate load on aft tip weight box without failure or permanent set. 211% radial limit load achieved on swept tip assembly without failure.
 - c. 100% radial limit load achieved on fwd. and aft tip weight boxes without failure.
 - d. 108,000 cycles; representing eight times three GAG cycles per hour for a service life of 4500 hours achieved without failure.
2. Root-Midspan Static and GAG tests.
 - a. 100% radial limit load applied statically without yielding or permanent set. Failure at the club end occurred at 149% limit load.
 - b. 108,000 cycles, representing eight times three GAG cycles per hour for a service life of 4500 hours achieved without failure. Lug failed at 33,200 cycles of 125% GAG load.
3. Root Fatigue Tests
 - a. Tests conducted on specimens 1 and 2 were considered invalid due to overheating of the test specimen resulting from an excessive test cyclic load rate.
 - b. A premature failure of specimen No. 3 indicated insufficient fatigue strength of the blade attachment lugs as originally designed.
 - c. Specimen 4, which incorporated design configuration changes yielded greatly improved fatigue strength in the lug area although lateral expansion of the lugs was still present.
 - d. Specimen 5, with shimmed lugs which simulated the additional lateral restraint of the longo fibers obtainable from the future use of double flanged lug bushings showed no damage or lateral expansion of the lugs after 947,700 cycles at increased load levels. The last 50,400 cycles were obtained at the mean 1 hour load level. The required number of cycles at the 1 hour load level is 17,340. The root end of the blade could still support centrifugal force when the test was terminated due to increased deflections.

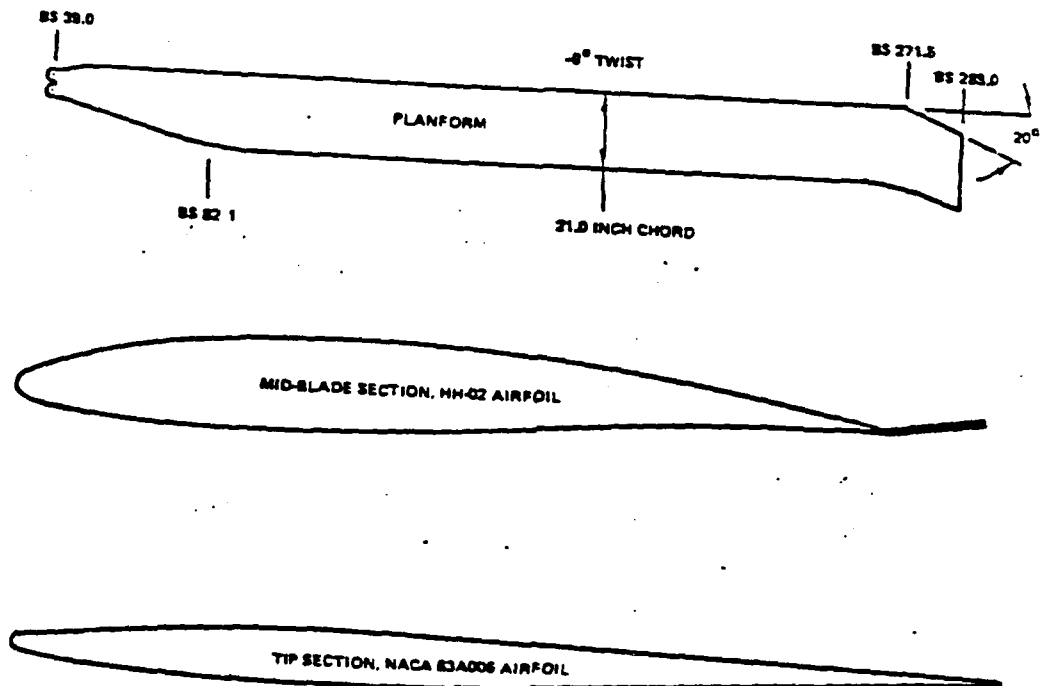
REPORT TITLE YAH-64 Static and Fatigue Analysis		REPORT NO. CMRB-79-005
PREPARED BY APC	3/9/82	CHECKED BY
SUBJECT YAH-64 CMRB		MODEL NO. YAH-64

MINIMUM MARGINS OF SAFETY

Station	Load Condition	Type of Stress	Margin of Safety
39 Attach Lugs	$n_z=3.5, V_f=180 \text{ Kn}$ RPM=289	Tension in Kevlar Windings	.40
191.7 Constant Section	$n_z=3.5, V_f=180 \text{ Kn}$ RPM=289	Compression in Kevlar spar longos in the constant section	.06
87 Constant Section	$n_z=3.5, V_f=180 \text{ Kn}$ RPM=289	Shear due to torsion in $+45^\circ$ layers of the constant section	.05
84 Constant Section	RPM = 0 Max Torque V=0 $n_z=1.0$	Compression in Kevlar spar longos after the T.E. longos have buckled	High
270 Blade Tip	RPM = 376 $V_f=150 \text{ Kn}$ $n_z=3.5$	Tension load applied to tip weight housings and blade tip	High

Hughes Helicopters

A15.02
CMRB-79-005



YAH-64 CMRB Geometry

Figure 1

REPORT TITLE		REPORT NO
PREPARED BY	3/25/82	CHECKED BY
APC		CMRB-79-005
SUBJECT		MODEL NO
YAH-64 CMRB		YAH-64

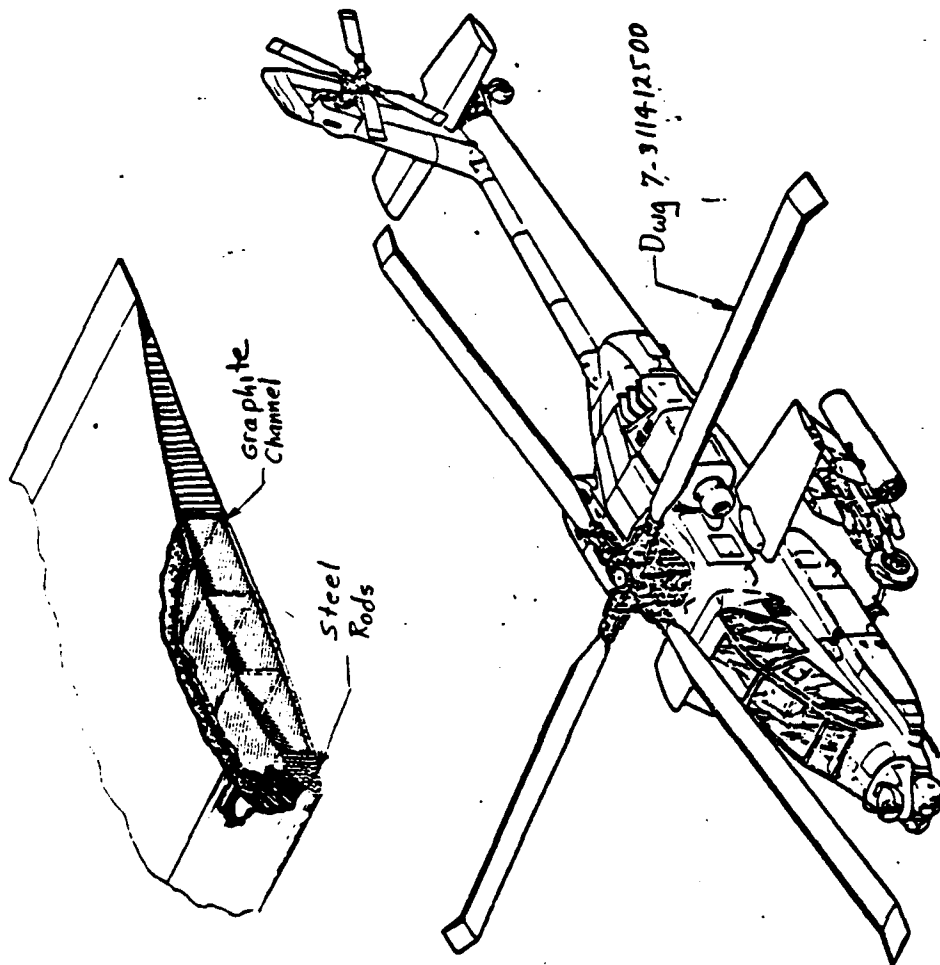
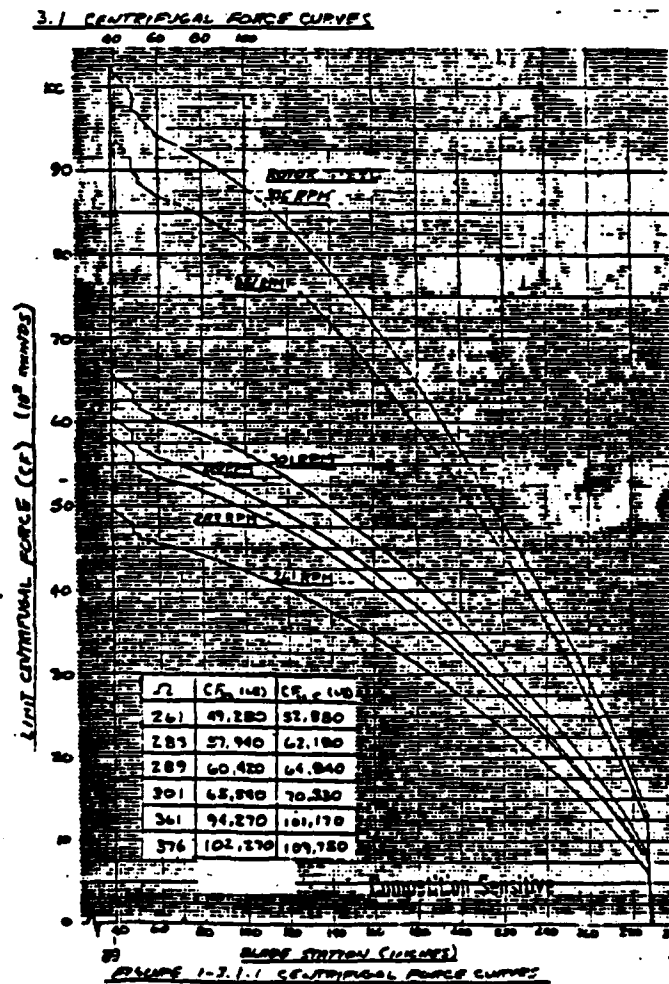


Figure 2

REPORT TITLE		REPORT NO.
PREPARED BY	CHECKED BY	CMRB-79-005
<u> </u>	<u> </u>	MODEL NO.
SUBJECT		<u>YAH-69</u>

CMRB Centrifugal Force



REPORT TITLE		REPORT NO. <u>CMRB-77-005</u>
PREPARED BY <u>APC</u>	CHECKED BY <u>3/3/82</u>	MODEL NO. <u>YAH-64</u>
SUBJECT		

CMRB loads

Main Rotor Blade Preliminary Limit LoadsPower On $n_2 = 3.5$, $V = 180$ kn, RPM = 289

r (in.)	M_F (in-lb)		M_C (in-lb)		M_T (in-lb)	
	Mean	Cyclic	Mean	Cyclic	Mean	Cyclic
11.0	← N.A. →				-15000	42000
25.0	+8400	36400	← N.A. →			
34.5	+4400	49700	60000	60900	-15000	33000
44.5	-8800	55300	55900	79400	-12000	33000
59.5	-5000	48700	50000	106000	- 9000	32000
87.0	-3500	26300	37700	133000	- 8000	32000
121.9	-5500	23600	29100	149000	- 5600	32800
156.8	-6000	28300	19900	136000	- 4300	32000
191.7	-8000	42900	12400	97500	- 3500	32000
226.6	-4000	44000	6600	60100	- 2200	22000
256.0	+2000	25200	1200	22900	- 1700	10500
273.0	+4500	14800	300	8300	- 900	4300

NOTE. Lds in tables are from Ref 1

REPORT TITLE		REPORT NO.
PREPARED BY	3/3/82	CHECKED BY
SUBJECT		MODEL NO.

CMRB LoadsMain Rotor Blade Preliminary Limit LoadsPower Off, (Limit Rotor Speed) $n_2 = 3.5$, $V = 150$ kn, RPM = 376

r (in.)	M_p (in-lb)		M_c (in-lb)		M_T (in-lb)	
	Mean	Cyclic	Mean	Cyclic	Mean	Cyclic
11.0			N.A.			
25.0	- 3600	10200			-11000	18000
34.5	- 4000	13900	-29000	42700		
44.5	- 1510	15400	-26600	55700	-11000	14100
59.5	- 940	13600	-23800	74300	- 9100	14300
87.0	- 4000	7300	-18000	93300	- 7100	13500
121.9	- 7600	6600	-13900	104000	- 5800	13400
156.8	-11500	7900	- 9500	95300	- 4200	13300
191.7	-13100	12000	- 5900	68400	- 3200	13500
226.6	- 9300	12300	- 3100	42100	- 2900	13400
256.0	+ 6100	7000	- 570	16100	- 2600	9300
273.0	+ 2700	4100	- 140	5800	- 1600	4500
					- 650	1900

REPORT TITLE		REPORT NO.
PREPARED BY	CHECKED BY	MODEL NO.
SUBJECT		

CMRB Loads

Main Rotor Blade Preliminary Limit LoadsPower Off $n_2 = 3.5$, $V = 150$ kn, RPM = 301

r (in.)	M_F (in-lb)		M_c (in-lb)		M_T (in-lb)	
	Mean	Cyclic	Mean	Cyclic	Mean	Cyclic
11.0	N.A.				-14000	23800
25.0	+8400	23700	N.A.			
34.5	+4400	32400	-25700	54400	-14000	18600
44.5	-8800	36000	-23900	71000	-11500	18900
59.5	-5000	31700	-21400	94800	- 9100	17800
87.0	-3500	17100	-16100	119000	- 7400	17700
121.9	-5500	15400	-12500	133000	- 5400	17500
156.8	-6000	18400	- 8500	122000	- 4100	17800
191.7	-8000	27900	- 5300	87200	- 3700	17700
226.6	-4000	28600	- 2800	53700	- 3300	12300
256.0	+2000	16400	- 500	20500	- 2100	6000
273.0	+4500	9600	- 130	7400	- 800	2500

REPORT TITLE		REPORT NO.
PREPARED BY	CHECKED BY	CMRB-79-005
SUBJECT		MODEL NO.
		YAH-64

CMRB Loads

Main Rotor Blade Preliminary Limit LoadsPower Off, (Design Minimum Rotor Speed) $n_2 = 3.3$, $V = 150$ kn, $KPH = 261$

r (in.)	M _y (in-lb)		M _c (in-lb)		M _T (in-lb)	
	Mean	Cyclic	Mean	Cyclic	Mean	Cyclic
11.0	N.A.				-14000	30000
25.0	+8400	36400	N.A.			
34.5	+4400	49700	-23000	58000	-14000	23500
44.5	-8800	55300	-21400	72000	-11500	23700
59.5	-5000	48700	-19200	101000	- 9100	22400
87.0	-3500	26300	-14500	127000	- 7400	22100
121.9	-5500	23600	-11200	142000	- 5400	22000
156.8	-6000	28300	- 7600	130000	- 4100	22400
191.7	-8000	42900	- 4750	92900	- 3700	22300
226.6	-4000	44000	- 2500	57200	- 3300	15400
256.0	+2000	25200	- 460	21800	- 2100	7500
273.0	+4500	14800	- 115	7900	- 800	3100

REPORT TITLE		REPORT NO.
PREPARED BY <u>W-L</u>		<u>CMRB-79-005</u>
3/3/82	CHECKED BY	MODEL NO. <u>YAH-64</u>
SUBJECT		

CMRB Loads

Main Rotor Blade Preliminary Limit LoadsPower On $n_2 = 2.5$, $V = 204$ kn, RPM = 289

r (in.)	M _F (in-lb)		M _C (in-lb)		M _T (in-lb)	
	Mean	Cyclic	Mean	Cyclic	Mean	Cyclic
11.0			N.A.		-14000	20900
25.0	- 820	29600			N.A.	
34.5	-11900	40500	60000	46300	-14000	17500
44.5	- 8600	45000	55900	60400	-11500	17700
59.5	- 6100	39600	50000	80600	- 9100	16700
87.0	- 9000	21400	37700	101000	- 7400	16600
121.9	- 7900	19200	29100	113000	- 5400	16400
156.8	- 6200	23000	19900	103000	- 4100	16700
191.7	- 8300	34900	12400	74100	- 3700	16700
226.6	- 5200	35800	6600	45700	- 3300	11500
256.0	0	20500	1200	17400	- 2100	5600
273.0	+ 1480	12000	300	6300	- 800	2300

REPORT TITLE		REPORT NO.
PREPARED BY	CHECKED BY	CMRB-77-005
APC	3/3/82	MODEL NO.
SUBJECT		YAH-64

CMRB Loads

Main Rotor Blade Preliminary Limit LoadsPower On, (Limit Rotor Speed) $n_2 = 3.5$, $V = 180$ kn, RPM = 361

r (in.)	M _p (in-lb)		M _c (in-lb)		M _t (in-lb)	
	Mean	Cyclic	Mean	Cyclic	Mean	Cyclic
11.0	N.A.				-14000	17000
25.0	-3600	15200	N.A.			
34.5	-4000	20800	34000	48700	-14000	13300
44.5	-1510	23100	31700	44300	-11500	13500
59.5	- 940	20300	28300	59200	- 9100	12700
87.0	-4000	11000	21400	74300	- 7400	12600
121.9	-7600	9900	16500	83200	- 5400	12500
156.8	-11500	11800	11300	75900	- 4100	12700
191.7	-13100	17900	7000	54400	- 3700	12600
226.6	-9300	18300	3700	33600	- 3300	8800
256.0	+6100	10500	700	12800	- 2100	4300
273.0	+2700	6200	200	4600	- 800	1800

REPORT TITLE		REPORT NO.
PREPARED BY	CHECKED BY	MODEL NO.
<u>APC</u>	<u>3/3/82</u>	<u>CMRB-79-005</u>
SUBJECT		<u>YAH-64</u>

CMRB LoadsMain Rotor Blade Preliminary Limit Loads

(Zero Rotor Speed, Maximum Torque)

 $n_z = 1.0$, $V = 0$ kn, RPM = 0

r (in.)	M _p (in-lb)		M _c (in-lb)		M _T (in-lb)	
	Mean*	Cyclic	Mean	Cyclic	Mean	Cyclic
11.0	26500	Negli- gible	N.A.	Negli- gible	Negli- nible	Negli- gible
34.5	19600		79900			
44.5	18100		74400			
59.5	16100		66600			
87.0	12660		50200			
121.85	8910		38800			
156.75	5780		26500			
191.65	3270		16500			
226.55	1390		8800			
256.0	320		1600			
273.0	40		400			

* 1g static droop moment with respect to a horizontal reference plane.

REPORT TITLE		PAGE <u>A30.01</u> OF <u> </u>
PREPARED BY <u>APC</u>		REPORT NO. <u>CURB-79-001</u>
<u>2/23/82</u>	CHECKED BY	MODEL NO. <u>YAH-64</u>
SUBJECT		
<p style="text-align: center;"><u>SECTION PROPERTIES</u></p> <p>Section properties are listed in Table 30-1 in this section. EI_c, EI_f and GJ are shown graphically on page A30.03. On page A30.07 the shear flows due to a 1000 in-lb torque applied to the blade are shown. On page A30.08 is listed the test data from which the calculated torsional stiffness of the blade was verified.</p>		

FORM 870a (REV 4/77)



REPORT TITLE		REPORT NO. <u>CMRB-79-005</u>
PREPARED BY <u>APC</u>	2/19/82	CHECKED BY
SUBJECT		MODEL NO. <u>YAH-67</u>

CMRB Section Properties

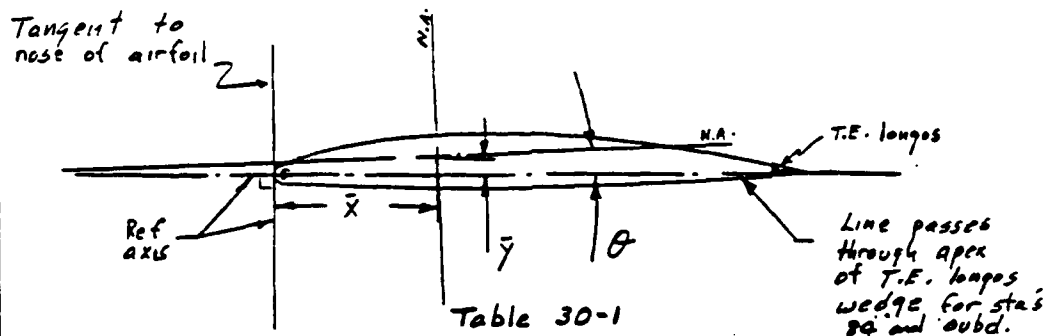


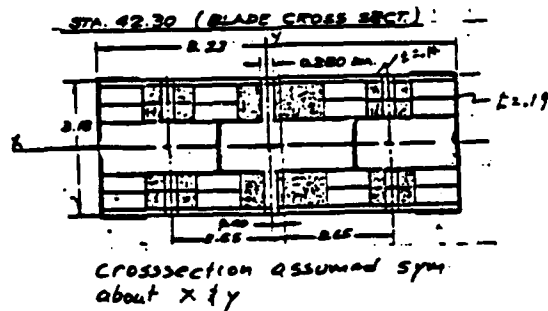
Table 30-1

Blade Sta	EA $\times 10^6$	EIF $\times 10^6$	EI _c $\times 10^6$	GJ $\times 10^6$	\bar{x} in	\bar{y} in	ϕ deg
42	23.16	96	596.2	34	See below		0°
55	71.51	49.12	854.4	49.07	4.61	.35	1.66
65	53.04	29.51	897.5	30.49	4.88	.32	1.23
75	42.94	21	946.2	24.74	5.09	.30	.57
84	32.10	15.52	924.0	16.2	4.974	.30	.52
130	35	13.4	898		4.92		.49
160	33.98	12.7	890.72		4.86		.45
Trim Tabs start	175.5	23.98	890.72		4.86	.30	
020 Stl	175.5	34.39	983.49		5.04	.26	
201	34.39	12.7	983.49		5.04		
Back-up strip	201	35.91	995.49		4.914		
260	35.91	13.4	995.49	16.2	4.914		

106 rods in N. wt.

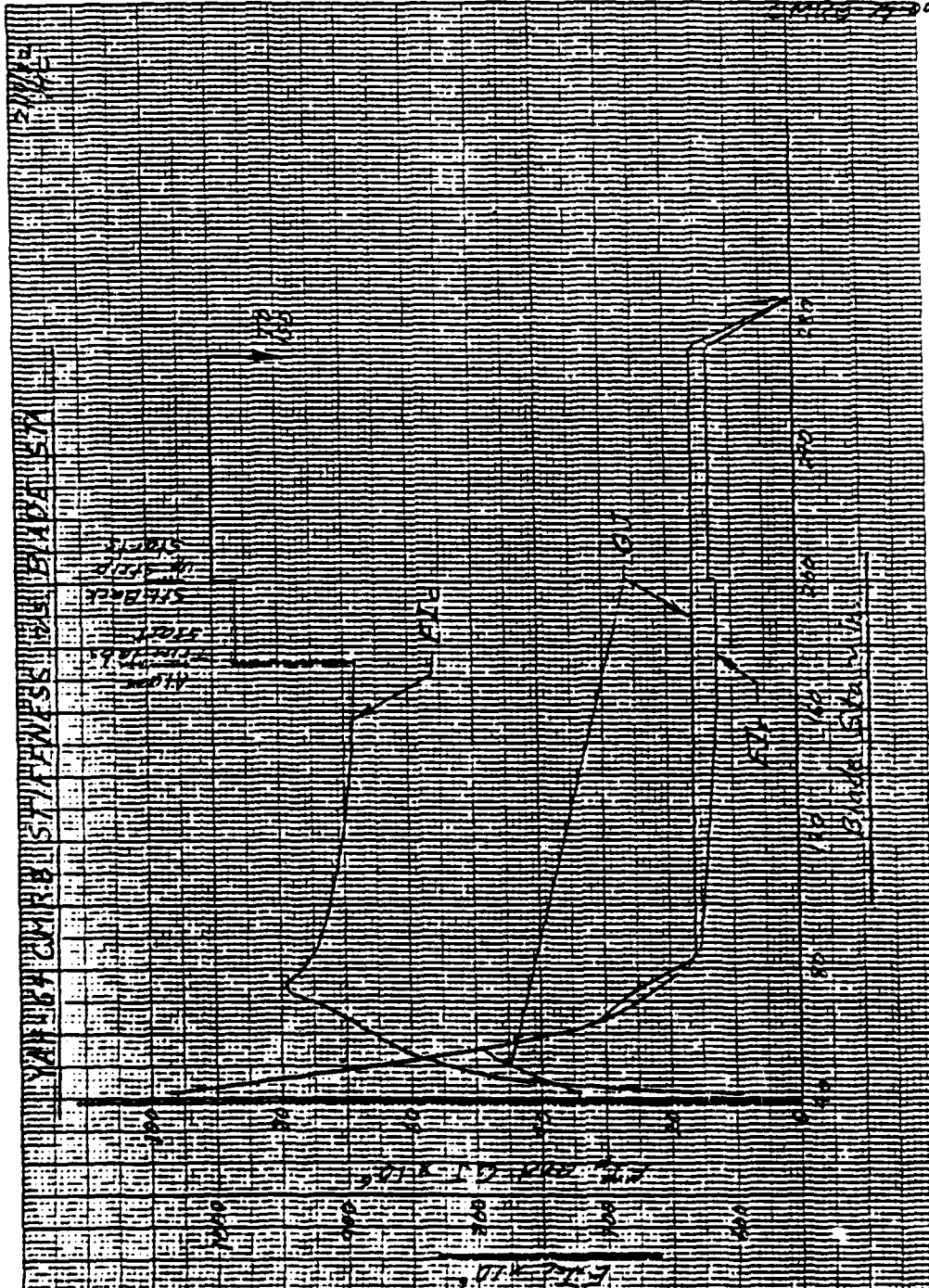
68 rods in N. wt.

*Tip wt housing starts at sta 260.



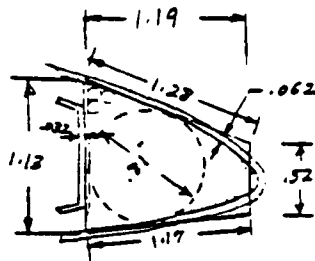
A30.03

~~CONFIDENTIAL~~ 05



REPORT TITLE		REPORT NO.
PREPARED BY	CHECKED BY	CMRB-79-005
186	7/3/79	MODEL NO.
SUBJECT		YAH-64
YAH-64 CMRB		

Torsion Stiffness - Sta 84



$$NWT \text{ area} = .8626 \text{ in}^2$$

$$\text{Rod area} = \left(\frac{.033}{2}\right)^2 \pi 68 = .464$$

$$V_f = \frac{.464}{.8626} = .54$$

$$V_m = \frac{.8626 - .464}{.8626} = .46$$

Skin

$$A_1 = \frac{.52 + 1.13}{2} \times 1.19 = .982 \text{ in}^2$$

$$\frac{S}{t} = \frac{1.19 + .52 + 1.17}{.024} + \frac{1.13}{.032} = 120 + 35.3 = 155.3$$

$$G \frac{A F^2}{s/t} = \frac{4 \times .982^2}{155.3} \times 2.532 \times 10^6 = .063 \times 10^6$$

Rods + Resin

$$GJ = \frac{1}{2} \pi \times .405^4 \times .56 \times 10^6 = .024 \times 10^6$$

Total GJ for Call 1

$$(.063 + .024) \times 10^6 = \frac{4 \times .982^2}{(143 + 128 + .52 + 1.17)/t} \times 2.532 \times 10^6$$

$$t = .092$$

$$\left(\frac{S}{t}\right) = (1.13 + 1.28 + .52 + 1.17) / .042 = 98$$

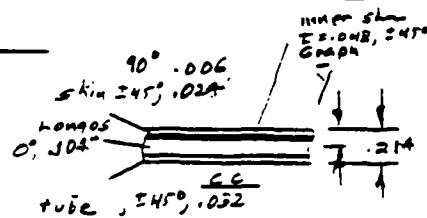
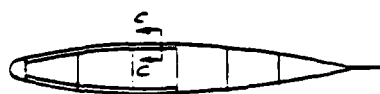
FIBER NO. 1	
EM= ?	0.46
UM= ?	4.7 05
NF= ?	0.35
FIBER NO.	1
VF= ?	0.54
EFL= ?	2.6 06
EFT= ?	2.6 06
GF= ?	0.8
EL=	1.1 07
ET=	1690357.616
GLT=	1168075.837
GLT=	3211397098
GLT=	556064.6481



REPORT TITLE		REPORT NO.
PREPARED BY <u>JPC</u>		<u>CMRB-79-005</u>
CHECKED BY <u>7/3/79</u>	MODEL NO. <u>YAH-64</u>	
SUBJECT <u>YAH-64 CMRB</u>		

Torsion Stiffness - Sta 84

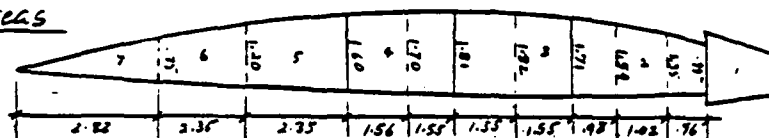
Slr C.g for laminate of Main Box



$$\bar{Y} = \frac{.024 \times 2.532 \times 0.15 + .048 \times 4.421 \times .054 + .104 \times .2349 \times .13 + .032 \times 2.532 \times .198}{(.024 + .072) \times 2.532 + .104 \times .2349 + .048 \times 4.421}$$

$$\bar{Y} = .084$$

Cell Areas



$$A_1 = .982$$

$$A_2 = \frac{.99 + 1.35}{2} \times .96 + \frac{1.35 + 1.59}{2} \times 1.02 + \frac{1.59 + 1.71}{2} \times .98 = 1.123 + 1.499 + 1.617 = 4.24$$

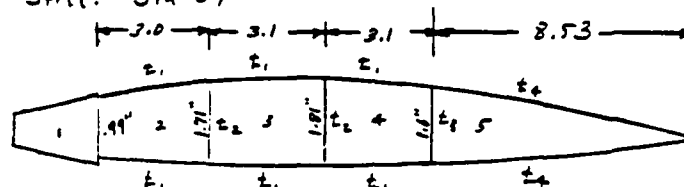
$$A_3 = \frac{1.71 + 1.82}{2} \times 1.55 + \frac{1.82 + 1.91}{2} \times 1.55 = 2.736 + 2.813 = 5.549$$

$$A_4 = \frac{1.31 + 1.70}{2} \times 1.55 + \frac{1.70 + 1.80}{2} \times 1.56 = 2.72 + 2.496 = 5.216$$

$$A_5 = \frac{1.60 + 1.20}{2} \times 2.35 + \frac{1.2 + .75}{2} \times 2.35 + \frac{.75 + 3.82}{2} = 7.02$$

REPORT TITLE		REPORT NO. <u>CMR3-79-005</u>
PREPARED BY <u>HC</u>	11/19/81	CHECKED BY
SUBJECT		MODEL NO. <u>YAH-64</u>

Torsional Stiff. Sta 84

Effective Skin Thickness

$$t_1 = .032 + \frac{.2349}{2.532} \times .104 + \frac{4.421}{2.532} \times .048 + .024 + .006 \frac{.229}{2.532} = .150$$

$$t_2 = .064, \quad t_3 = \frac{9.921}{2.532} \times .075 + .032 = .163, \quad t_4 = .0245$$

$$\left(\frac{S}{t}\right)_1 = 98$$

$$\left(\frac{S}{t}\right)_2 = \frac{6}{.15} + \frac{.99}{.042 + .032} + \frac{1.71}{.064} = 80.1$$

$$\left(\frac{S}{t}\right)_3 = \frac{6.2}{.15} + \frac{1.71 + 1.81}{.064} = 96.3$$

$$\left(\frac{S}{t}\right)_4 = \frac{1.81}{.064} + \frac{1.6}{.163} + \frac{6.2}{.15} = 79.4$$

$$\left(\frac{S}{t}\right)_5 = \frac{1.6}{.163} + \frac{2 \times 8.53}{.0254} = 682$$

$$\left(\frac{S}{t}\right)_{1,2} = \frac{.99}{.042 + .032} = 13.4$$

$$\left(\frac{S}{t}\right)_{2,3} = \frac{1.71}{.064} = 26.7$$

$$\left(\frac{S}{t}\right)_{3,4} = \frac{1.81}{.064} = 28.3$$

$$\left(\frac{S}{t}\right)_{4,5} = \frac{1.6}{.163} = 9.82$$

REPORT TITLE		REPORT NO.
PREPARED BY <u>JFL</u>		<u>CMRB-79-005</u>
11/17/81	CHECKED BY	MODEL NO.
SUBJECT <u>YAH-64 CMRB</u>		<u>YAH-64</u>

Torsional Stiff Sta 84

$$\begin{bmatrix}
 98 & -13.4 & 0 & 0 & 0 \\
 -13.4 & 80.1 & -26.7 & 0 & 0 \\
 0 & -26.7 & 96.3 & -28.3 & 0 \\
 0 & 0 & -28.3 & 81.5 & -9.82 \\
 0 & 0 & 0 & -9.82 & 682
 \end{bmatrix}
 \begin{bmatrix}
 X_1 \\
 X_2 \\
 X_3 \\
 X_4 \\
 X_5
 \end{bmatrix}
 =
 \begin{bmatrix}
 .982 \\
 4.24 \\
 5.55 \\
 5.216 \\
 7.02
 \end{bmatrix}$$

23.008

where

$X_1 = 0.0229$
 $X_2 = 0.0942$
 $X_3 = 0.1123$
 $X_4 = 0.1044$
 $X_5 = 0.0118$

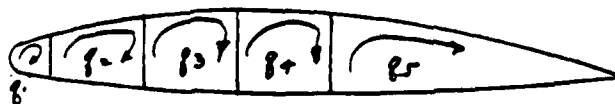
$.0229 \times .982 = .0225$
 $.0942 \times 4.24 = .40$
 $.1123 \times 5.55 = .6233$
 $.1044 \times 5.216 = .545$
 $.0118 \times 7.02 = .0828$

$$1.674 \times 4 = 6.69 = J$$

$$\begin{aligned}
 GJ &= 2.54 \times 10^6 \times 6.69 \\
 &= 17 \times 10^6 \text{ By calculation}
 \end{aligned}$$

$$\begin{aligned}
 g_1 &= \frac{2 \times 1000}{6.69} \times .0229 = 6.85 \text{ \%/in} \\
 g_2 &= \text{ " } \times .0942 = 28 \text{ \%/in} \\
 g_3 &= \text{ " } \times .1123 = 33.6 \text{ \%/in} \\
 g_4 &= \text{ " } \times .1044 = 31.2 \text{ \%/in} \\
 g_5 &= \text{ " } \times .0118 = 3.5 \text{ \%/in}
 \end{aligned}$$

"g" for 1000" of torque



REPORT TITLE	REPORT NO.
PREPARED BY <u>APC</u>	<u>CMRB-77-005</u>
CHECKED BY <u>11/19/81</u>	MODEL NO.
SUBJECT <u>YAH-64 CMRB</u>	<u>YAH-64</u>

Torsional Stiffness Test Data

Table 30-2

Composite M/R Blade 100% = 12,000 "lb
YAH: 7-311412500
S/N: 1002

STA % LAST	DEGREES/MIN										LE, YD, T	
	54	69	84	107	130	153	176	199	222	245	265	
0	6/30	6/0	5/27	4/50	4/08	3/23	2/40	2/10	1/32	0/45	-0/49	
20	6/34	5/44	5/03	4/15	3/20	2/24	1/32	0/40	-0/81	-1/05	-2/50	
40	6/09	5/33	4/55	3/53	2/45	1/36	0/29	-0/34	-1/34	-2/40	-4/36	
60	6/04	5/22	4/41	3/23	2/07	0/47	-0/31	-1/47	-3/60	-4/13	-6/33	
80	6/00	5/21	4/30	3/00	1/50	0/00	-1/13	-3/60	-1/24	-5/59	-8/12	
100	5/59	5/16	4/16	2/40	0/58	-0/48	-2/28	-4/05	-5/45	-7/27	-10/00	
80	6/00	5/21	4/24	3/00	1/30	0/00	-1/33	-3/60	-4/26	-6/00	-8/19	
60	6/04	5/26	4/37	3/23	2/03	0/37	-0/34	-1/52	-3/05	-4/55	-6/31	
40	6/06	5/31	4/51	3/27	2/40	1/29	0/22	-0/22	-1/42	-2/53	-4/50	
20	6/11	5/40	5/00	4/10	3/17	2/20	1/24	0/35	-0/24	-1/11	-3/00	
0	6/28	5/57	5/29	4/49	4/06	3/22	2/40	2/00	1/26	0/40	-0/49	
20	6/49	6/20	5/56	5/29	4/57	4/27	3/57	3/28	3/02	2/38	1/14	
40	6/53	6/24	6/03	5/55	5/37	5/14	4/57	4/41	4/28	4/12	2/55	
60	6/57	6/33	6/15	6/15	6/11	6/00	5/58	5/53	5/53	5/45	4/50	
80	6/58	6/41	6/29	6/41	6/47	6/49	6/56	7/04	7/14	7/22	6/34	
100	7/00	6/47	6/43	7/02	7/19	7/22	7/52	8/09	8/34	8/52	8/14	
80	6/59	6/42	6/32	6/43	6/49	6/52	6/58	7/06	7/18	7/28	6/44	
60	6/55	6/35	6/19	6/18	6/13	6/04	6/00	6/00	6/00	5/56	5/03	
40	6/52	6/27	6/04	5/51	5/39	5/19	5/00	4/47	4/35	4/16	3/10	
20	6/46	6/20	5/56	5/20	5/01	4/27	4/00	2/54	2/12	2/43	1/23	
0	6/33	6/05	5/32	4/58	4/16	3/32	2/52	2/10	1/40	0/58	-0/33	

REPORT TITLE		REPORT NO. <u>CMRB-79-005</u>
PREPARED BY <u>APC</u>	11/20/81 CHECKED BY	MODEL NO. <u>YAH-64</u>
SUBJECT <u>YAH-64 CMRB</u>		

Sta 84 to 176, Blade Torsional Stiffness
Ref Torsional Stiffness Data

$$\begin{aligned} \text{Ave torsional } \left. \begin{array}{l} \text{Def Sta 84} \end{array} \right\} &= \frac{[-40'16" + (5^{\circ}29' + 5^{\circ}27')/2] + [1^{\circ}43' - (5^{\circ}27' + 5^{\circ}32')/2]}{2} \\ &= 1^{\circ}12.75' = 1.2125^{\circ} \\ \text{Ave torsional } \left. \begin{array}{l} \text{Def Sta 176} \end{array} \right\} &= \frac{[20'28" + (2^{\circ}40')] + [7^{\circ}52' - (2^{\circ}40' + 2^{\circ}52')/2]}{2} \\ &= 5^{\circ}7' = 5.117^{\circ} \\ GJ \text{ sta 84 to 176 } \left. \begin{array}{l} \end{array} \right\} &= \frac{57.3 \times 12000(176-84)}{5.117^{\circ} - 1.2125^{\circ}} = 16.2 \times 10^6 \text{ Measured} \end{aligned}$$

REPORT TITLE		REPORT NO CMRB-77-005
PREPARED BY APC	11/19/81	CHECKED BY
SUBJECT YAH-64 CMRB		MODEL NO. YAH-64

Sta 84 to 69, Blade Torsional Stiffness

Ref Torsional Stiffness Data

$$\begin{aligned} \text{Ave torsional } \left. \begin{array}{l} \text{Def Sta 69} \end{array} \right\} &= \frac{[-5^{\circ}16' + (6^{\circ}0' + 5^{\circ}59')/2] + [6^{\circ}47' - (6^{\circ}5' + 5^{\circ}59')/2]}{2} \\ &= .7375^{\circ} \end{aligned}$$

$$GJ = \frac{57.3 \times 12000 (84-69)}{1.2125 - .7375} = 21.7 \times 10^6 \quad \text{sta 84 to 69}$$

measured

Sta 54 to 69

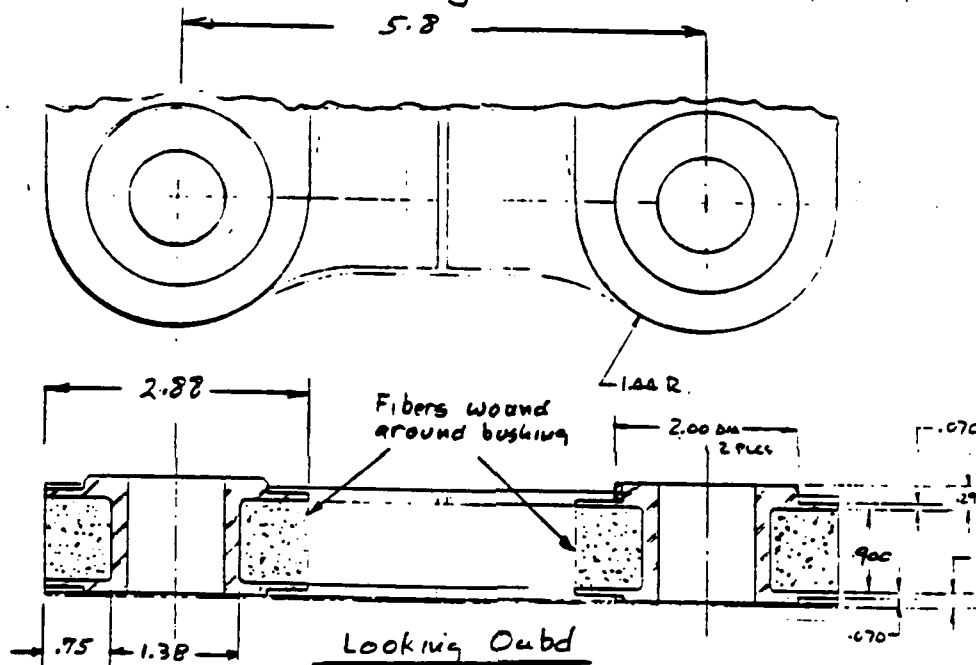
$$\begin{aligned} \text{Ave torsional } \left. \begin{array}{l} \text{Def Sta 54} \end{array} \right\} &= \frac{[-5^{\circ}59' + (6^{\circ}30' + 6^{\circ}28')/2] + [7^{\circ} - (6^{\circ}28' + 6^{\circ}33')/2]}{2} \\ &= .4958^{\circ} \end{aligned}$$

$$GJ = \frac{57.3 \times 12000 (69-54)}{.7375 - .4958} = 42.6 \times 10^6 \quad \text{Sta 54 to 69}$$

measured

REPORT TITLE		REPORT NO.
PREPARED BY	3/2/82	CARB-79-005
SUBJECT	CHECKED BY	MODEL NO.
		YAH-60

Crosssection Root Lugs



Cross-section of lug bushings now being used on the CARB.

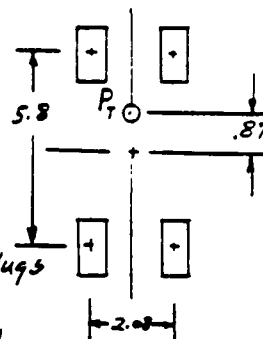
REPORT TITLE		REPORT NO
PREPARED BY	CHECKED BY	CMRB-79-005
APC	3/4/82	MODEL NO
SUBJECT		YAH-64

Root Lugs; Calculated Strength Compared with Static Test Applied Ld

$$P_T = 187,869 \# \text{ ult Ref 3 P. A-1}$$

$$\begin{aligned} \text{Max lug Load} \left. \begin{array}{l} \text{applied during} \\ \text{static test} \end{array} \right\} &= \frac{3.77 \times 187,869}{2 \times 5.8} \times \frac{1.49}{150} \\ &= 60,450 \# \quad \text{Ref. 2} \end{aligned}$$

For the above load the specimen failed at the club end (Sta 123) not at the lugs which are at Sta 39. Ref 2 Fig. 4



$$K = \frac{1.3(R/r)^2 + .7}{R/r + 1} \quad \text{strength reduction factor due to wrapping keular around lug bushing. Ref 3 P. 30.12 Vol II}$$

CMRB Lug Geometry

$$\text{Allowable tension stress} = \left\{ [162,500] \div \left[\frac{1.3(1.49/1.69)^2 + .7}{1.44/1.69 + 1} \right] \right\} \times \text{Reduction factor, environmental etc } .80 = 63,200 \text{ PSI}$$

$$\text{Lug Strength} = 2 \times .9 \times .75 \times 63,200 = 85,600 \#$$

Calculated lug strength is 42% higher than what was applied during static test; The calculated M.S. is:

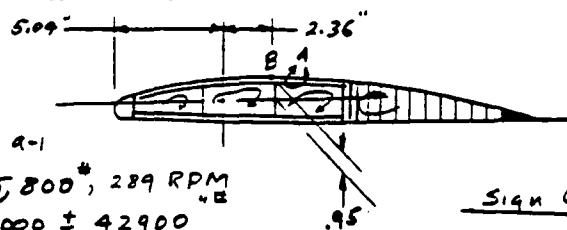
$$\text{Ult Lug Load} = \frac{150}{149} \times 60,450 = 61,000 \#$$

$$MS = \frac{85,600}{61,000} - 1 = \frac{.40}{\text{ult Attach Lugs}}$$

REPORT TITLE	REPORT NO.
PREPARED BY <u>HC</u>	CHECKED BY
SUBJECT <u>YAH-64 CMRB</u>	MODEL NO <u>YAH-64</u>

Sta 191.7 Pt. "B"

CK. Spar Longos, Critical Bending Section



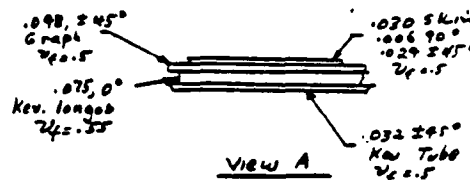
Ref Table A-1

C.F. = 35,800[#], 289 RPM $M_F = -8000 \pm 42900$ $M_C = 12400 \pm 97500$ " " $M_T = 3900 \pm 32000$

It is assumed the the longos resist bending and C.F. load, and the $\pm 45^\circ$ layers resist torsion.

Sign Convention

- + M_F ~ Com. Upper Surface
- + M_C ~ Com. Trailing Edge
- + Torsion ~ Nose Up



$$E_{Ten} = \frac{35800}{39.39} = 1041 \mu\% \text{ Ten.}$$

$$E_f = \frac{-8000 \times .95}{12.7} = 598 \mu\% \text{ Ten.}$$

$$E_c = -\frac{12400 \times 2.36}{984} + \frac{(21/4 - 5.04) 35800 \times 2.36}{984} = -12 \mu\% \text{ Com}$$

$$E_{alt} = \frac{42900 \times .95}{12.7} + \frac{97500 \times 2.36}{984} = 3890 + 234 = 3443 \mu\% \text{ alt}$$

 $f E, K_{ov}, \nu_f = .55$

$$\text{Max Ax. Ten Str} = (1041 + 724 - 12 + 3443) 10.66 = 55400 \text{ psi Ten}$$

$$\text{Min Ax Str} = (1041 + 598 - 12 - 3443) 10.66 = -19400 \text{ psi Com}$$

$$F_{tu} = 162500 \times .8 = 130,000 \text{ psi}$$

Reduction factor
Environmental etc

$$F_{cu} = 38500 \times .8 = 30,800 \text{ psi}$$

 $\nu_f = .55$

$$MS = \frac{30800}{1.5 \times 19400} - 1 = .06$$

Bend. C.K.
Pt. "B"
Spar longos

REPORT TITLE		REPORT NO. CMRB-77-605
PREPARED BY HFC	3/8/82	CHECKED BY
SUBJECT YAH-CMRB		MODEL NO. YAH-64

Sta 87, Ck. $\pm 45^\circ$ layers

It is assumed the $\pm 45^\circ$ layers resist shear due to torsion.

$$t_{kevlar} = .032 + .024 = .056"$$

$$t_{graph} = .048"$$

$$q = 33.6 \times (8000 + 32000) = 1344 \frac{\#}{in} \quad \text{lim}$$

$P. 30.07$ $P. 20.02$ $2016 \frac{\#}{in} \quad \text{ult}$

Reduction factor
Environmental effects
etc.

$$\text{Shear capability of the } \pm 45^\circ \text{ layers} = (.048 \times 37098 + .056 \times 15600) \cdot 8$$

$P. 100.06$

$$= 2123 \frac{\#}{in} \quad \text{P. 20.11}$$

$$MS = \frac{2123}{2016} - 1 = .05$$

Shr. Ck
 $\pm 45^\circ$ layers

Stress applied to spar cap longerons during static test

$$\text{Stress applied to } \left. \begin{array}{l} \text{longerons during test} \end{array} \right\} = \frac{187869}{38.1} \frac{149}{150} \times 10.66 = 52,000 \text{ PSI}$$

$P. 30.02$ $P. 190.02$

$$\text{Ratio of stress applied during test and calculated ultimate stress} = \frac{52,000}{1.5 \times 55,400} = .63$$

$P. 150.01$

REPORT TITLE		REPORT NO CMRB-79-005	
PREPARED BY APC	3/26/82	CHECKED BY	MODEL NO. YAH-64
SUBJECT YAH-64 CMRB			

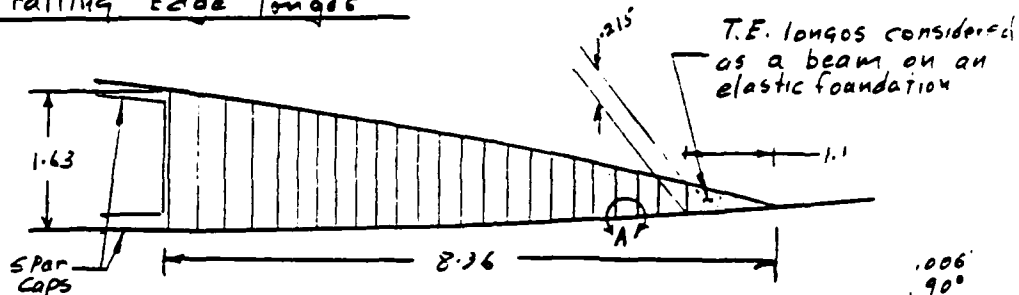
TRAILING EDGE

The buckling load for the trailing edge is calculated assuming it to be a column on an elastic foundation. Comparing the buckling load with the applied load it can be seen that the trailing edge will not buckle at limit load for the Maximum Rotor Torque condition.

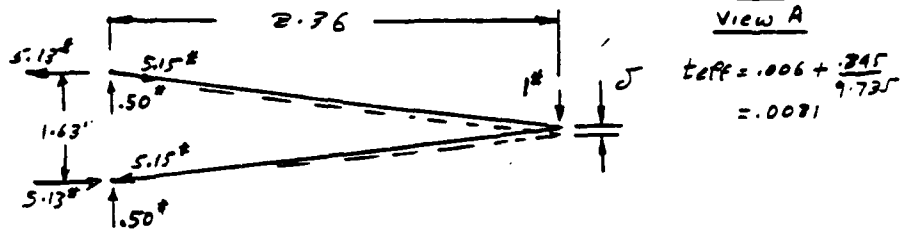
The analysis shows that the spar caps can resist the remaining bending load after the trailing edge buckles above limit load. That is the instant the trailing edge buckles elastically at a stress of 16,900 psi; the spar caps will pick up the remaining load preventing any inelastic buckling of the trailing edge. Since only elastic buckling occurs, no failure results.

REPORT TITLE	REPORT NO.
PREPARED BY JFC	CMRB-77-005
CHECKED BY 3/5/82	MODEL NO.
SUBJECT	YAH-64

Trailing Edge Longos



From the T.E. longos to the spar caps will be idealized as a truss.



$$\delta = \frac{PL}{AE} = \frac{5.13 \times 8.36}{.0081 \times 9.735 \times 10^6} = .000544"$$

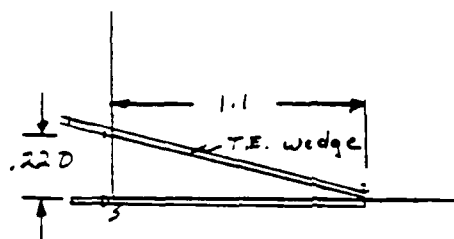
$$\text{Internal Energy } \delta = \frac{1}{2} \delta \times 5.15 \times 2 = .000544 \times 5.15 = .0028$$

$$\text{External Energy } \delta = \frac{1}{2} \delta ; \delta = 2 \times .0028 = .0056$$

$$\text{Spring Rate} = \frac{1}{.0056} = .179 \text{ #/in}$$

REPORT TITLE		REPORT NO <u>CMRB-79-005</u>
PREPARED BY <u>ACE</u>	3/5/82	CHECKED BY
SUBJECT		MODEL NO <u>YAH-64</u>

Trailing Edge Lougas



$$X = .37$$

$$Y = .073$$

$$A = .121$$

$$I_x = 325 \times 10^{-6}$$

$$I_y = 8 \times 10^{-3}$$

$$I_{xy} = 873 \times 10^{-6}$$

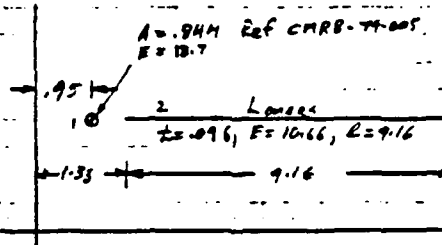
$$EI = 17.23 \times 10^6 \times 309 \times 10^{-6}$$

$$= 5600 \text{ T.E. wedge only}$$

	X	Y
0	0	0
1	0	.220
2	1.1	0
3	0	0

REPORT TITLE	REPORT NO. CMRB-79-005
PREPARED BY A. Cilli	CHECKED BY
SUBJECT YAH-64 CMRB	MODEL NO. YAH-64

Calculation of I chord. Aft skin and T.E. assumed Buckled



Item	A	E	EA	X	EAx	EAx ²	I _o
1	.844	10.7	15.73	.45	14.99	14.99	0
2	1.91	10.66	19.29	5.91	114.0	673.8	135.18
			35.07		129	688.8	135.18

$$EI_{long} = \frac{2 \times 1.099 \times 9.16^3}{12} \times 10.66 = 135.18$$

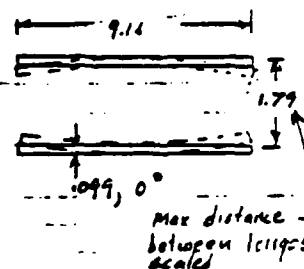
$$\bar{X} = \frac{129}{35.07} = 3.68$$

$$EI_{chord} = 135.18 + 688.8 - 3.68 \times 129 = 349$$

To account for curvature of long

$$I_{Flap} = \left(.90 \times \frac{1.79}{2} \right)^2 \times 9.16 \times .099 \times 10.66 \times 2$$

$$= 12.54 \quad \text{Long only}$$



REPORT TITLE		REPORT NO.
PREPARED BY <u>APC</u>		<u>CMRB-79-005</u>
3/5/82	CHECKED BY	MODEL NO.
SUBJECT <u>YAH-64 CMRB</u>		<u>YAH-64</u>

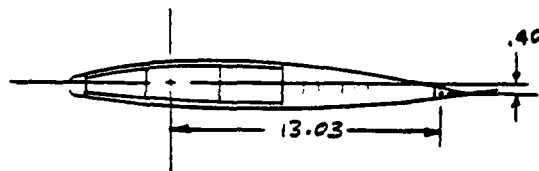
Trailing Edge Longos

$$m = \left[\frac{KL^4}{\pi^4 EI} \right]^{1/4} = \left[\frac{179 \times (288-82)^4}{\pi^4 \times 5600} \right]^{1/4} = 28$$

Ref 3
P. 97
Main body
of Rp.

$$P_{cr} = \frac{2m^2 \pi^2 EI}{L^2} = \frac{2 \times 28^2 \times \pi^2 \times 5600}{206^2} = 2042$$

$$T.E. \text{ Buckling stress} = 2042 / .121 = 16,900 \text{ PSI}$$



Ref 3 P. 9
Vol II
Zero Rotor Speed
Max Torque

$$f = \left[\frac{54795 \times 13.03}{924} + \frac{790 \times .4}{15.52} \right] 17.23$$

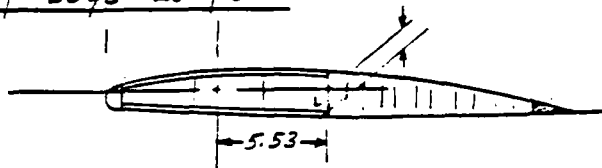
$$= 13,660 \text{ PSI}$$

$$MS = \frac{16900}{13660} - 1 = .23$$

Limit
Stability

Shows that for
LIMIT LOADS
the T.E. longos
will not buckle.

REPORT TITLE		REPORT NO.
PREPARED BY <u>AKC</u>		<u>CMRB-74-005</u>
<u>3/5/82</u>	CHECKED BY	MODEL NO.
SUBJECT <u>YAH-CMRB</u>		<u>YAH-64</u>

Trailing Edge Longos

$$\text{Stress at Pt. 'L' due to 1.23 times limit load} \left\} = \left[\frac{54795 \times 5.53}{924} + \frac{790 \times .70}{15.52} \right] 10.66 \times 1.23 = 4,800 \text{ psi}$$

$$\text{Stress at Pt. 'L' due to balance of ultimate load} \left\} = \left[\frac{54795 \times 6.81}{349} + \frac{790 \times .7}{12.54} \right] (1.5 - 1.23) \times 10.66 = 3204 \text{ psi}$$

$$\text{Stress at Pt. 'L' after the T.E. longos have buckled} \left\} = 4800 + 3204 = 8000 \text{ psi com.}$$

$$\text{Allowable com. stress for Kevlar, } \nu_f = .55 \left\} = .8 \times 38500 = 30800 \text{ psi}$$

$B_{20.14}$

Reduction factor, Environmental effects etc.

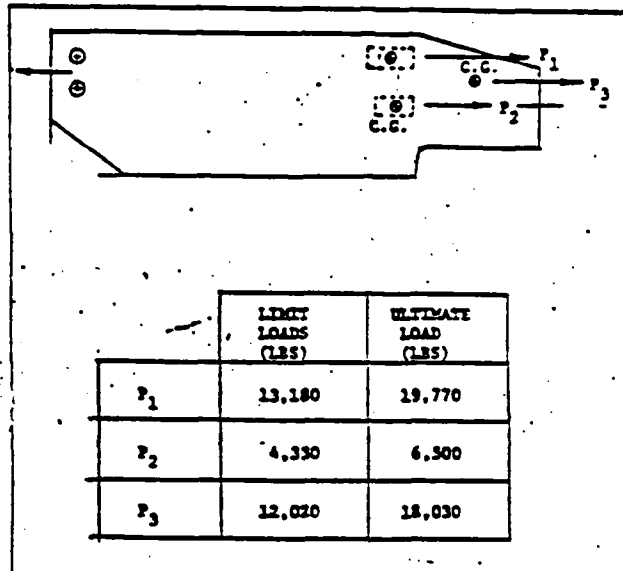
$$MS = \frac{30800}{8000} - 1 = \text{High}$$

ABOVE LIMIT LOAD

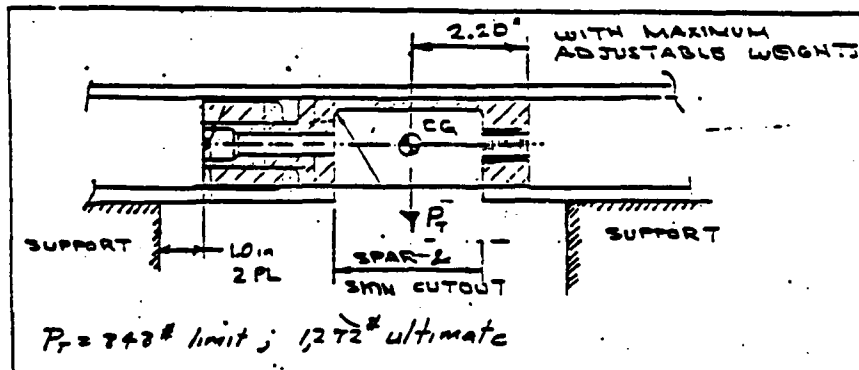
This shows that after the T.E. longos have buckled the spar cap longos will resist the remaining bending and that ultimate can be applied to the blade without failure.

LONG

REPORT TITLE		REPORT NO
PREPARED BY <u>AFC</u>		<u>CMRB-77-005</u>
3/8/82		CHECKED BY
SUBJECT <u>YAH-64 - CMRB</u>		MODEL NO <u>YAH-64</u>

Blade Tip ~ Substantiated by Test

Load Configuration, Sump; Tip Radial Static Test

NOTE: Tip resisted 356% of the above limit loads without failure (Ref. 2, P3 &) or; MS = High

Load Configuration, Aft Weight Assy. Vertical Load Test

APPENDIX B

FATIGUE ANALYSIS OF THE COMPOSITE MAIN ROTOR
BLADE FOR THE AH-64A HELICOPTER

REPORT TITLE		REPORT NO.
Fatigue Analysis for the YAH-64 CMRB		CMRB-79-006
PREPARED BY	CHECKED BY	MODEL NO.
APC	3/25/82	YAH-64
SUBJECT		
CMRB Fatigue Analysis		

TABLE OF CONTENTS

<u>Section</u>		<u>Page</u>
B10	References	B10.02
B10	Introduction	B10.03
B10	Summary of Component Lives	B10.04
B10	Summary of Test Results	B10.05
B15	Root Fatigue Test Results and Applied Loads	B15.01
B15	Swept Tip Test Results and Applied Loads	B15.02
B20	Fatigue Test Results Plotted	B20.01
B30	CMRB and Metal Blade Flight Allowables Compared	B30.01
B40	Graphs Substantiating CMRB Fatigue Strength Compared to Blade Flight Loads and Metal Blade Allowables	B40.01



REPORT TITLE		Fatigue Analysis for the YAH-64 CMRB		REPORT NO.	CMRB 79-006
PREPARED BY	APC	3/25/82	CHECKED BY	MODEL NO.	YAH-64
SUBJECT					
CMRB - Fatigue Analysis					
 <u>REFERENCES</u> 					
1. CMRB-79-004 Basic Loads Report for the Composite Main Rotor Blade for the YAH-64 Advanced Attack Helicopter 1 June 1979 Revised July 1979 Revised March 1982					
2. Structural Test Report for the CMRB YAH-64/AAH Feb. 1982					
3. CMRB 79-041 Safety of Flight Review Airworthiness Substantiation Document Composite Main Rotor Blade for the YAH-64/AAH May 1980, Vol. I and II					

REPORT TITLE Fatigue Analysis for the YAH-64 CMRB		REPORT NO. CMRB-79-006
PREPARED BY APC 3/25/82	CHECKED BY	MODEL NO. YAH-64
SUBJECT CMRB Fatigue Analysis		

INTRODUCTION

Fatigue life of the CMRB is equal to or greater than 4500 hours as required per Specification Number AMC-SS-AAH-H10000. Also with a critical element failed the CMRB is capable of a minimum of thirty (30) minutes of flight after initial failure.

The revised fatigue life of the CMRB has been substantiated by a combination of analysis and component fatigue tests. A summary of test results is shown on Pg. A10.05. Fatigue analysis of the blade before testing is presented in the main body of the report.

Five root specimens were tested. The first two specimens were root-midspan specimens. The purpose being to test the blades root-end and mid-span simultaneously. During testing of the specimens 1 and 2 premature lug failures occurred at 8000 and 24000 respectively due to the high rate of cyclic loading (approximately 13 Hz), which cause heating of the lugs and an undue rise in temperature leading to early failure. 13-Hz was the resonant frequency of the specimen.

A premature failure of specimen No. 3 indicated insufficient fatigue strength of the blade attachment lugs as originally designed. Specimen 4, which incorporated design configuration changes yielded greatly improved fatigue strength in the lug area although lateral expansion of the lugs was still present.

The present design of the blade lugs has a double flange bushing (spool) to contain the fibers because they tend to spread or flatten out when loaded. The previous tested blade specimens had bushings with only a single flange. To structurally simulate the current design in the fatigue test, shims were placed between the link assembly and the blade lugs for specimen 5.

Specimen 5, with shimmed lugs showed no damage or lateral expansion of the lugs after 947,700 cycles at increased load levels. The last 50,400 cycles were obtained at the mean 1 hour load level. The required number of cycles at the 1 hour load level is 17,340. The root end of the blade could still support centrifugal force when the test was terminated due to increased deflections.

REPORT TITLE <u>Fatigue Analysis for the YAH-64 CMRB</u>		REPORT NO. <u>CMRB-79-005</u>
PREPARED BY <u>APC</u>	<u>3/26/82</u>	CHECKED BY <u>YAH-64</u>
SUBJECT <u>CMRB Fatigue Analysis</u>		

INTRODUCTION - (Cont'd)

Other changes to the original design that increase the fatigue strength are as follows:

1. .048" graphite inner skin; was .010" Kevlar.
2. Honeycomb supporting the trailing edge skin and swept tip; was Kevlar tubes and Kevlar ribs respectively.
3. .075 graphite channel that runs the length of the blade; was .048 Kevlar web.

A summary of loads and test results is given on Pg. B15.01 for specimens 3, 4, and 5; and on Pg. B10.05 is a summary of all testing done on the CMRB.

One swept tip was tested. Loads and results are shown on Pg. B15.02. The swept tip is of original design with .010" Kevlar inner skin and Kevlar ribs supporting the skin. The present design has honeycomb supporting the skin and is stronger.

From test results shown on Pg. B15.01 and Pg. B15.02, flight L-N fatigue curves are developed starting on Pg. B20.01. For flap bending and chord bending curves, the most conservative combination of 45° and 0° curve shapes is used. This is because either the 45° or 0° fibers may fail first. For torsion, only the 0° curve shape is used since torsion is resisted as axial load in the $\pm 45^\circ$ fibers. The attach lug curve shape is based on the 0° fibers. The mean test curve at the endurance limit is reduced as follows:

L-N CURVE SCATTER REDUCTION FACTORS

Number of Fatigue Test Specimens	Percent of Mean L-N Curve Used
1	50%
2	65%
3	75%
4 or more	Statistical analysis (M-3σ)

REPORT TITLE		REPORT NO.	
Fatigue Analysis for the YAH-64 CMRB		CMRB-79-006	
PREPARED BY	APC 3/26/62	CHECKED BY	MODEL NO.
SUBJECT		YAH-64	
CMRB Fatigue Analysis			

INTRODUCTION - (Cont'd)

Values obtained for endurance limit, 10 hour and 1 hour flight allowables are shown on Pg. B30.01 and compared to metal blade allowables.

Starting on Pg. B40.01 the values on Pg. B30.01 for endurance limit and one hour are shown graphically along with the applied blade load curve. From these curves the fatigue strength of the CMRB can be compared to the metal blade and the load applied to the blade.

REPORT TITLE Fatigue Analysis for the YAH-64 CMRB	REPORT NO. CMRB-79-006
PREPARED BY AFC	CHECKED BY 3/25/82
MODEL NO. YAH-64	
SUBJECT CMRB Fatigue Analysis	

REPORT TITLE FATIGUE ANALYSIS FOR THE YAH-64 ADVANCED ATTACK HELICOPTER COMPOSITE MAIN ROTOR BLADE	REPORT NO. CMRB-79-006		
PREPARED BY AFC	CHECKED BY 11-5-79		
MODEL NO. YAH-64			
SUBJECT CMRB - FATIGUE ANALYSIS			
<u>SUMMARY OF COMPONENT LIVES</u>			
ITEM	CONDITION	PAGE	LIFE
ROOT LGS	WEIGHTED FATIGUE	30.20	> 4500 HOURS
	GAC	30.21	100,000 HOURS
	VULNERABILITY (ONE LGS FAILED)	30.22	MORE THAN 30 MINUTES
VIBRATION ABSORBER BRACKET	FATIGUE	31.13	INFINITE
		31.17	
		31.19	
ROOT CLOSE-OUT	WEIGHTED FATIGUE	40.04	INFINITE
STA 55	WEIGHTED FATIGUE	50.04	> 4500 HOURS
STA 84	WEIGHTED FATIGUE	60.04	> 4500 HOURS
STA 160	WEIGHTED FATIGUE	70.03	> 4500 HOURS
STA 192	WEIGHTED FATIGUE	70.06	> 4500 HOURS
TIP COMPONENTS	GAC	80.01	INFINITE



SUMMARY OF TESTS RESULTS

This page presents the results of tests conducted on the Composite Main Rotor Blade for the YAH-64 Advanced Attack Helicopter. The tests were conducted at the Hughes Helicopters Inc. Structures Test Laboratory, Culver City, CA., between January 1980 and August 1981.

One each, Swept Tip specimens were subjected to Static, Ground-Air-Ground, and Fatigue loading. One each, Root-Midspan specimens were subjected to Static and Ground-Air-Ground loading. Five Root specimens were tested under fatigue loading.

Significant test results are as follows:

1. Swept Tip Static, GAG and Fatigue tests.
 - a. 100% radial limit load achieved on swept tip section without failure or permanent set.
 - b. 100% vertical limit load and ultimate load on aft tip weight box without failure or permanent set. 211% radial limit load achieved on swept tip assembly without failure.
 - c. 336% radial limit load achieved on fwd. and aft tip weight boxes without failure.
 - d. 108,000 cycles, representing eight times three GAG cycles per hour for a service life of 4500 hours achieved without failure.
2. Root-Midspan Static and GAG tests.
 - a. 100% radial limit load applied statically without yielding or permanent set. Failure at the club end occurred at 149% limit load.
 - b. 108,000 cycles, representing eight times three GAG cycles per hour for a service life of 4500 hours achieved without failure. Lug failed at 33,200 cycles of 125% GAG load.
3. Root Fatigue Tests
 - a. Tests conducted on specimens 1 and 2 were considered invalid due to overheating of the test specimen resulting from an excessive test cyclic load rate.
 - b. A premature failure of specimen No. 3 indicated insufficient fatigue strength of the blade attachment lugs as originally designed.
 - c. Specimen 4, which incorporated design configuration changes yielded greatly improved fatigue strength in the lug area although lateral expansion of the lugs was still present.
 - d. Specimen 5, with shimmed lugs which simulated the additional lateral restraint of the longo fibers obtainable from the future use of double flanged lug bushings showed no damage or lateral expansion of the lugs after 947,700 cycles at increased load levels. The last 50,400 cycles were obtained at the mean 1 hour load level. The required number of cycles at the 1 hour load level is 17,340. The root end of the blade could still support centrifugal force when the test was terminated due to increased deflections.

REPORT TITLE			REPORT NO.				
Fatigue Analysis for the YAH-64 CMRB			CMRB-79-006				
PREPARED BY			CHECKED BY				
LPC			YAH-64				
SUBJECT			MODEL NO.				
CMRB Fatigue Analysis			YAH-64				
Root Fatigue Test Results and Applied Loads							
See Pgs 38 & 39 Ref 2.							
Specimen Description	3	Original Design	4		5		
			1st Specimen	Redesigned Specimen	2nd Specimen (Shimmed Lug)	Redesigned Specimen (Shimmed Lug)	
39	LL-1	.4xLL-2	LL-3	LL-4	LL-5	LL-6	
							5/N
Mid Flap	39	39,200 ± 32,100 ± 35,200 ± 24,100	15,600 ± 14,400 ± 11,900 ± 5,600	39,200 ± 36,000 ± 30,000 ± 16,000	43,950 ± 40,360 ± 30,800 ± 18,400	43,950 ± 40,360 ± 31,500 ± 20,400	54,500 ± 50,000 ± 40,300 ± 32,000
Mid Flap	39	50,400 ± 51,900 ± 55,900 ± 53,900	20,160 ± 20,760 ± 22,360 ± 21,200	50,400 ± 52,500 ± 55,900 ± 53,500	87,900 ± 85,100 ± 79,300 ± 93,300	87,900 ± 85,000 ± 79,300 ± 93,300	109,000 ± 94,520 ± 72,352 ± 57,000
Mid Flap	39	83,900 ± 79,900 ± 68,000	2,356 ± 3,196 ± 2,720	13,830 ± 13,600 ± 13,000	18,500 ± 19,300 ± 17,600	18,500 ± 18,300 ± 17,600	23,100 ± 22,407 ± 20,328
Mid Flap	39	83,900 ± 79,900 ± 68,000	2,356 ± 3,196 ± 2,720	13,830 ± 13,600 ± 13,000	18,500 ± 19,300 ± 17,600	18,500 ± 18,300 ± 17,600	23,100 ± 22,407 ± 20,328
Mid Flap	39	83,900 ± 79,900 ± 68,000	2,356 ± 3,196 ± 2,720	13,830 ± 13,600 ± 13,000	18,500 ± 19,300 ± 17,600	18,500 ± 18,300 ± 17,600	23,100 ± 22,407 ± 20,328
Mid Flap	39	83,900 ± 79,900 ± 68,000	2,356 ± 3,196 ± 2,720	13,830 ± 13,600 ± 13,000	18,500 ± 19,300 ± 17,600	18,500 ± 18,300 ± 17,600	23,100 ± 22,407 ± 20,328
Mid Flap	39	83,900 ± 79,900 ± 68,000	2,356 ± 3,196 ± 2,720	13,830 ± 13,600 ± 13,000	18,500 ± 19,300 ± 17,600	18,500 ± 18,300 ± 17,600	23,100 ± 22,407 ± 20,328
Mid Flap	39	83,900 ± 79,900 ± 68,000	2,356 ± 3,196 ± 2,720	13,830 ± 13,600 ± 13,000	18,500 ± 19,300 ± 17,600	18,500 ± 18,300 ± 17,600	23,100 ± 22,407 ± 20,328
Mid Flap	39	83,900 ± 79,900 ± 68,000	2,356 ± 3,196 ± 2,720	13,830 ± 13,600 ± 13,000	18,500 ± 19,300 ± 17,600	18,500 ± 18,300 ± 17,600	23,100 ± 22,407 ± 20,328
Mid Flap	39	83,900 ± 79,900 ± 68,000	2,356 ± 3,196 ± 2,720	13,830 ± 13,600 ± 13,000	18,500 ± 19,300 ± 17,600	18,500 ± 18,300 ± 17,600	23,100 ± 22,407 ± 20,328
Mid Flap	39	83,900 ± 79,900 ± 68,000	2,356 ± 3,196 ± 2,720	13,830 ± 13,600 ± 13,000	18,500 ± 19,300 ± 17,600	18,500 ± 18,300 ± 17,600	23,100 ± 22,407 ± 20,328
Mid Flap	39	83,900 ± 79,900 ± 68,000	2,356 ± 3,196 ± 2,720	13,830 ± 13,600 ± 13,000	18,500 ± 19,300 ± 17,600	18,500 ± 18,300 ± 17,600	23,100 ± 22,407 ± 20,328
Mid Flap	39	83,900 ± 79,900 ± 68,000	2,356 ± 3,196 ± 2,720	13,830 ± 13,600 ± 13,000	18,500 ± 19,300 ± 17,600	18,500 ± 18,300 ± 17,600	23,100 ± 22,407 ± 20,328
Mid Flap	39	83,900 ± 79,900 ± 68,000	2,356 ± 3,196 ± 2,720	13,830 ± 13,600 ± 13,000	18,500 ± 19,300 ± 17,600	18,500 ± 18,300 ± 17,600	23,100 ± 22,407 ± 20,328
Mid Flap	39	83,900 ± 79,900 ± 68,000	2,356 ± 3,196 ± 2,720	13,830 ± 13,600 ± 13,000	18,500 ± 19,300 ± 17,600	18,500 ± 18,300 ± 17,600	23,100 ± 22,407 ± 20,328
Mid Flap	39	83,900 ± 79,900 ± 68,000	2,356 ± 3,196 ± 2,720	13,830 ± 13,600 ± 13,000	18,500 ± 19,300 ± 17,600	18,500 ± 18,300 ± 17,600	23,100 ± 22,407 ± 20,328
Mid Flap	39	83,900 ± 79,900 ± 68,000	2,356 ± 3,196 ± 2,720	13,830 ± 13,600 ± 13,000	18,500 ± 19,300 ± 17,600	18,500 ± 18,300 ± 17,600	23,100 ± 22,407 ± 20,328
Mid Flap	39	83,900 ± 79,900 ± 68,000	2,356 ± 3,196 ± 2,720	13,830 ± 13,600 ± 13,000	18,500 ± 19,300 ± 17,600	18,500 ± 18,300 ± 17,600	23,100 ± 22,407 ± 20,328
Mid Flap	39	83,900 ± 79,900 ± 68,000	2,356 ± 3,196 ± 2,720	13,830 ± 13,600 ± 13,000	18,500 ± 19,300 ± 17,600	18,500 ± 18,300 ± 17,600	23,100 ± 22,407 ± 20,328
Mid Flap	39	83,900 ± 79,900 ± 68,000	2,356 ± 3,196 ± 2,720	13,830 ± 13,600 ± 13,000	18,500 ± 19,300 ± 17,600	18,500 ± 18,300 ± 17,600	23,100 ± 22,407 ± 20,328
Mid Flap	39	83,900 ± 79,900 ± 68,000	2,356 ± 3,196 ± 2,720	13,830 ± 13,600 ± 13,000	18,500 ± 19,300 ± 17,600	18,500 ± 18,300 ± 17,600	23,100 ± 22,407 ± 20,328
Mid Flap	39	83,900 ± 79,900 ± 68,000	2,356 ± 3,196 ± 2,720	13,830 ± 13,600 ± 13,000	18,500 ± 19,300 ± 17,600	18,500 ± 18,300 ± 17,600	23,100 ± 22,407 ± 20,328
Mid Flap	39	83,900 ± 79,900 ± 68,000	2,356 ± 3,196 ± 2,720	13,830 ± 13,600 ± 13,000	18,500 ± 19,300 ± 17,600	18,500 ± 18,300 ± 17,600	23,100 ± 22,407 ± 20,328
Mid Flap	39	83,900 ± 79,900 ± 68,000	2,356 ± 3,196 ± 2,720	13,830 ± 13,600 ± 13,000	18,500 ± 19,300 ± 17,600	18,500 ± 18,300 ± 17,600	23,100 ± 22,407 ± 20,328
Mid Flap	39	83,900 ± 79,900 ± 68,000	2,356 ± 3,196 ± 2,720	13,830 ± 13,600 ± 13,000	18,500 ± 19,300 ± 17,600	18,500 ± 18,300 ± 17,600	23,100 ± 22,407 ± 20,328
Mid Flap	39	83,900 ± 79,900 ± 68,000	2,356 ± 3,196 ± 2,720	13,830 ± 13,600 ± 13,000	18,500 ± 19,300 ± 17,600	18,500 ± 18,300 ± 17,600	23,100 ± 22,407 ± 20,328
Mid Flap	39	83,900 ± 79,900 ± 68,000	2,356 ± 3,196 ± 2,720	13,830 ± 13,600 ± 13,000	18,500 ± 19,300 ± 17,600	18,500 ± 18,300 ± 17,600	23,100 ± 22,407 ± 20,328

NOTE: Original design had kevlar inner skin and tubes in T.E. of airfoil. Redesigned specimen has graphite inner skin and honeycombs in T.E. of airfoil. None of the above specimens had the double flange bushing (spool) that is now being used. Lugs of the 2nd redesigned specimen were shimmed to simulate the spool bushing.

REPORT TITLE <i>Fatigue Analysis for the VAH-64 CMRB</i>	REPORT NO. <i>CMRB-77-006</i>
PREPARED BY <i>ACC</i>	CHECKED BY
<i>2/26/82</i>	MODEL NO. <i>VAH-64</i>
SUBJECT <i>CMRB Fatigue Analysis</i>	

Swept Tip Fatigue Results and Applied Loads

Ref 3 Pg 24

Test Results, Swept Tip Fatigue Test

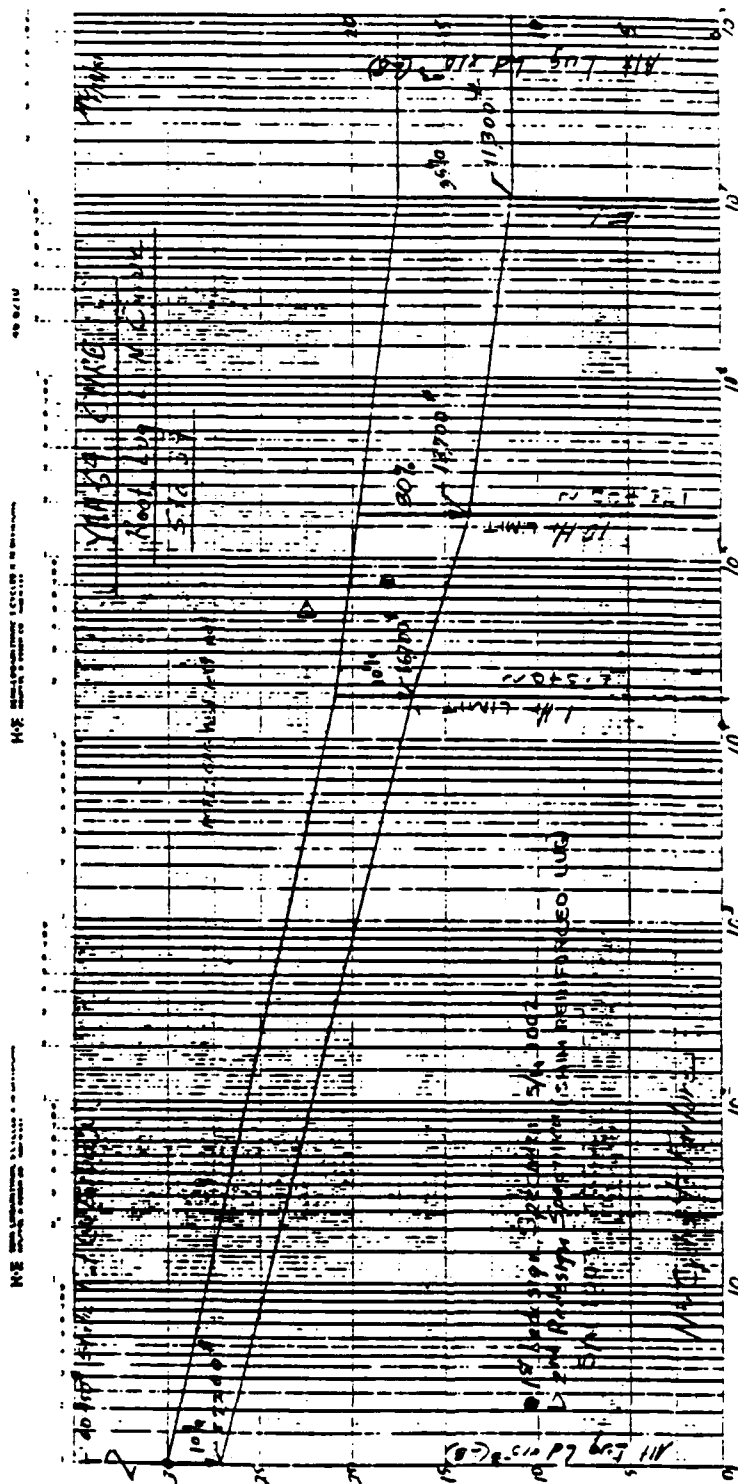
LOAD LEVEL	FATIGUE MOMENTS (IN-LB.)			COMMENTS
	Sta. 266.5		Sta. 260	
	M _{Flap}	M _{Chord}	M _{Torsion}	
1	+9227	+5670	+1100	1 X 10 ⁶ CYCLES. NO FAILURE
2	+11534	+7088	+1376	1 X 10 ⁶ CYCLES. NO FAILURE
3	+13841	+8505	+1650	162,000 CYCLES. NO FAILURE TEST TERMINATED.

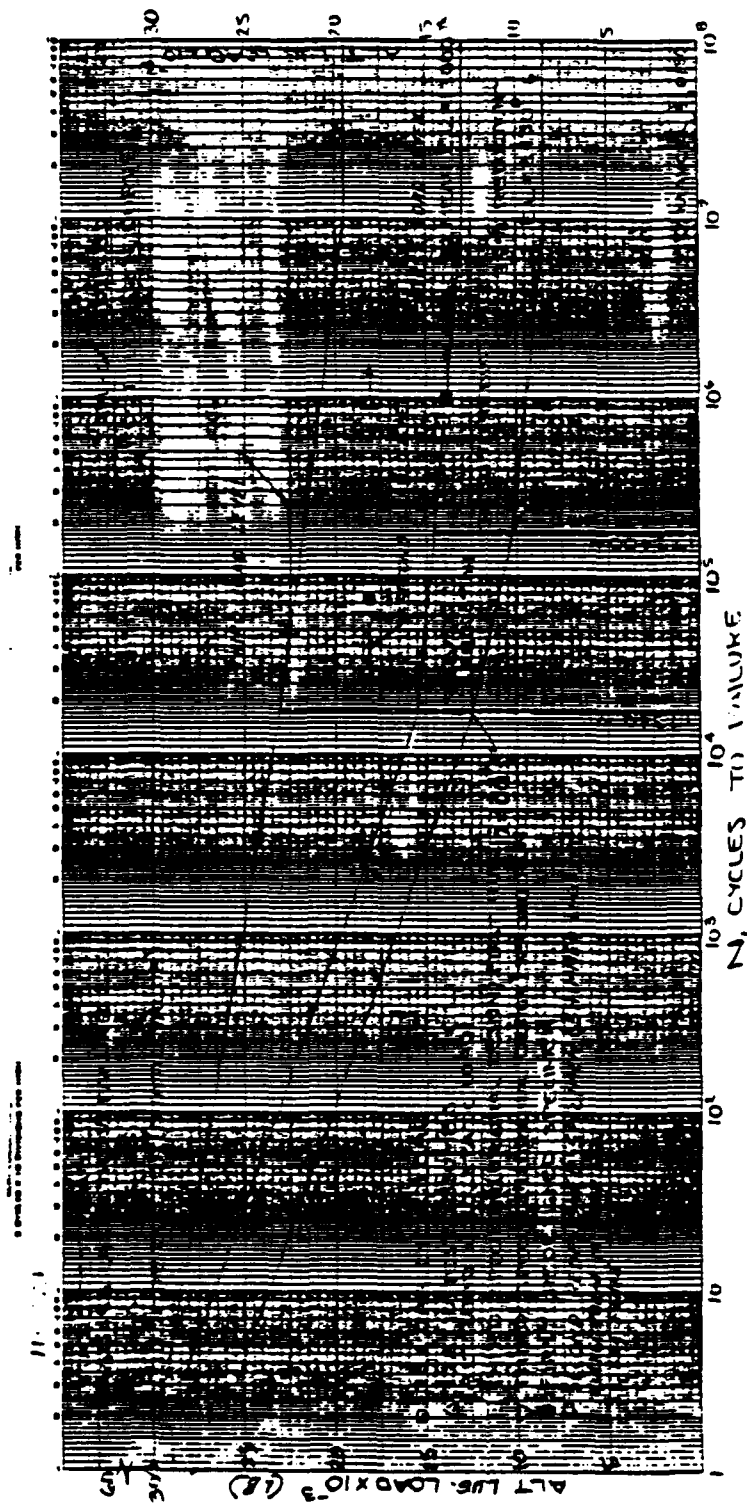
Fatigue Bending Moment Distribution, Load Level 1
Swept Tip Fatigue Test

CYCLES	STATION (IN.)	M _C	M _T
		+(1a.-1b)	+(1a.-1b)
5600	250	17013	16653
	260	4186	10680
	266.5	2670	9227
22590	250	17532	16965
	260	4069	10679
	266.5	5670	9227
29300	250	15268	16742
	260	N.A.	10679
	266.5	5670	9227

NOTE: Specimen was the original design (Kevlar inner skin). Present design has an graphite inner skin which has greater strength.

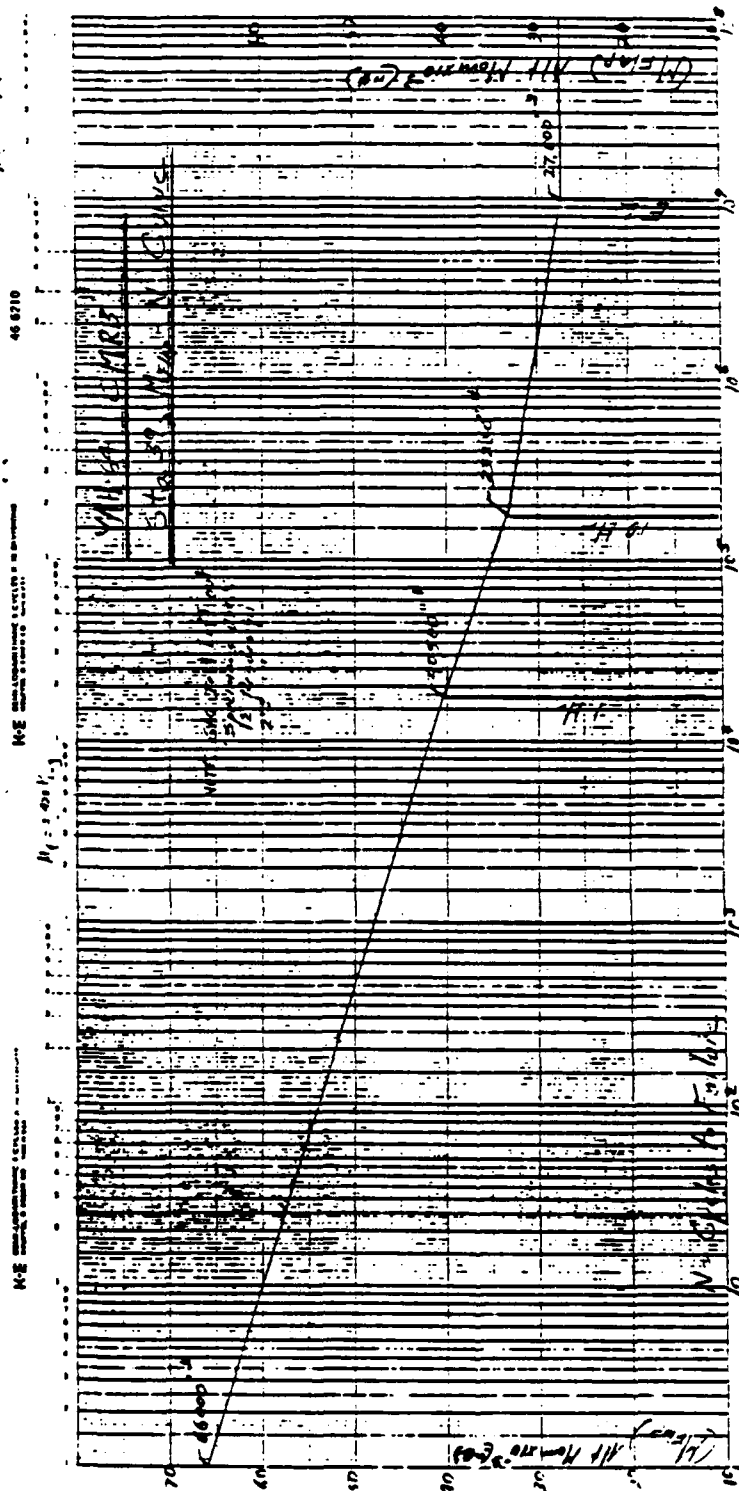
CMRB-79-006





Above data is just for added information on testing of the blade lugs.

B20.01.1
CIRS-79-006



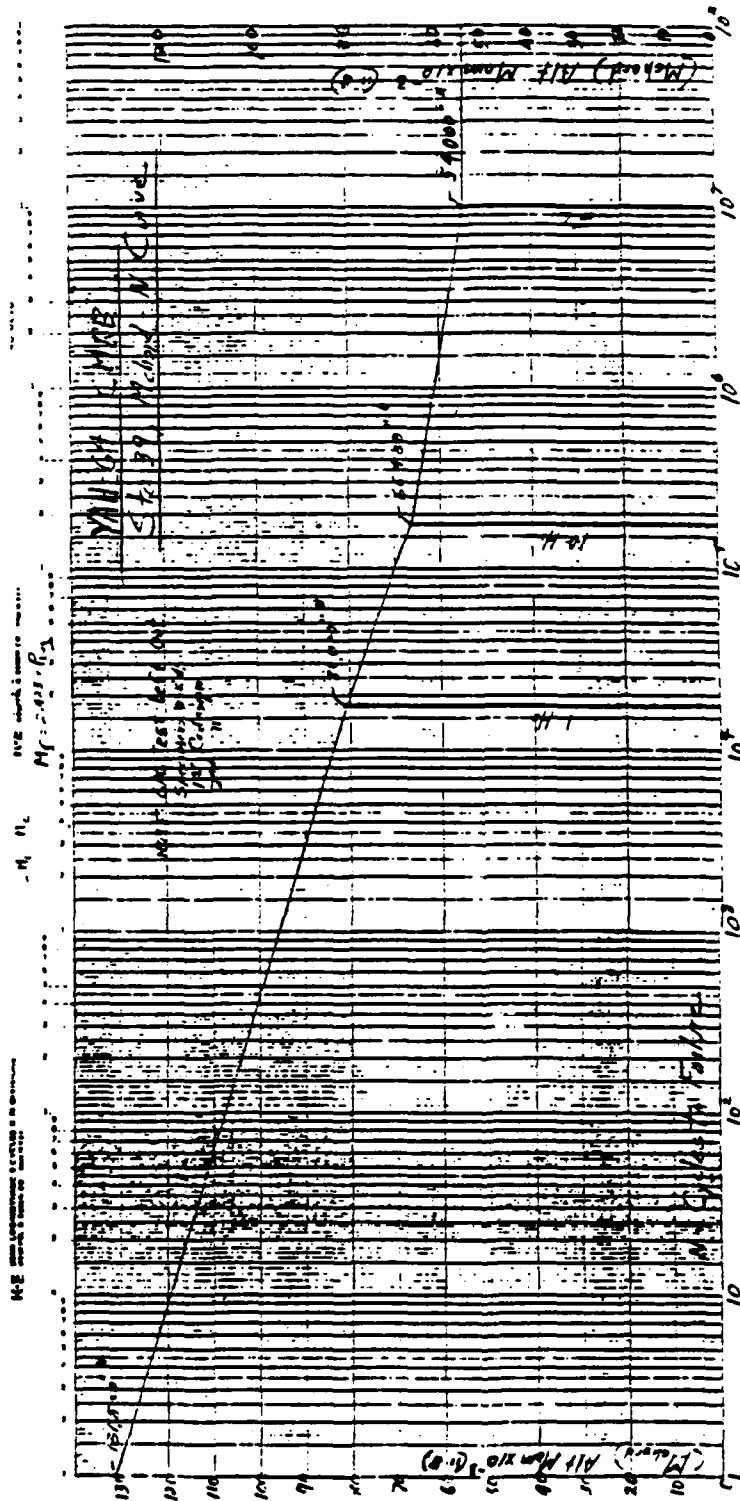
820.02
CIRB-79-006

Assumed:
at Stg 39
Then:

$$M_c = 2 M_F$$

$$P_{Lug} = \frac{M_F}{2 \times 2.08} + \frac{2 M_F}{2 \times 5.8}$$

where P_{Lug} is from Pg A20.01



B20.03
CIRB-79-006

Assumed: $M_c = 2 M_F$
at Sta 39
Then: See $P_{A20.02}$

Alt. Mon 10-20

Alt. Mon 10-20

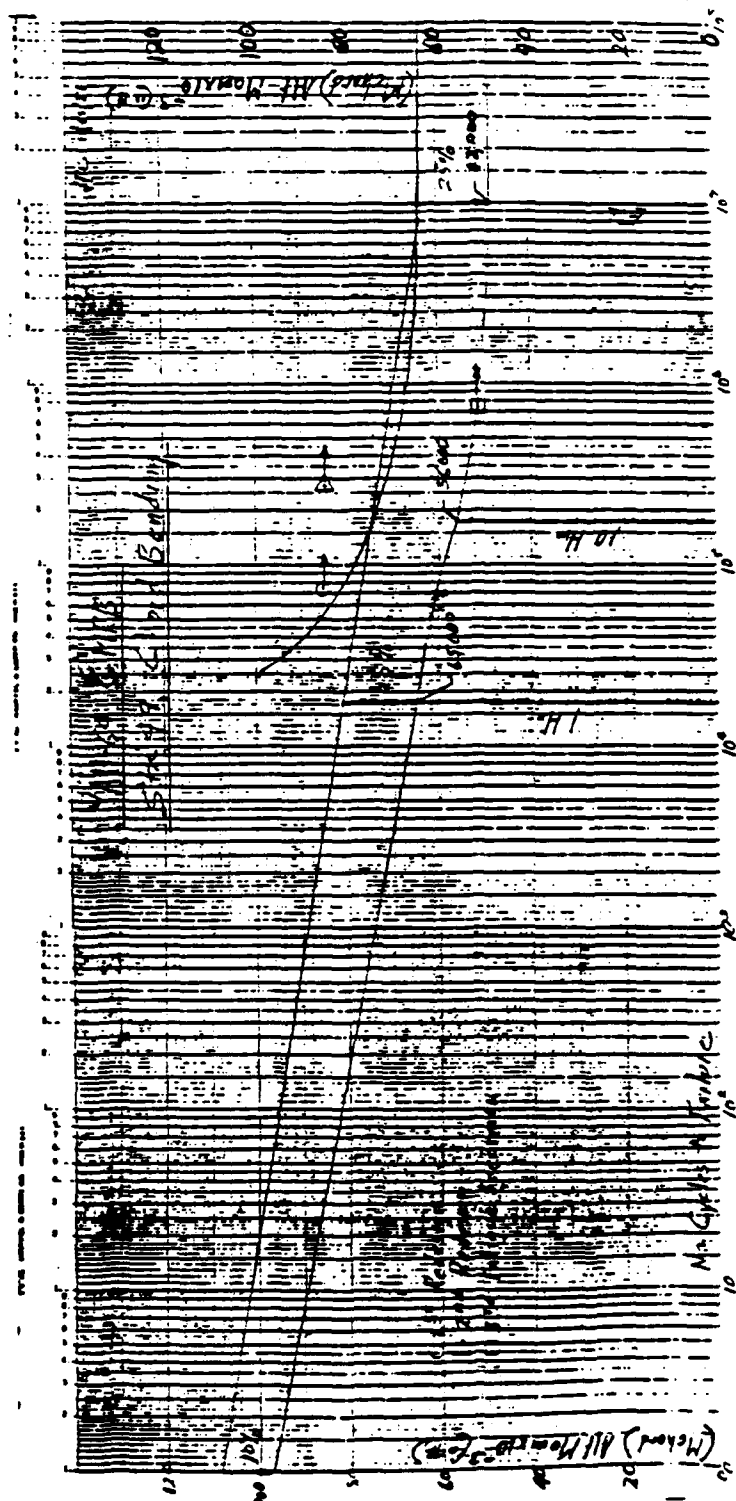
10-20

20-30

10-20

Time

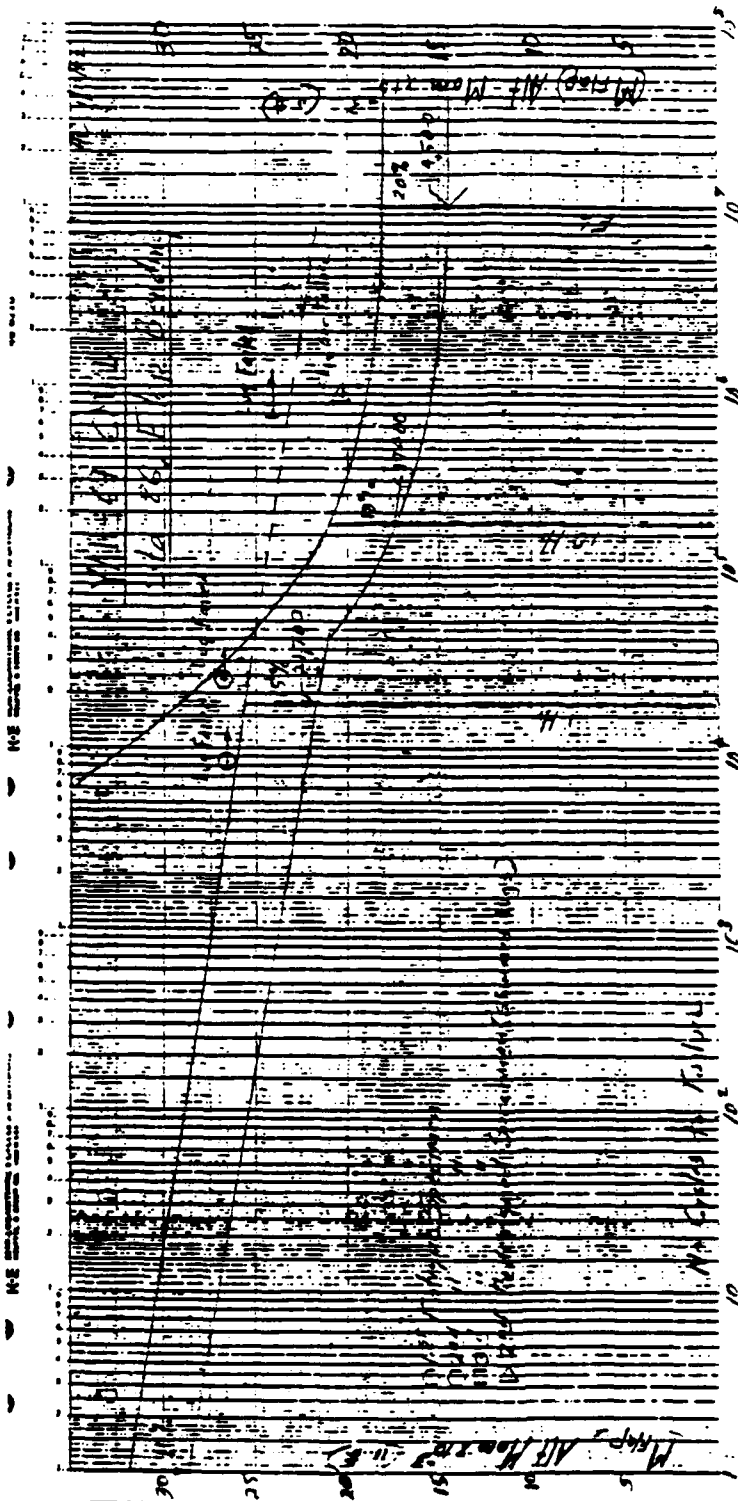
10 20 30 40 50 60 70 80 90 100

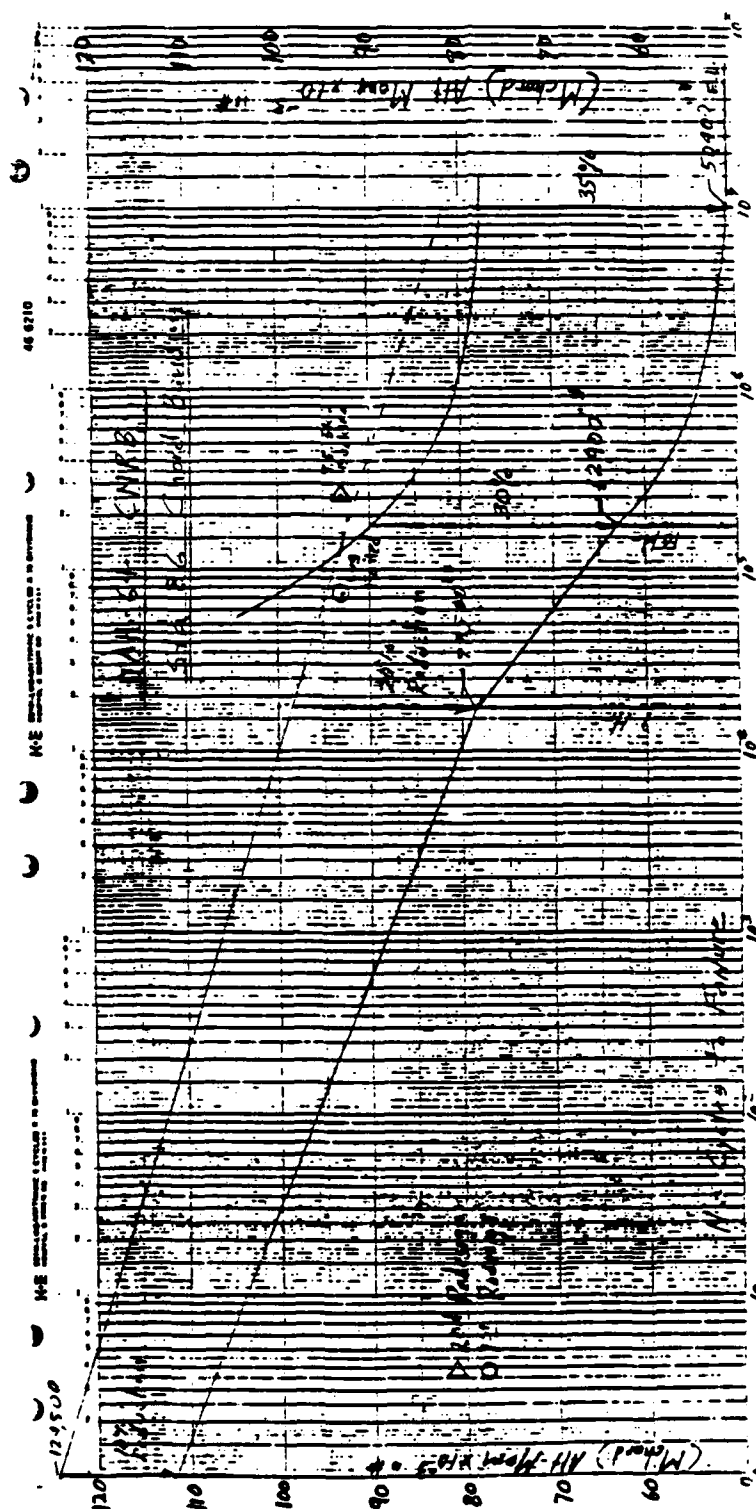


B20.05
CHRB-79-006

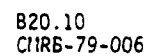
Hand-drawn graph on a grid. The vertical axis is labeled "M (lb)" and "At. Moment" with values 0, 20, 40, 60, 80, 100. The horizontal axis is labeled "At. Moment" with values 0, 10, 20, 30, 40, 50, 60, 70, 80, 90, 100. Two curves are plotted: one starting at (0,0) and rising to (100,100), and another starting at (0,0) and rising to (100,25). Handwritten text includes "M (lb)" and "At. Moment" at the top, "M (lb)" and "At. Moment" on the left, and "M (lb)" and "At. Moment" on the right.

B20.08
CIRG-79-006

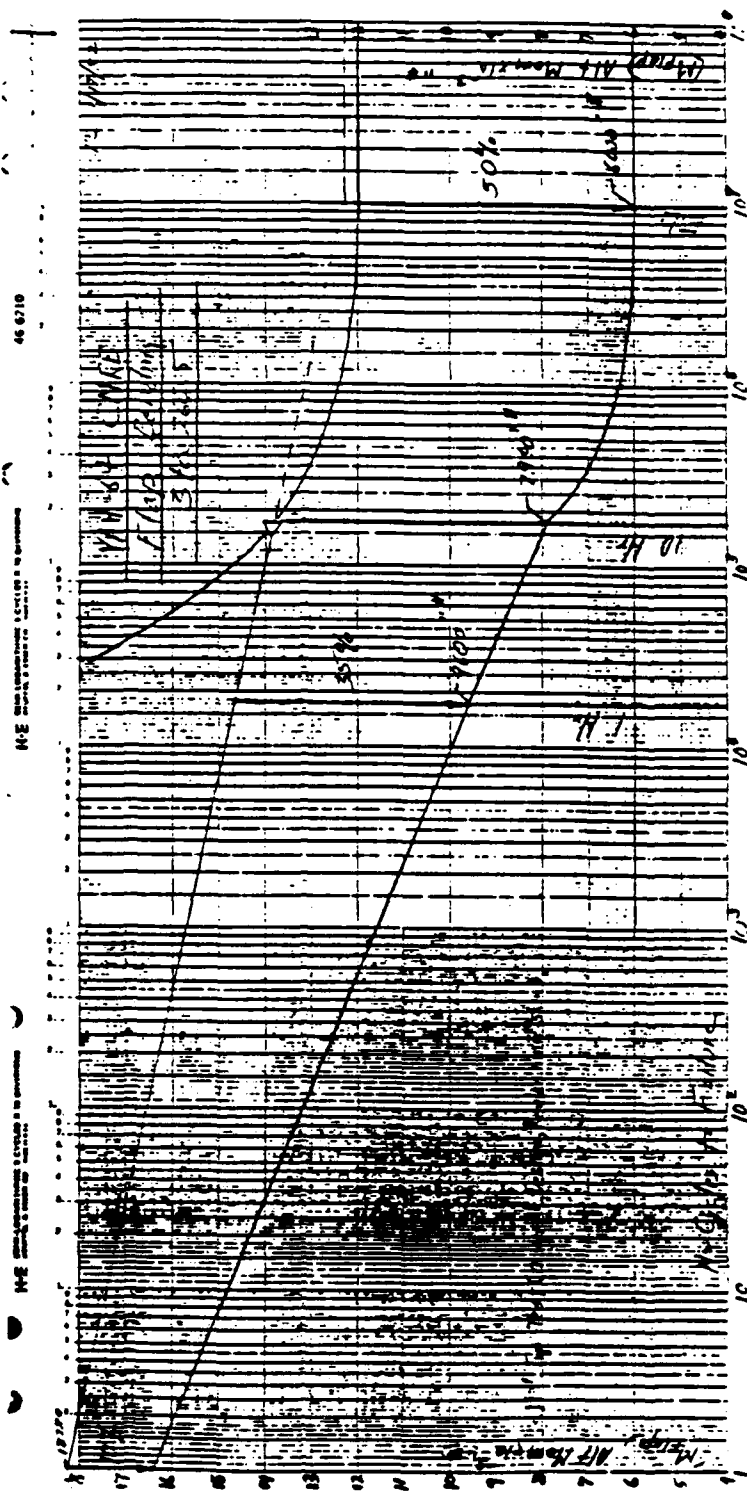




B20.09
CIRB-79-006



B20.11
CMRB-79-006



[illegible]

[illegible]

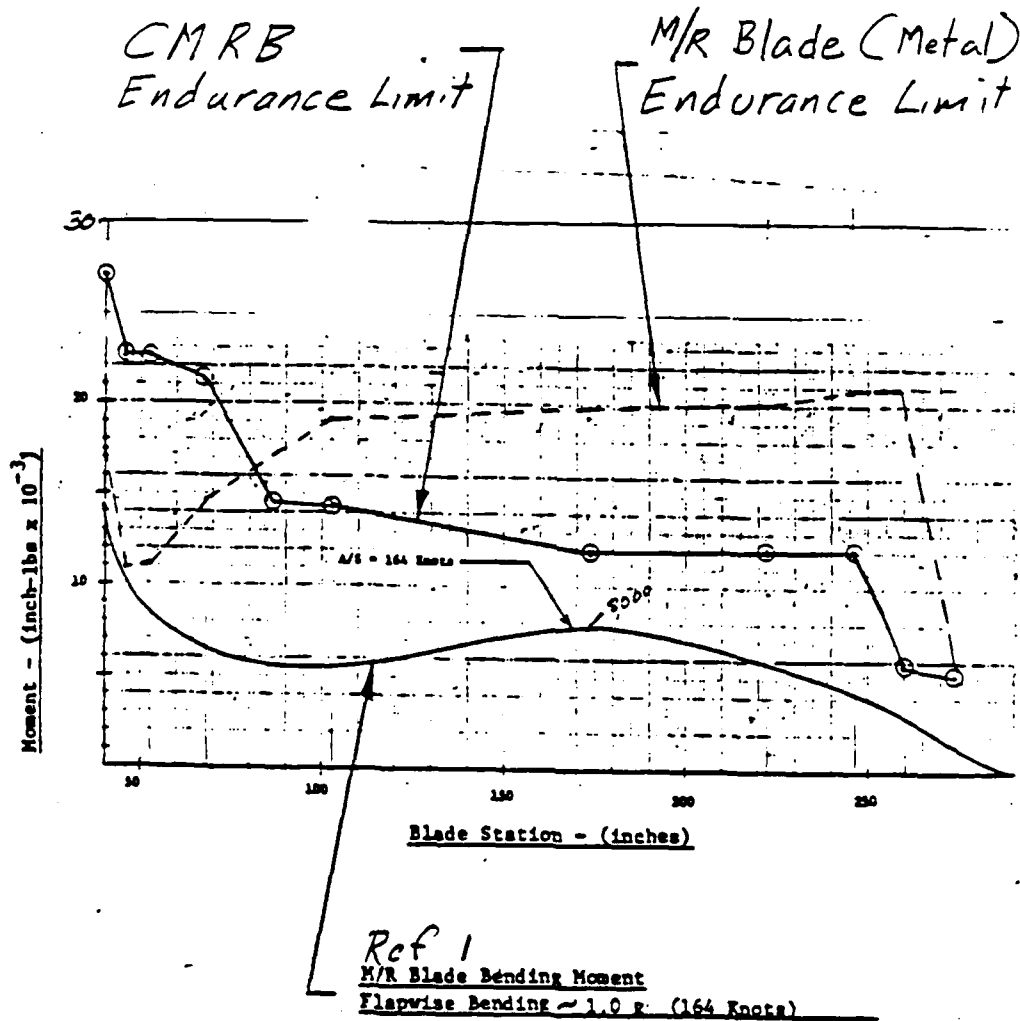
COMPARISON OF THE COMPOSITE M/R BLADE
ALLOWABLES WITH THE METAL BLADE

		Allowable Loads (Cyclic)					
		Composite Blade			Metal Blade		
Sta	Mom	Endurance Limit (n #)	10 Hour Limit (n #)	1 Hour Limit (n #)	Endurance Limit (n #)	10 Hour Limit (n #)	1 Hour Limit (n #)
39	M _f	27,000	33,200	40,500	17,435	25,800	43,580
	M _c	54,000	66,400	81,000	34,860	51,600	87,160
46	M _f	22800	28000	37200	10845	16130	27240
	M _c	48000	56000	65000	34,860	51600	87160
51.3	M _f	22800	28000	37200	11,300	12,090	19,970
	M _c	48000	56000	65,000	X	X	X
53	M _f	22800	28000	37200	X	X	X
	M _c	48000	56000	65,000	32,470	34,700	57,390
69	M _f	21200	25000	30,000	14,700	15,700	26,000
	M _c	46000	54000	60800	49,600	51,500	66,400
103	M _f	13920	16700	20,800	19,000	20,500	33,400
	M _c	50400	62,900	78,500	50,000	52,000	67,000
174	M _f	12,000	14,300	18,000	19,900	21,500	35,000
	M _c	50,400	62,900	78,500	58,100	60,400	77,800
222	M _f	12,000	14,300	18,000	20,400	22,000	35,900
	M _c	50,400	62,900	78,500	X	X	X
246	M _f	12,000	14,300	18,000	21,100	22,800	37,100
	M _c	50,400	62,900	78,500	57,000	59,300	76,400
260	M _c	6000	7900	9600	21,100	22,800	37,100
266.5	M _c	3700	4900	5800	X	X	X
274	M _f	5300	6770	8400	4090	4900	9300
	M _c				X	X	X
104.5	M _c	10,850	13,000	15,800	8000	8640	14,000

* 45° and 0° Curve shapes used
□ 0° Curve Shape used

FLAP BENDING

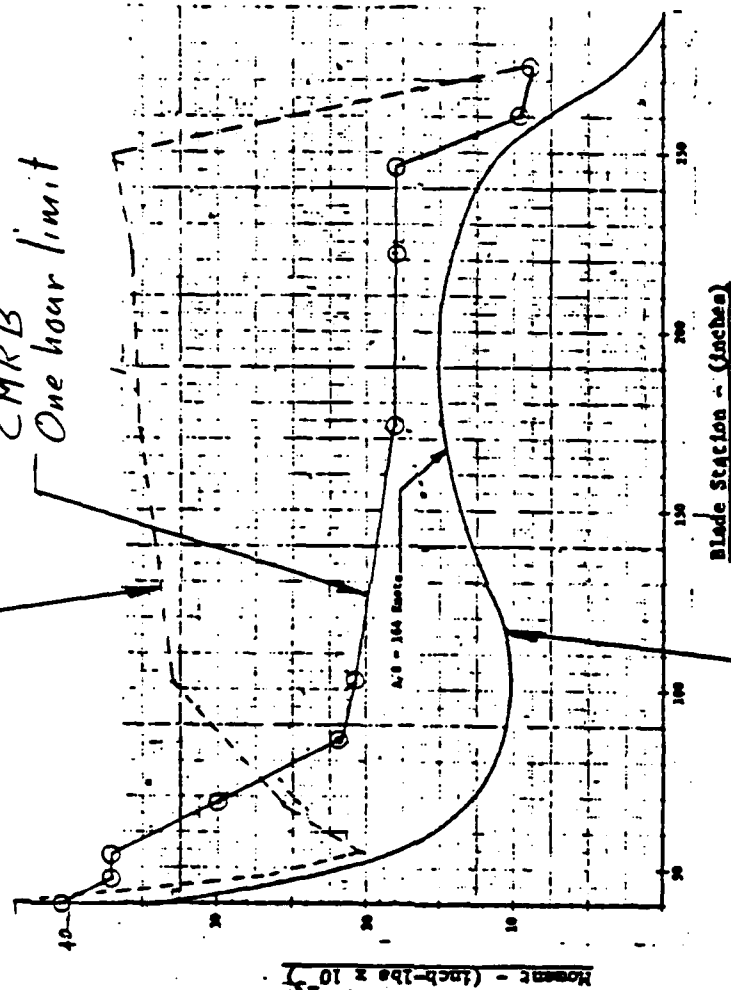
26 BLADE STA.



Flap Bending vs Blade t_a

M/R Blade (Metal)
One hour limit

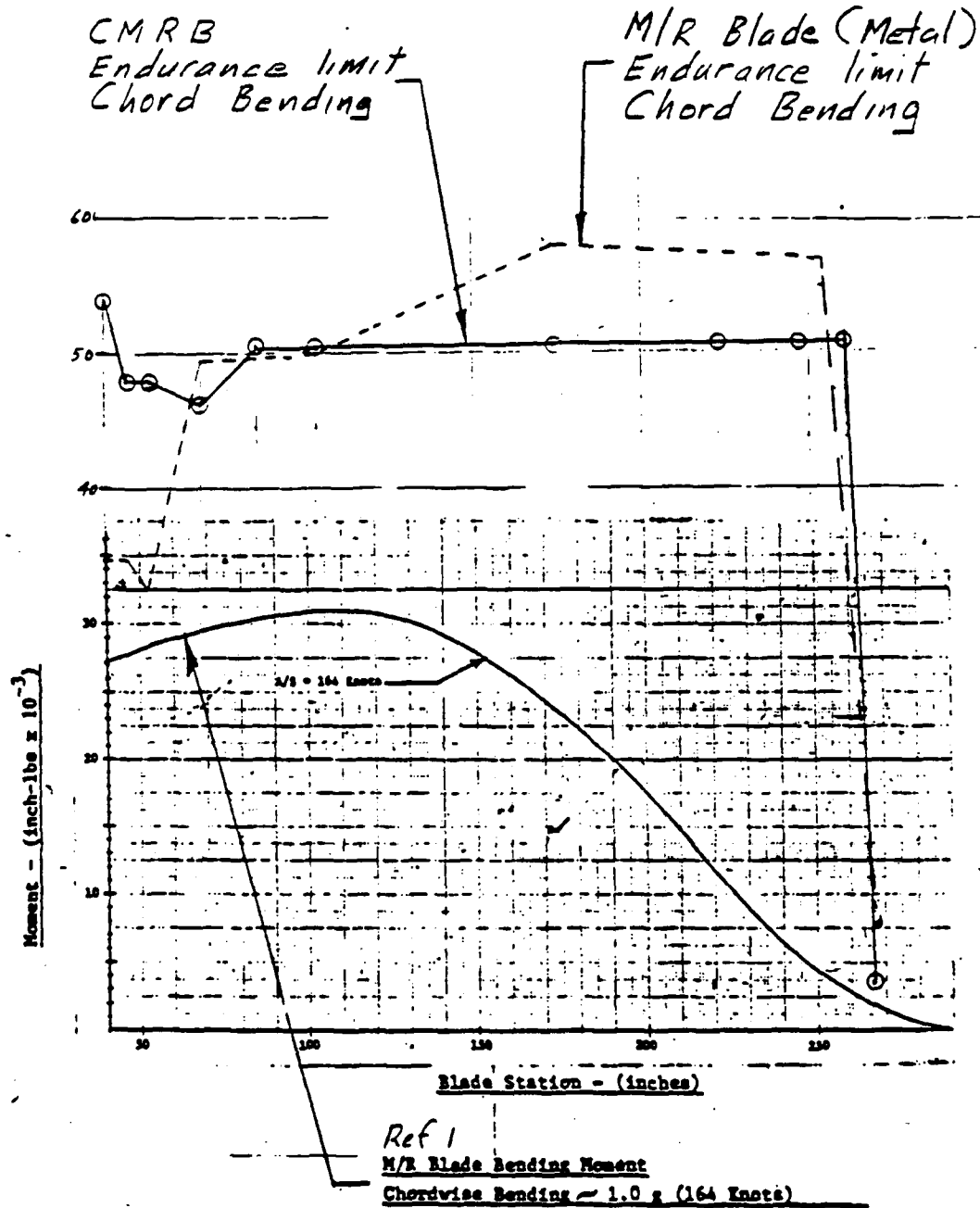
CMRB
One hour limit



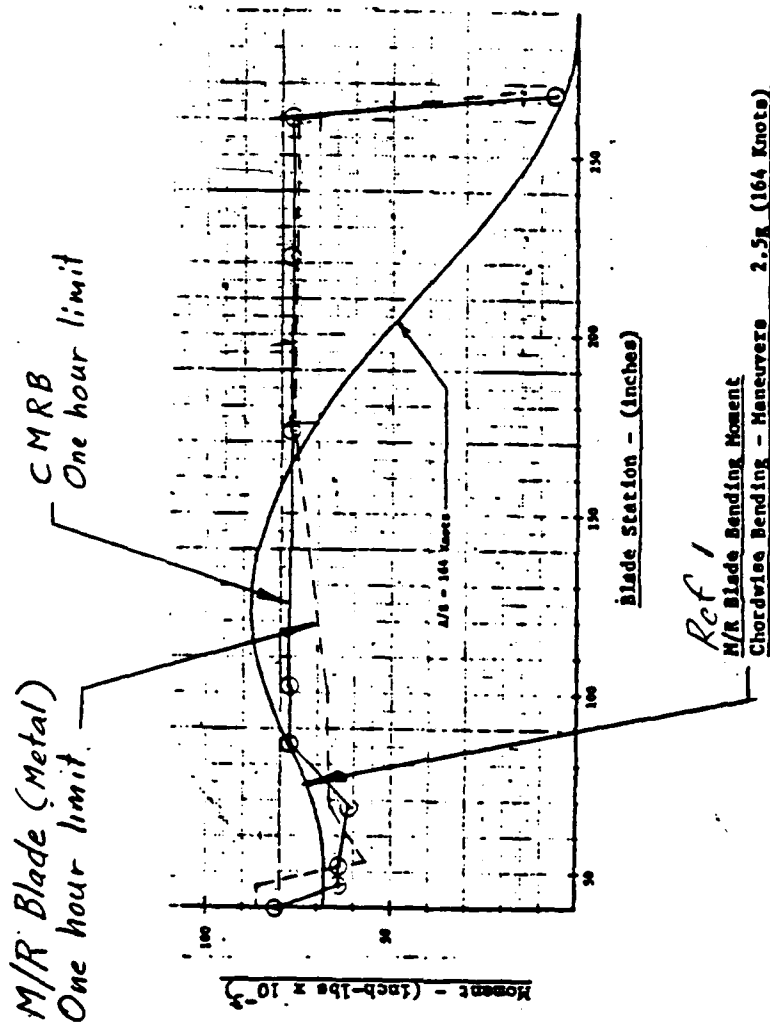
Ref 1
M/R Blade Bending Moment
Flap-line Bending - Maneuvers 2.5g (164 knots)

B40.02
CMRB-79-006

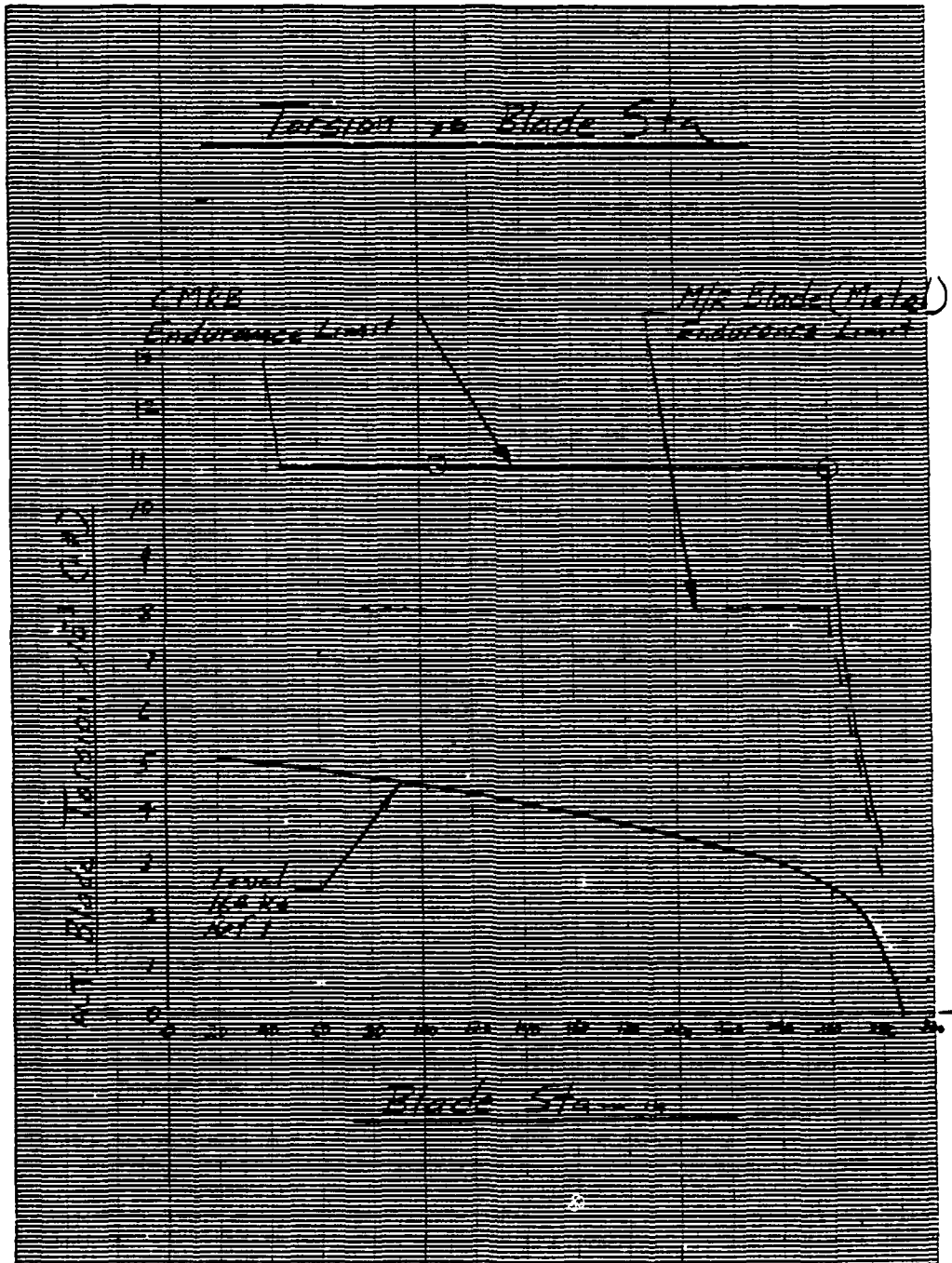
Chord Bending vs Blade Sta.

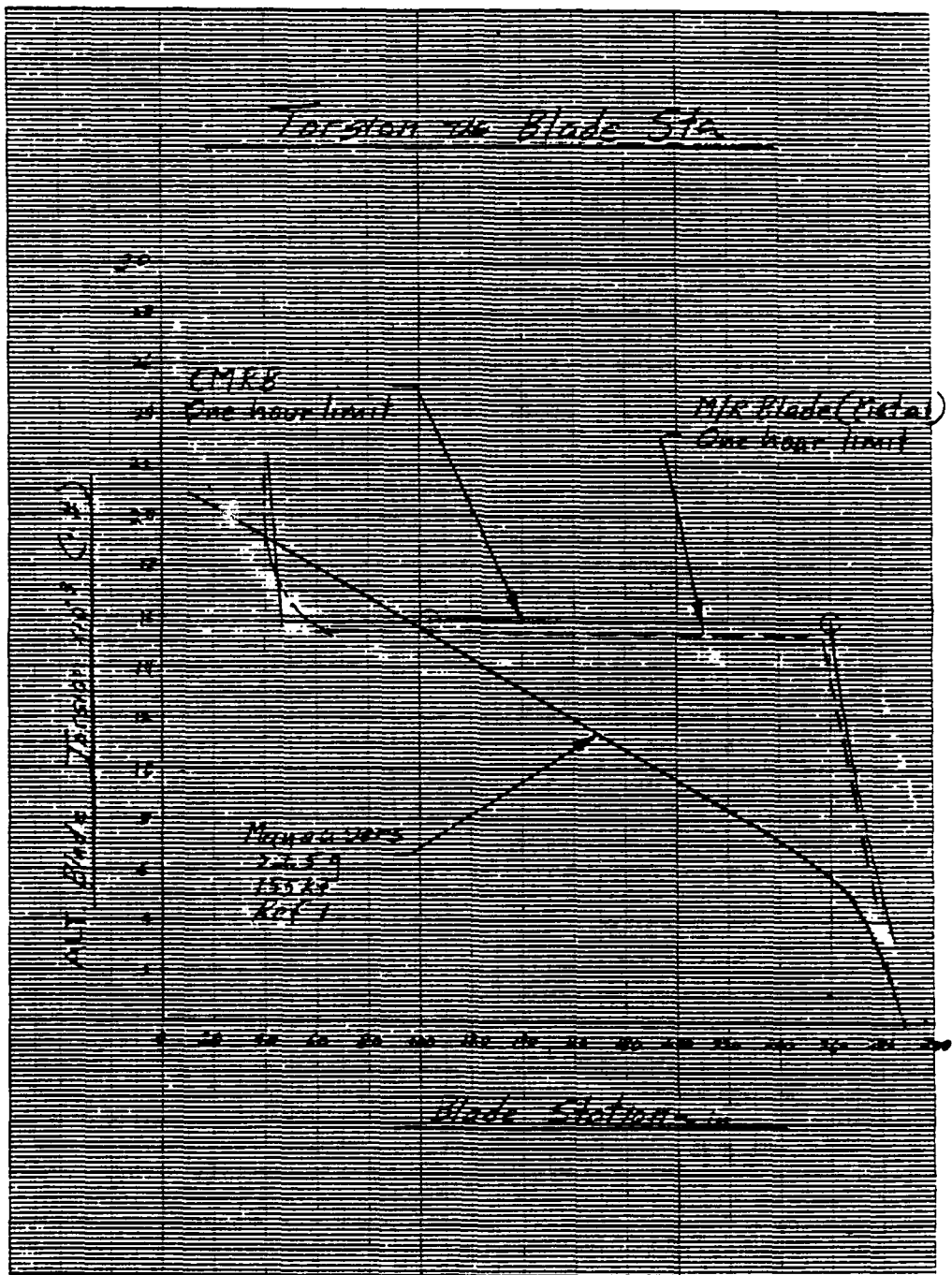


Chord Bending vs Blade Sta



B40.04
CMRB-79-006





APPENDIX C

STRUCTURAL ANALYSIS OF A BALLISTICALLY
DAMAGED COMPOSITE MAIN ROTOR
BLADE FOR THE
AH-64A HELICOPTER

REPORT TITLE Static Stress Analysis for the YAH-64 AAH CMRB		REPORT NO. CMRB-79-005
PREPARED BY D. Mancill	4-7-82	CHECKED BY
		MODEL NO. YAH-64
SUBJECT		

INTRODUCTION

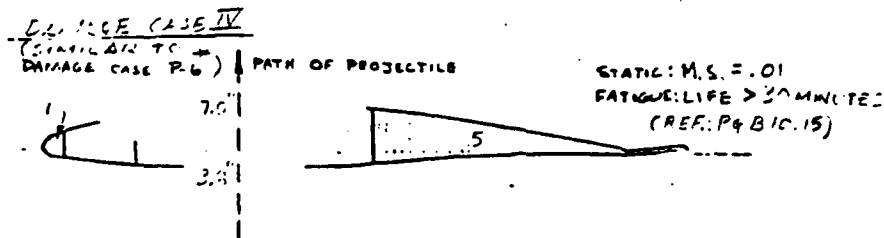
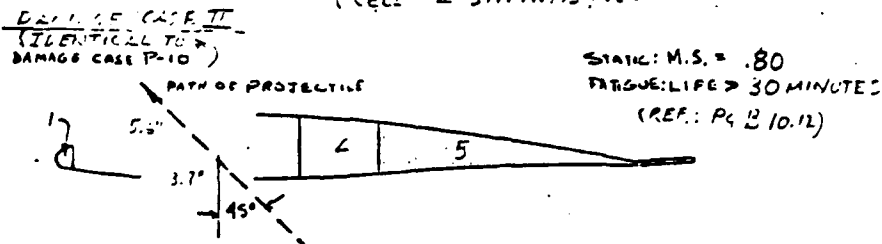
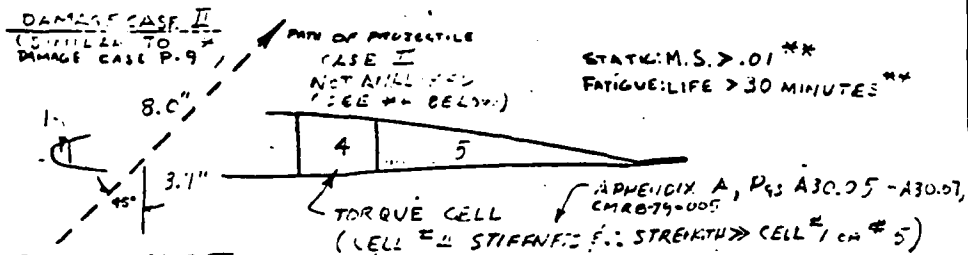
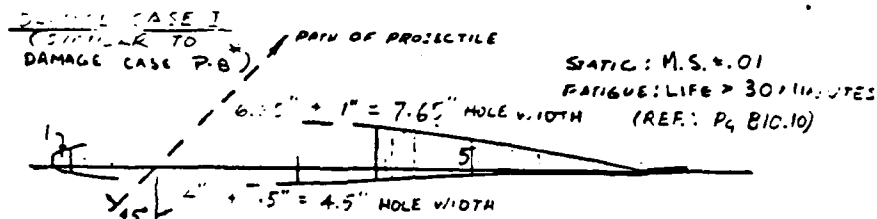
This appendix contains the structural analysis of the ballistically damaged YAH-64 CMRB.

Based on this analysis, there will be no failure at the limit vulnerability condition ($N_2 = 2.0g$, $V = 150$ kn, RPM 289). The fatigue life of the CMRB after sustaining ballistic damage is greater than 30 minutes.

The damage model is based on an impact by a 23mm high explosive incendiary (HEI) projectile. Extent of the ballistic damage is based on experience with the metal YAH-64 main rotor blade and the composite multi-tubular spar main rotor blade for the AH-1G.

REPORT TITLE STATIC STRESS ANALYSIS FOR THE YAH-64 AAH CMRE		REPORT NO. CMRB-79-005
PREPARED BY J. CRANDELL 11-15-82	CHECKED BY	MODEL NO. YAH-64
SUBJECT		

SUMMARY



- * REF: P4 5.35, HUGHES HELICOPTERS REPORT NO. 77-5-1002, STRUCTURAL ANALYSIS OF BALLISTICALLY DAMAGED MRE FOR YAH-64 AAH, 30 APR 1974.
- ** SIMILAR TO DAMAGE CASE I, BUT WITH 3 TORQUE CELLS REMAINING INSTEAD OF 2; ∴ LESS CRITICAL BY INSPECTION (NO DIFFERENTIAL BENDING).

Table C-1. Main Rotor Blade Preliminary Vulnerability Loads

$n_z = 2.0g$, $V = 150$ kn, $RPM = 289$

r (in.)	M_F (in-lb)		M_C (in-lb)		M_T (in-lb)	
	Mean	Cyclic	Mean	Cyclic	Mean	Cyclic
11.0	N.A.				-8200	15900
25.0	+3500	20200	N.A.			
34.5	+5600	27600	32000	50200		
44.5	+3900	30800	29800	52500	-8200	8500
59.5	+ 900	27100	26700	55300	-6800	8600
					-5300	8100
87.0	-2900	14700	20100	69400	-4300	8000
121.9	-4300	13200	15500	77800	-3100	7900
156.8	-5700	15800	10600	71000	-2400	8100
191.7 *	-5700	24000	6600	50900	-2200	8000
226.6	-3200	24600	3500	31400	-1900	5600
256.0	+4100	14100	640	12000	-1200	2700
273.0	+1700	8300	160	4300	- 500	1110

REF.: Table C-1, Pg. 11, Hughes Helicopters Report No. 77-5-8000-2, Apr. '81

SIGN CONVENTION:

- (+) M_F ~ COMPRESSION IN UPPER SURFACE
- (+) M_C ~ COMPRESSION IN TRAILING EDGE
- (+) M_T ~ NOSE UP

* CRITICAL STATION DUE TO THE HIGHEST COMBINATION OF MOMENTS AND TORSION, GOVERNED BY FLAPWISE BENDING.

Table C-2. Main Rotor Blade Preliminary Vulnerability Fatigue Spectrum

r (in.)	Number of Cycles	M _F (in-lb)		M _C (in-lb)		M _T (in-lb)	
		Mean	Cyclic	Mean	Cyclic	Mean	Cyclic
25	20	3500	13700	-	-	-8200	10800
	29	3500	13700	-	-	-6800	8500
	96	3500	8200	-	-	-4800	5400
	983	negl.	2800	-	-	-2900	2500
	7542	negl.	1900	-	-	-1900	1850
34.5	20	5600	18700	32000	31800	-8200	8400
	29	5600	18700	32000	29600	-6800	6600
	96	5600	11200	30000	22700	-4800	4200
	983	negl.	3700	-4000	14500	-2900	2000
	7542	negl.	2500	-4000	11600	-1900	1450
44.5	20	3900	20800	29800	41500	-7500	8600
	29	3900	20800	29800	38600	-6200	5900
	96	3900	12400	27700	29600	-4400	3700
	983	negl.	5000	-3700	14900	-2700	1000
	7542	negl.	3400	-3700	11900	-1700	700
226.55*	20	-3200	16600	3500	31400	-2100	6800
	29	-3200	16600	3500	29200	-1700	5400
	96	-3200	9900	3500	22400	-1200	3400
	983	negl.	3400	negl.	4100	-700	1600
	7542	negl.	2300	negl.	3300	-500	1200

REF: Table A-10, Hughes Helicopters Report No. 77-5-8000-2, April 1981

NUMBER OF LOAD CYCLES FOR 30 MINUTES FOR
ONCE/REVOLUTION OCCURRENCE:

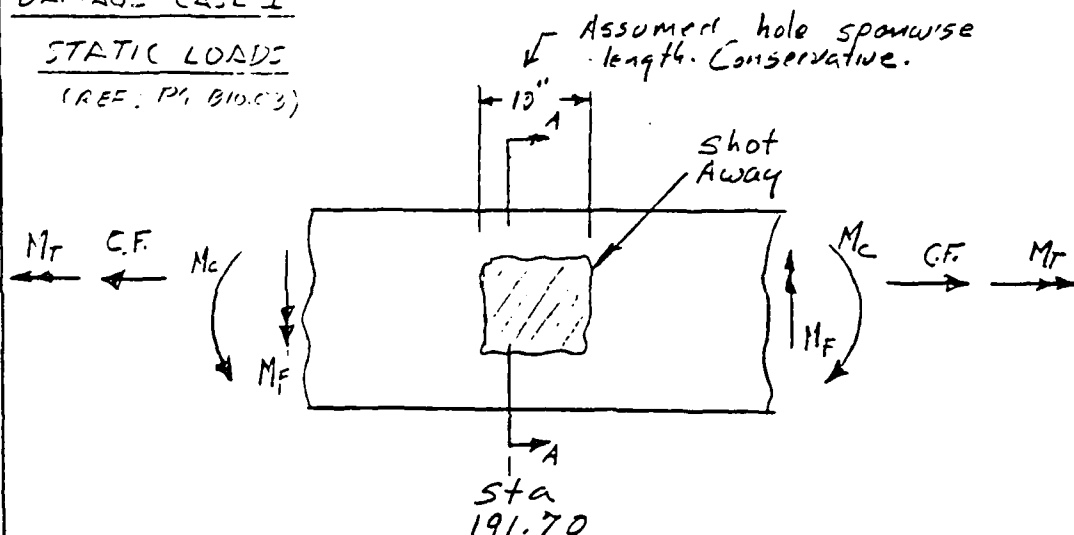
$$N = 30 \times 289 = 8670 \text{ CYCLES}$$

* CRITICAL STATION FOR MAXIMUM LOADING AT CONSTANT
SPEEDS OF STA. 870.

REPORT TITLE		REPORT NO. CMRB-79-005
PREPARED BY MZ	4/12/83	CHECKED BY
SUBJECT CMRB Ballistic Ana		MODEL NO. YAH-64

DAMAGE CASE ISTATIC LOADS

(REF: PG B10.03)



$$M_F = (-5700 \pm 24,000) \cdot 0.8^* = -4560 \pm 19,200$$

$$M_C = 6600 \pm 50,900$$

$$M_T = -2200 \pm 8,000$$

AND

$$CF = 36,000^{\#} \text{ FOR } 285 \text{ RPM (REF: PG 20.01)}$$

* Testing of ballistically damaged rotor blades at Hughes indicates that the damage area acts like a partial elastic hinge which will reduce the flapwise moment by 20%. This is shown on pg 9 of the following ref:

Paper No. 12

Damage Tolerant Design of the YAH-64 Main Rotor Blade

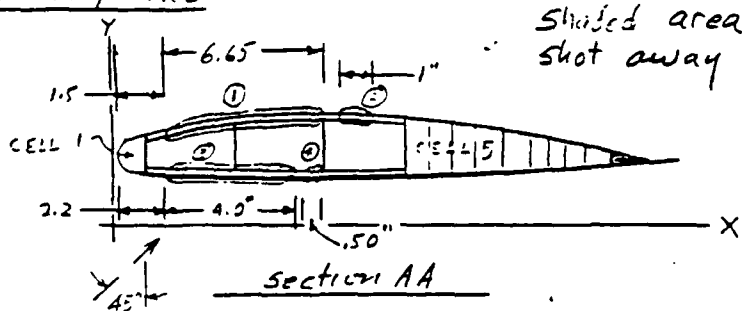
Malcolm F. Symonds
Chief, Rotor Analysis

Hughes Helicopters
Division of Summa Corporation
Culver City, California

Presented at the AHS/Ames Conference on Helicopter Structures Technology, Nov. 16-18, 1977.

REPORT TITLE		REPORT NO.
PREPARED BY APC		CMRB-79-005
4/9/82		CHECKED BY
SUBJECT CMRB Ballistic Aug.		MODEL NO. YAH-69

Section Properties (DAMAGE CASE I)



* Ref AppA CMRB-79-505 P. A20.02

	EA	X	Y	EAX	EAY	EI _{xx}	EAY	EAY ²	EI _{xy}
Basic Section*	34.39	5.09	1.491	173.32	275.56	983.5	51.27	76.45	12.7
①	-6.17	4.33	2.43	-30.54	-145.1	-23.17	-14.49	-36.43	-2.02
②	-9.361	9.8	2.553	-9.17	-90.0	-1.08	-2.39	-6.10	0
③	-3.83	4.272	.772	-16.2	-68.6	-5.2	-2.96	-2.28	-.014
④	-.468	7.04	.747	-3.29	-23.2	-9.8	-.35	-.261	0
	22.99			114.6	546.7	945.3	30.58	31.38	12.48

$$\bar{X} = \frac{114.6}{22.99} = 5.0''$$

$$\bar{Y} = \frac{30.58}{22.99} = 1.33''$$

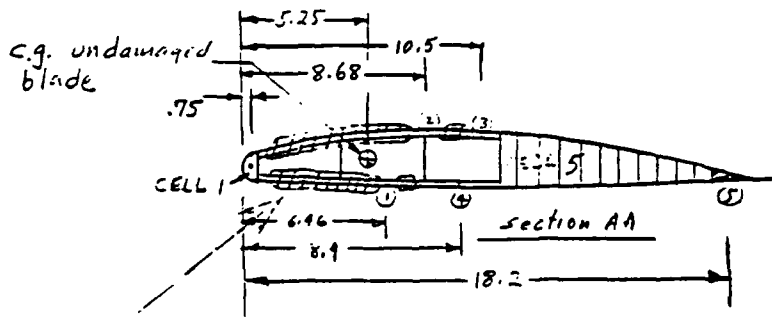
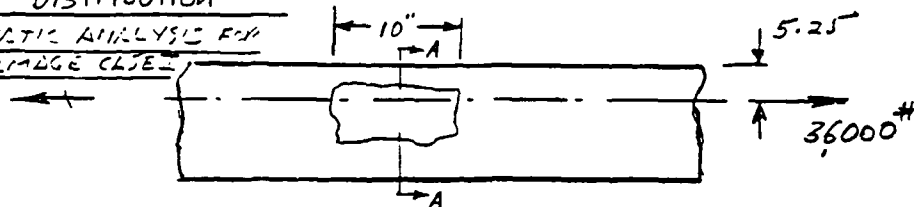
$$EI_x = 12.48 + 31.38 - 1.33 \times 50.58 = 3.2 \text{ LB-IN}^2$$

$$EI_y = 546.7 + 945.3 - 5.0 \times 114.6 = 919 \text{ LB-IN}^2$$

REPORT TITLE		REPORT NO.
PREPARED BY APC		C MRB-79-005
4/12/82	CHECKED BY	MODEL NO.
SUBJECT		YAH-64
CMPB Ballistic Ang.		

C.F. Distribution

STATIC ANALYSIS FOR
DAMAGE CASE



Cell		EA	X	EAx
1	.6 x .185 x 5.06	.562	6.46	3.63
2	1.15 x .185 x 5.06	1.08	8.68	9.40
3	.2 x .185 x 5.06	.187	10.5	1.97
4	3.2 x .185 x 5.06	3.0	8.9	26.66
5	.11 x 17.25	1.9	18.2	34.5
		6.7		76.13

$$x = \frac{76.13}{6.7} = 11.36$$

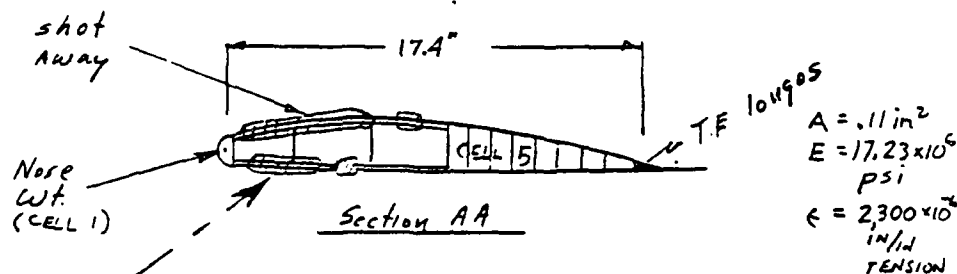
In the damaged area the c.f. distributes to the fwd and aft portion of the remaining structure as follows:

$$C.F. \text{ aft section} = \frac{5.25 - .75}{11.4 - .75} \times 36,000 = 15,200\#$$

$$\text{Strain on aft portion of remaining structure} = \frac{15,200}{6.7} = 2300 \text{ u/in. Ten. due to C.F.}$$

REPORT TITLE		REPORT NO.
PREPARED BY LPC		CMRB-79-005
4/12/82	CHECKED BY	MODEL NO.
SUBJECT CMRB Ballistic Area		YAH-64

Resistance of M_c (DAMAGE CASE I)



$$M_c = 6,600 \pm 50,900 = 57,500''^\# \text{ Com. in T.E. longos; Ten Nose wt.}$$

Assuming M_c is resisted as a couple load at the Nose wt and T.E. longos:

$$\text{Com. load in } T.E. \text{ longos } = \frac{57,500}{17.4} = 3,304''^\#$$

$$\text{C.F. load resisted by the T.E. longos } = .11 \times 2,300 \times 17.23 = 4,359''^\# \text{ Ten load.}$$

Ref CMRB 79-005 App. A, P. A51.05

$$\text{Column load that the T.E. longos can resist } = 16,900 \times .11 = 1,859''^\# \text{ Allowable compression load.}$$

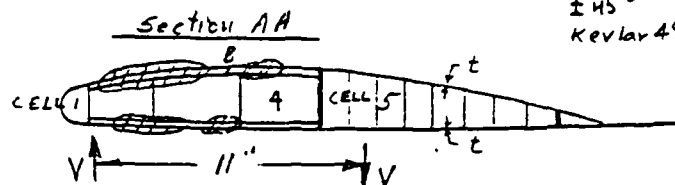
$$MS = \frac{4,359 + 1,859}{3,304} - 1 = .88$$

Above M.S. shows that the damaged blade will resist chordwise bending.

REPORT TITLE		REPORT NO. CMRB-79-005
PREPARED BY M/C	4/9/82	CHECKED BY
SUBJECT CMRB Ballistic Anal.		MODEL NO. YAH-64

Torque resisted by cell *5 (DAMAGE CASE I)

$t = .030"$
 $\pm 45^\circ$
Kevlar 49/Epoxy



"8" resisted }
by 5kmi } = $15,600 \times .030 = 468 \text{ #/in}$

$$q = \frac{T}{2A}$$

Allowable
Shear for
Kevlar/Epoxy

Appendix A P. A30.05 CMRB-79-005

$$T = 468 \times 2 \times 7.02$$

$$= 6,570 \text{ #}$$

Remaining torque is resisted as a couple as shown
where:

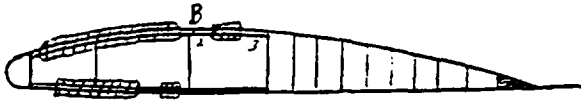
$$V = \frac{8000 + 2200 - 6,570}{11} = 330 \text{ #}$$

Remaining torque is resisted as differential banding. See
analysis for point "B" shown above.

* CELL 1 CONSERVATIVELY NEGLECTED (CONTRIBUTION SMALL).

REPORT TITLE		REPORT NO. CMRB-79-005
PREPARED BY LPC	4/12/82	CHECKED BY
SUBJECT CMRB Ballistic Ana		MODEL NO. YAH-64

Resistance of M_F , M_r and C.F. (DAMAGE CASE I)
Point "B" critical



$M_F = -4,560 \pm 17,200 = 14,640 \text{ " #}$ com. upper surface.

Mom at edge of damaged area due to differential bending $\} = \frac{10}{2} \times 330 = 1,650 \text{ " #}$
 (Damaged area length)

Strain at "B" $\} = 2,300 - \frac{1,650}{1.8 \times (1.27)} - \frac{14,640 \times 1.17}{3.2}$
 (Due to CF) (Distance between caps) (cap area)

$= 3,700 \mu \text{ " / in. com.}$
 (REF: Pg B10.15)

Ref stress strain curve (Pg B10.15)

$M_S = \frac{3,750}{3,700} - 1 = .01$

Above M_S shows damaged area of blade will resist M_F .

REPORT TITLE		REPORT NO.
PREPARED BY	CHECKED BY	CMRB-79-005
JC	4/15/82	MODEL NO. YAH-64
SUBJECT CMRB BALLISTIC ANA		

DIVISION CASE IFATIGUE ANALYSIS AT STA. 226.57 (SAME X-SECT. AS AT STA 191.7)

$$C.F. = 36,000 \text{ LB. @ } 209 \text{ RPM}$$

$$M_E = (-3,200 \pm 16,600) \times .8^* = -2,560 \pm 13,280 \text{ IN-LB}$$

$$M_C = 3,500 \pm 31,400 \text{ IN-LB (FATIGUE LOAD REF.: PG. B10.04)}$$

$$M_T = -2,100 \pm 6,800 \text{ IN-LB} \Rightarrow 0 \pm 2330 \text{ IN-LB}^{**}$$

VERY CONSERVATIVELY LET $N = 8670$ CYCLES; THEN:

$$F = \frac{-(-2,560 \pm 13,280) \cdot 1.17}{3.2} - \left(\frac{\pm 2330 \times 10}{11 \times 2} \right) / 1.8 \times 1.27 + 2,300 @ \text{PT. B}$$

$$= 936 \pm 4,856 \pm 463 + 2,300$$

$$= 3,236 \pm 5,319 \text{ IN-LB}$$

$$E = 10.66 \times 10^6 \text{ PSI FOR KEVLAR/EPXY LAMINATES}$$

$$F = FE = 34,500 \pm 56,700 \text{ PSI}$$

$$= 91,200 \text{ PSI (TENS.)}, -22,200 \text{ PSI (COMPR.)}$$

$$F_{T_u}' = 165,000 \text{ PSI (PG. B10.13 OR B10.17)}$$

$$F_{C_u}' = 31,980 \text{ PSI (PG. B10.13)}$$

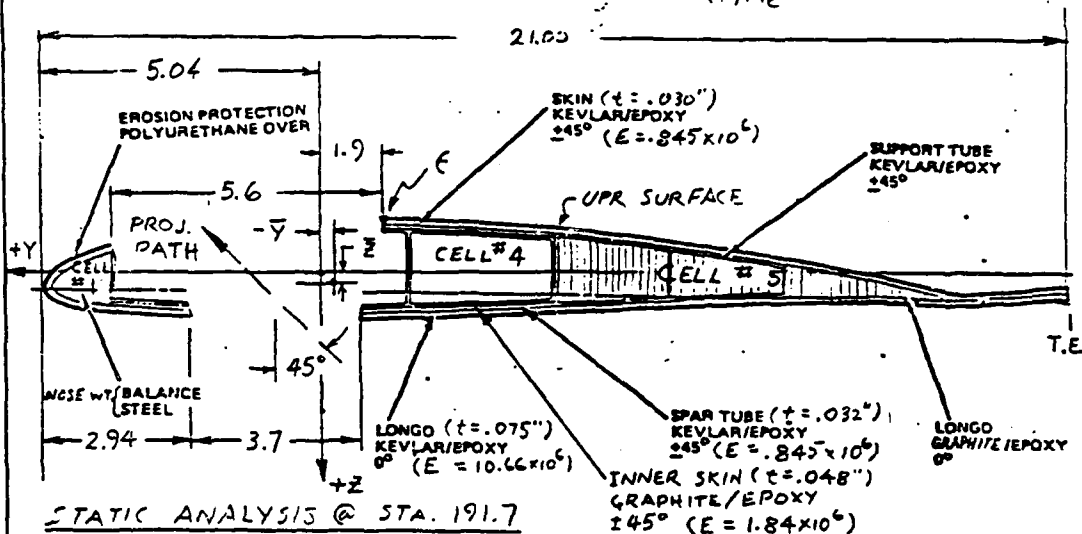
$$\left. \begin{aligned} \text{TENS. A.S.} &= \frac{165,000}{91,200} - 1 = \underline{\underline{.75}} \\ \text{COMPR. A.S.} &= \frac{31,980}{-22,200} - 1 = \underline{\underline{.44}} \end{aligned} \right\} > \text{STATIC A.S.} = .01$$

THEREFORE, BY INSPECTION, LIFE AFTER IMPLCT IS
MUCH GREATER THAN 30 MINUTES & LESS CRITICAL
THAN FOR THE STATIC CRD. (PG. B10.10).

* CELL 5 RESISTS 6,510 IN-LB (PG. B10.09).

* SEE PG. B10.15.

REPORT TITLE STATIC STRESS ANALYSIS FOR THE YAH-64 AAH CMRB		REPORT NO. CMRB-79-005
PREPARED BY J.L. CRANDELL	CHECKED BY	MODEL NO. YAH-64
SUBJECT VULNERABILITY ANALYSIS OF CMRB BLADE		

DAMAGE CASE III(+) M_F ~ COMPR. UPR SURFACE(+) M_C ~ COMPR. IN T.E.STATIC ANALYSIS @ STA. 191.7

C.F. = 36,000 LB. FOR 289 RPM

 $M_F = -5,700 \pm 24,000$ IN-LB $M_C = 6,600 \pm 50,900$ IN-LB @ $\frac{1}{4}$ CHORD $M_T = -2,200 \pm 8,000$ IN-LB $\bar{E}A = 25.65 \times 10^6$ LB, $\bar{E} = 5.08 \times 10^6$ $\bar{E}I_F = 6.46 \times 10^6$ LB-IN² $\bar{E}I_C = 963.05 \times 10^6$ LB-IN² $\bar{E} = .09$ IN, $-1.18 - \bar{E} = -1.27$ INMOMENTS FOR MAX. COMPR. STRAIN, ϵ , ARE: $\bar{Y} = -.22$ IN, $5.04 - \bar{Y} = 5.26$ IN. $M'_F = (.8)^* (M_F + C.F. \times \bar{E}) = .8 \times [-5,700 + 24,000 + 36,000 \times .09] = 17,232$ IN-LB $M'_C = M_C + [(5.04 - \bar{Y}) - \frac{21.00}{4}] \times C.F. = (6,600 + 50,900) + .01 \times C.F. = 57,860$ IN-LBRESULTING STRAIN IS (ALL OF M_T MAINLY REACTED BY STIFF, STRONG CELL #4):

$$\epsilon = \epsilon_F + \epsilon_C + \epsilon_{CF} = \frac{M'_F \times (-1.18 - \bar{E})}{\bar{E}I_F} + \frac{M'_C \times (-1.9 - \bar{Y})}{\bar{E}I_C} + \frac{C.F.}{\bar{E}A}$$

$$= \frac{17,232 \times -1.27}{6.46} + \frac{57,860 \times -1.68}{963.05} + \frac{36,000}{25.65} = -2,085 \mu\text{-IN/IN (COMPR.)}$$

$$\epsilon_{ALL} = 3,750 \mu\text{-IN/IN (PG B10.16)} \quad \& \quad \text{STATIC M.S.} = \frac{\epsilon_{ALL}}{|\epsilon|} - 1 = \frac{3750}{2085} - 1 = .80$$

ABOVE A.I.S. SHOWS DAMAGED AREA OF BLADE WILL RESIST THE APPLIED LOADS.

* SEE "*" ON PAGE B10.05.

FORM 8704 (REV 4/77)



REPORT TITLE STATIC STRESS ANALYSIS FOR THE YAH-64 ACH CMRB		REPORT NO. CMRB-79-005
PREPARED BY J.L. CRANDELL	CHECKED BY	MODEL NO. YAH-64
SUBJECT VULNERABILITY ANALYSIS OF CMRB BLADE		

FATIGUE ANALYSIS @ STA 226.55 (SAME X-SECT. AS @ STA 191.7)
(DAMAGE CASE III)

C.F. = 36,000 LB. @ 287 RPM (FATIGUE LOAD REF.: PG B10.04)

$$M_R = -3,200 \pm 16,600 \text{ IN-LB}$$

$$M_C = 3,500 \pm 31,400 \text{ IN-LB}$$

$$M_T = -2,100 \pm 6,800 \text{ IN-LB}$$

CONSERVATIVELY LET
 $N = 8670$ CYCLES
FOR 30 MINUTES

$$M_R' = .8 \times [(-3,200 + 36,000 \times .09) \pm 16,600] = 40 \pm 13,280 \text{ IN-LB}$$

$$M_C' = (3,500 \pm 31,400) + .01 \times \text{C.F.} = 3,860 \pm 31,400 \text{ IN-LB}$$

$$f = \frac{(40 \pm 13,280)(-1.27)}{6.46} + \frac{(3,860 \pm 31,400)(-1.68)}{963.05} + \frac{36,000}{25.65}$$

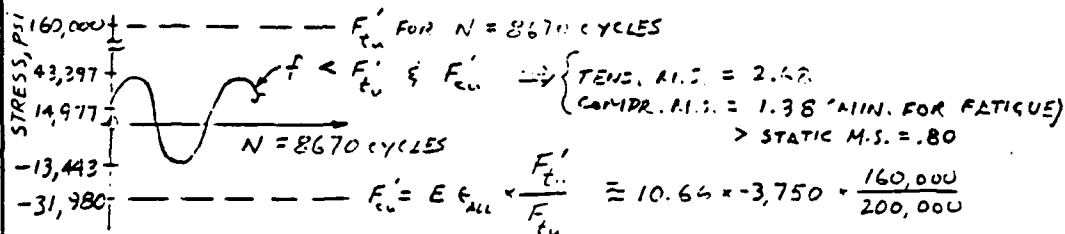
$$= (0 \pm 2,611) + (-7 \pm 55) + 1,404$$

$$= 1,405 \pm 2,616 \text{ } \mu\text{-IN/IN}^*$$

$E = 10.66 \times 10^6$ PSI FOR KEVLAR49/EPOXY LONGOS

$$f = \epsilon E = 14,977 \pm 28,420 \text{ } \mu\text{IN/IN} = 43,397 \text{ } \mu\text{IN/IN (TENS.)} / -13,443 \text{ } \mu\text{IN/IN (COMPR.)}$$

GRAPHICALLY f IS COMPARED WITH ALLOWABLES FOR $N=8670$ CYCLES
AS FOLLOWS:



THEREFORE, BY INSPECTION, LIFE AFTER IMPACT IS MUCH GREATER THAN 30 MINUTES & LESS CRITICAL THAN FOR THE STATIC COND. (PG B10.12).

* 10^{-6} IN/IN.

** SEE D-D-T DATA CURVE ON PG B10.17

REPORT TITLE		REPORT NO. CMRB-77-005
PREPARED BY JC	4/15/82	CHECKED BY
SUBJECT CMRB BALLISTIC ANA.		MODEL NO. YAH-64

DAMAGE CASE IVSTATIC LOADS:

$$M_F = .8 \cdot (-5,700 \pm 24,000) = -4,560 \pm 19,200$$

$$M_C = 6,600 \pm 5,090$$

$$C.F. = 36,000 \# \text{ FOR } 289 \text{ RPM}$$

$$M_T = -2,200 \pm 8,000$$

SECT. PROP.

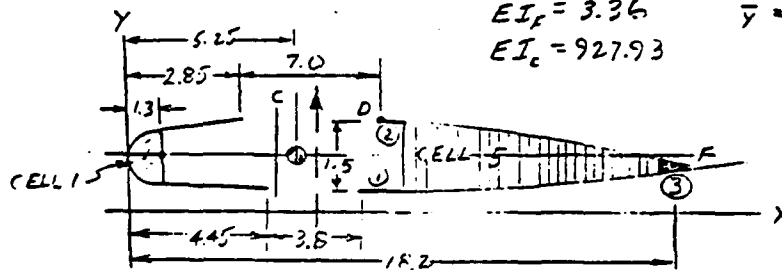
$$EA = 24.25$$

$$\bar{x} = 4.49$$

$$EI_F = 3.36$$

$$\bar{y} = 1.32$$

$$EI_C = 927.93$$

CF DISTRIBUTION

ELEM	EA	(x-1.3)	EA(x-1.3)
(1)	$3.25 \times 18.5 \times 5.06 = 3.05$	8.58	26.17
(2)	$1.65 \times 18.5 \times 5.06 = 1.55$	9.38	14.54
(3)	$.11 \times 17.23 = 1.90$	16.9	32.11
Σ	6.50	~	72.82

$$x = \frac{72.82}{6.50} = 11.20"$$

$$C_F \text{ AFT SECT.} = \frac{5.25 - 1.3}{11.20 - 1.3} \times 36,000 = 14,364 \#$$

$$e \text{ AFT SECT.} = \frac{14,364}{6.50} = 2,210 \text{ lb.}/\text{in.} \text{ TENS.}$$

* SEE "F" ON PAGE C10.05.

REPORT TITLE		REPORT NO. CMRB-79-005
PREPARED BY JC	4/15/82	CHECKED BY
SUBJECT		MODEL NO. YAH-64

STATIC ANALYSIS (DAMAGE CASE IV)RESISTANCE OF M_c

$M_c = 57,500 \text{ in}^2$ COMP. IN T.E. LONGS; TENS. NOSE WT.

ASSUMING M_c RESISTED AS A COUPLE LOAD AT THE NOSE WT. & T.E. LONGS:

$$\text{COMP. LOAD IN } \left. \begin{array}{l} \text{T.E. LONGS} \end{array} \right\} = \frac{57,500}{182-1.3} = 3,402 \#$$

$$\text{CF LOAD RESISTED } \left. \begin{array}{l} \text{BY THE T.E. LONGS} \end{array} \right\} = .11 \times 2,210 \times 17.23 = 4,189 \#$$

$$\text{COLUMN LOAD THAT } \left. \begin{array}{l} \text{T.E. LONGS CAN RESIST} \end{array} \right\} = 16,900 \times .11 = 1,859 \# \quad \text{ALLOW. COMP. LOAD}$$

$$A.S. = \frac{4,189 + 1,859}{3,402} = .77$$

RESISTANCE OF M_r , M_t & C.F.

$$M_r = 14,640 \text{ in}^2$$

$$\left. \begin{array}{l} \text{NOM. Q. EDGE OF DAMAGED} \\ \text{AREA DUE TO DIFF. BEND.} \end{array} \right\} = \frac{10}{2} \times 320 = 1,650 \text{ in}^2 \quad (\text{PG B10.10})$$

$$\text{STRAIN } \sigma = "D"(PG B10.14), \approx \left| 2,210 - \frac{1,650}{1.5-1.55} - \frac{14,640 \times 1.19}{3.36} \right|$$

$$= 3,685 \mu\text{-in/in COMP.}$$

$$e_{ALL} = 3,750 \mu\text{-in/in}$$

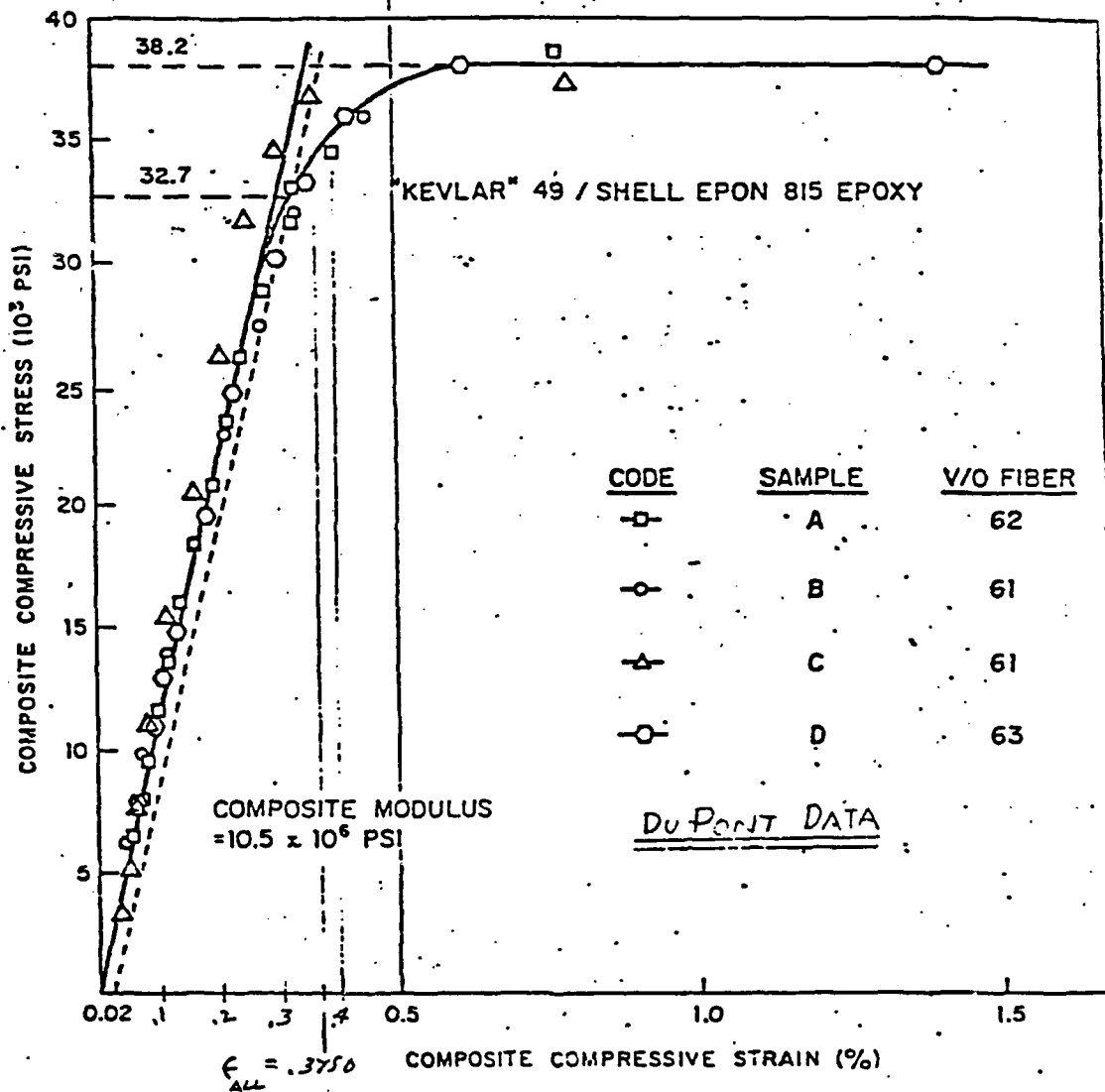
$$A.S. = \frac{3,750}{3,685} - 1 = .01$$

FATIGUE ANALYSIS (DAMAGE CASE IV)

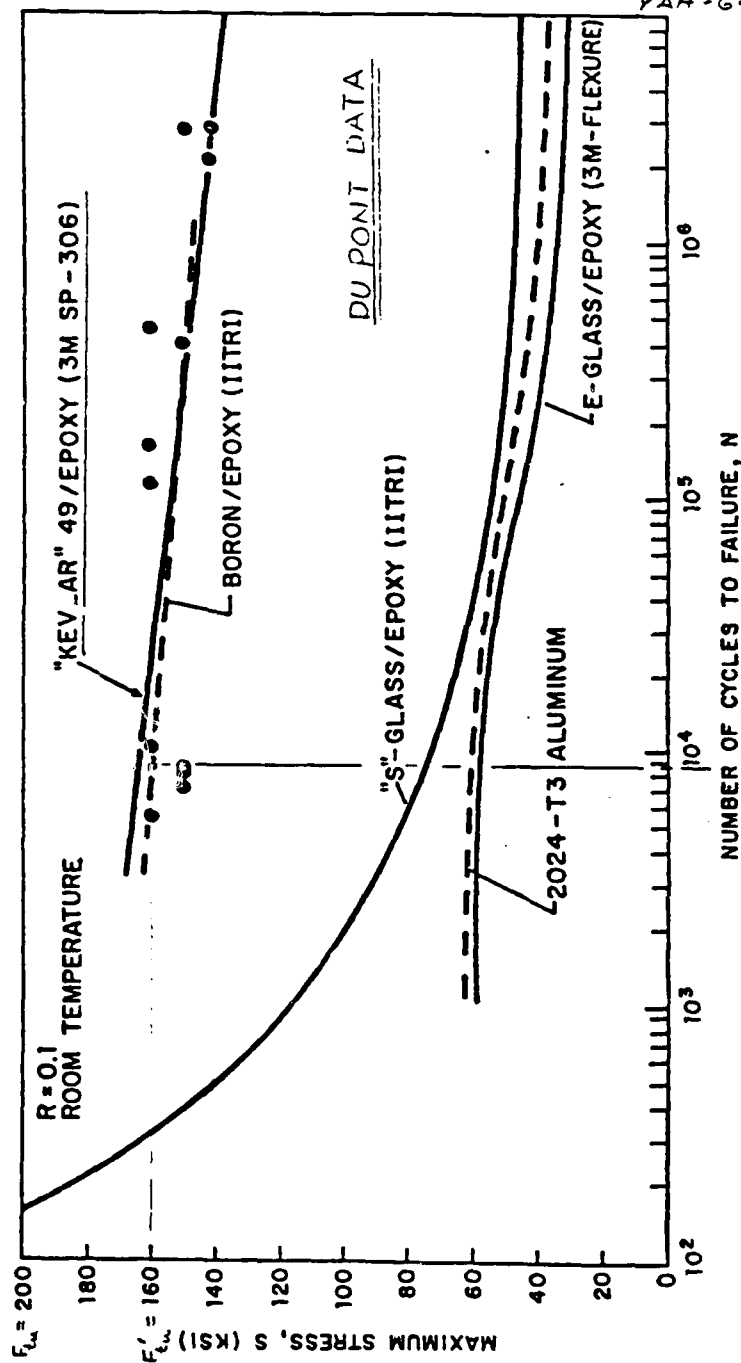
THIS CASE HAS THE SAME STATIC MARGIN-OF-SAFETY AS FOR CASE I; THEREFORE:

- FATIGUE LIFE ≥ 30 MINUTES
- FATIGUE M.S. $\approx .44$ (PG B10.11)

UNIDIRECTIONAL COMPOSITE
COMPRESSIVE STRESS-STRAIN CURVE



TENSION-TENSION FATIGUE BEHAVIOR OF UNIDIRECTIONAL COMPOSITES AND ALUMINUM



Hughes Helicopters

CMRB-79-005
YAH-64

$$\left. \begin{array}{l} \text{MAX STRESS} \approx \frac{160}{200} \cdot (\text{ULT. STRESS}) \\ \text{8670 CYCLES} \\ \text{(30 MINUTES} \\ \text{OF FLIGHT)} \end{array} \right\} = .80 \times (\text{ULT. STRESS})$$

C10.17

APPENDIX D

DYNAMIC ANALYSIS OF THE COMPOSITE
MAIN ROTOR BLADE FOR THE
AH-64A HELICOPTER

D-2

This appendix supplements the dynamics section of the CMRB final report. It summarizes mode shapes in Figures D-1a through D-1n that show mode shape plots for the CMRB with cyclic boundary conditions.

At frequencies where there are significant real and imaginary deflections, both components are plotted.

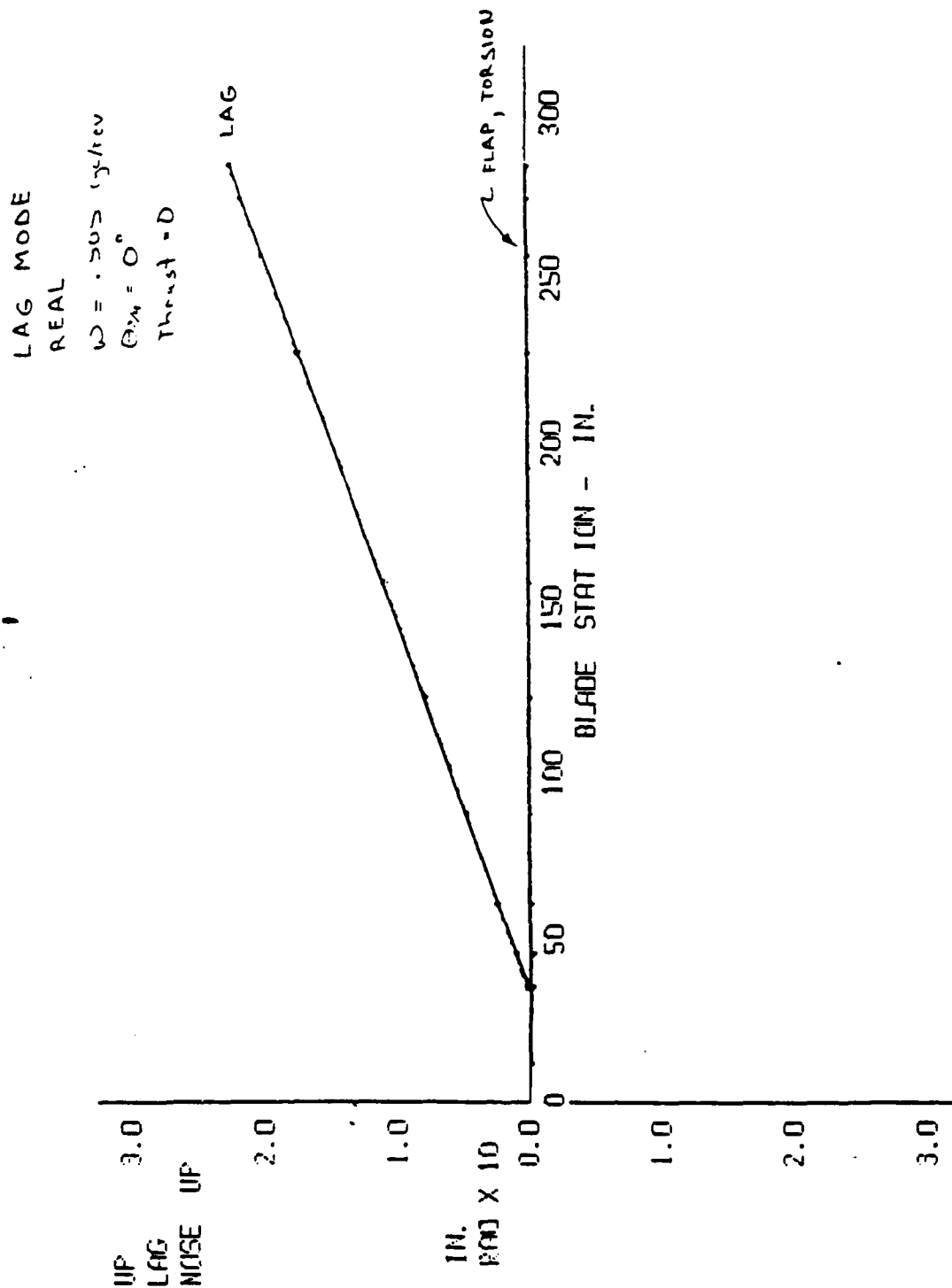


Figure D-1a. CMRB mode shapes.

FLAP MODE
 REAL
 $\omega = 1.051 \text{ cycles}$
 $\phi_{\omega} = 0^\circ$
 Thrust = 0

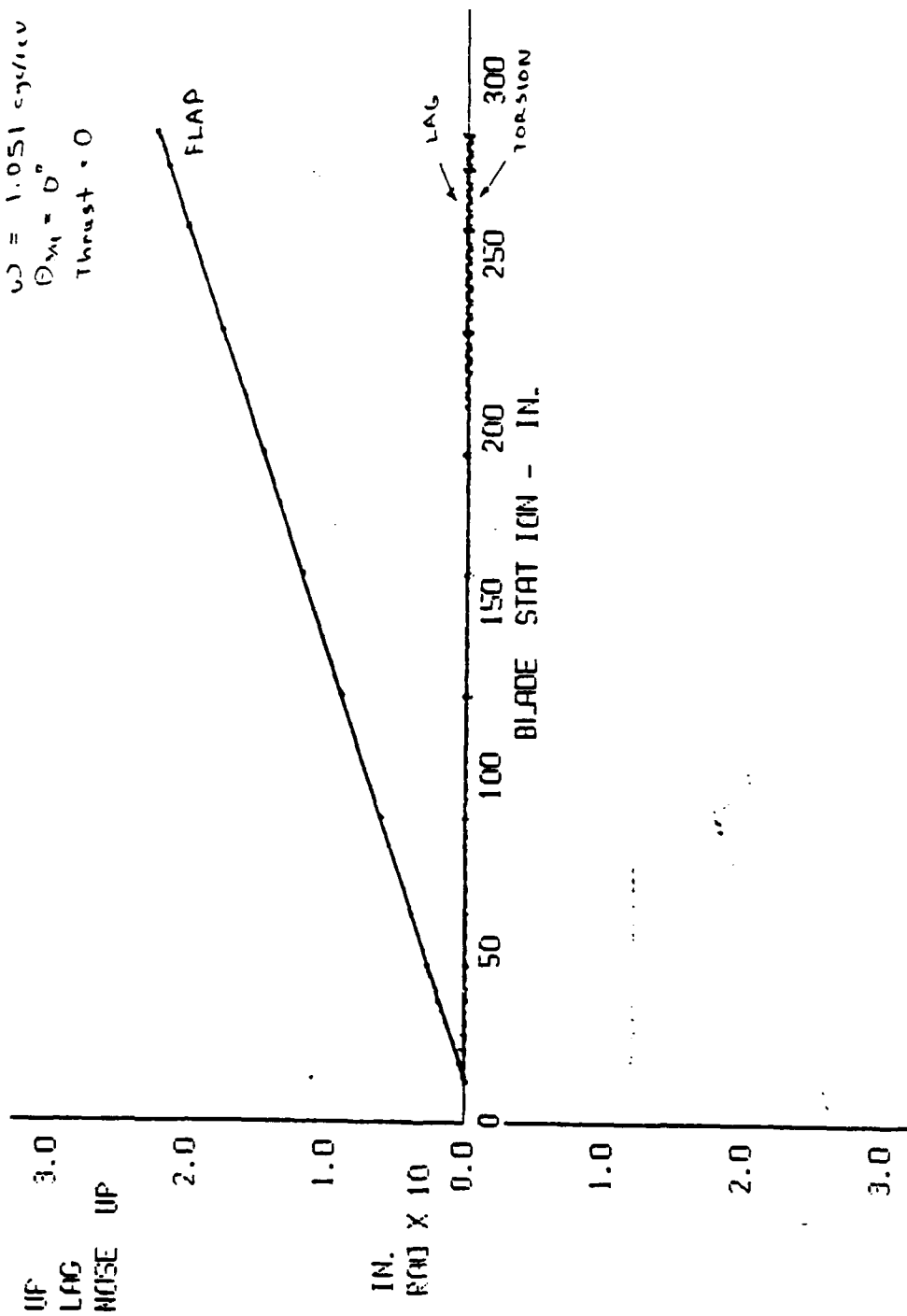


Figure D-1b. CMRB mode shapes.

1st FLAP BENDING MODE
 REAL
 $\omega = 2.739 \text{ cyc/rev}$
 $\phi_{\omega} = 0^\circ$
 Thrust = 0

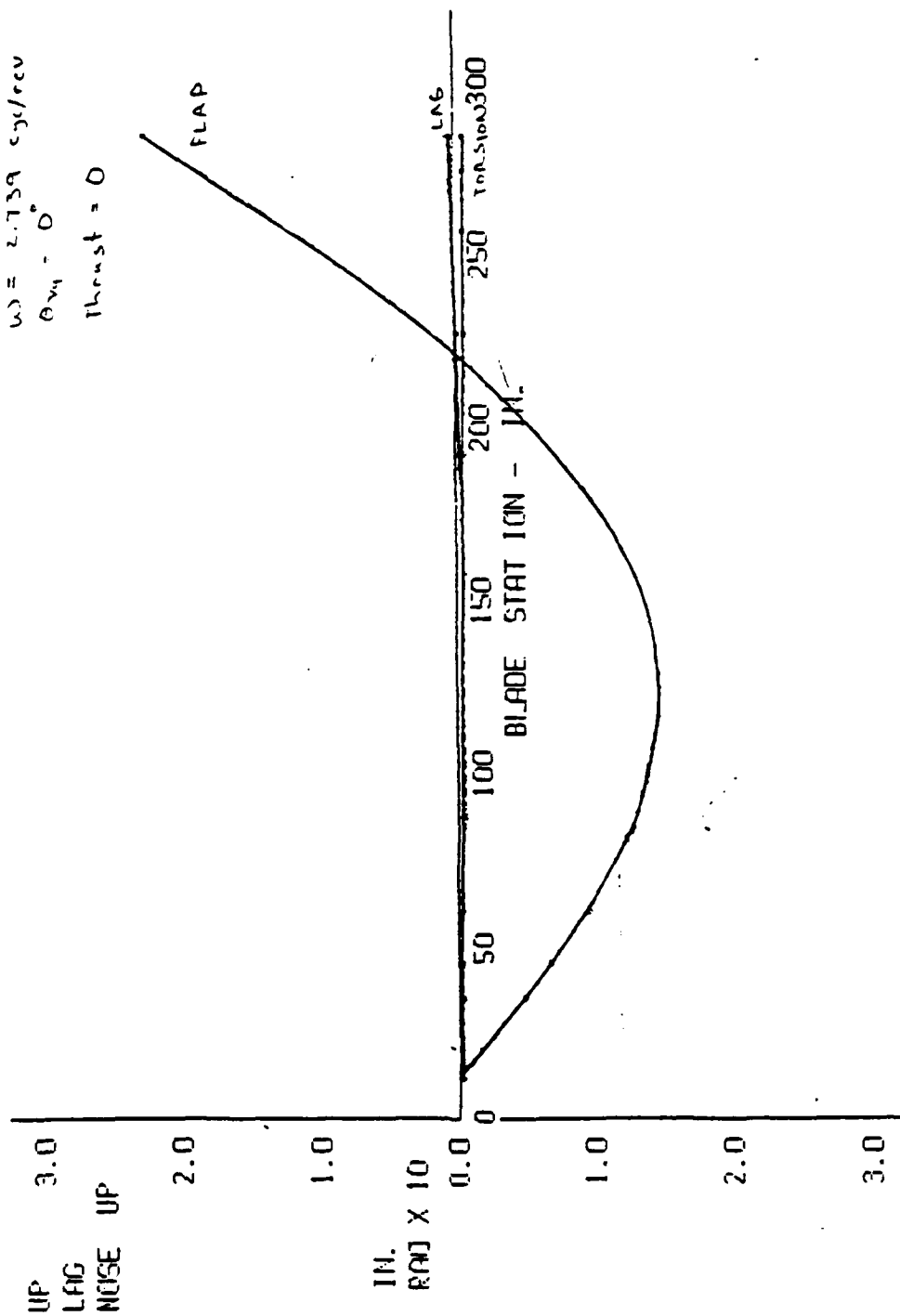


Figure D-1c. CMRB mode shapes.

1st FLAP BENDING MODE
 IMAGINARY
 $\omega = 2.739 \text{ cyc/rev}$
 $\phi_{\omega} = 0^\circ$
 THRUST = 0

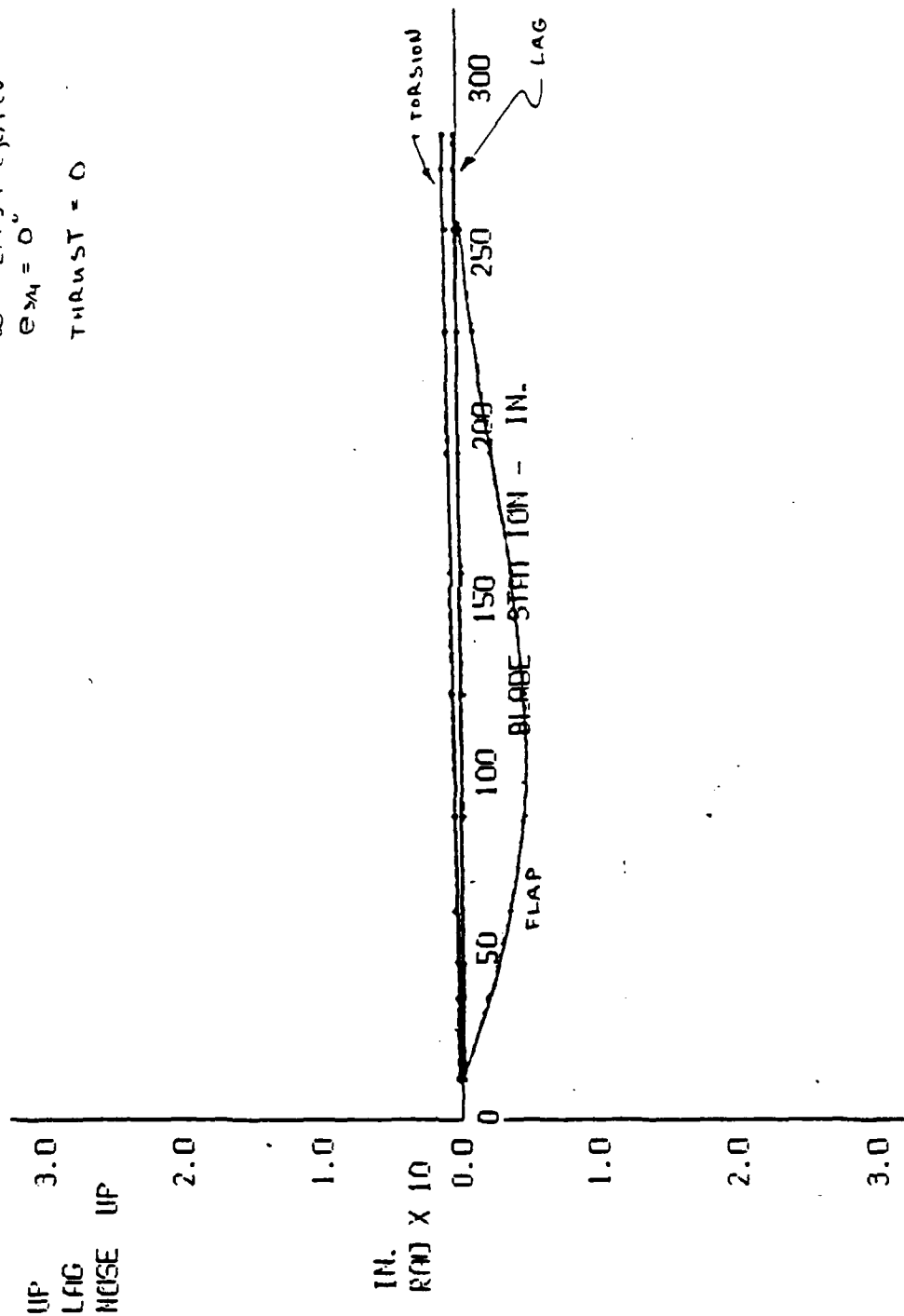


Figure D-1d. CMRB mode shapes.

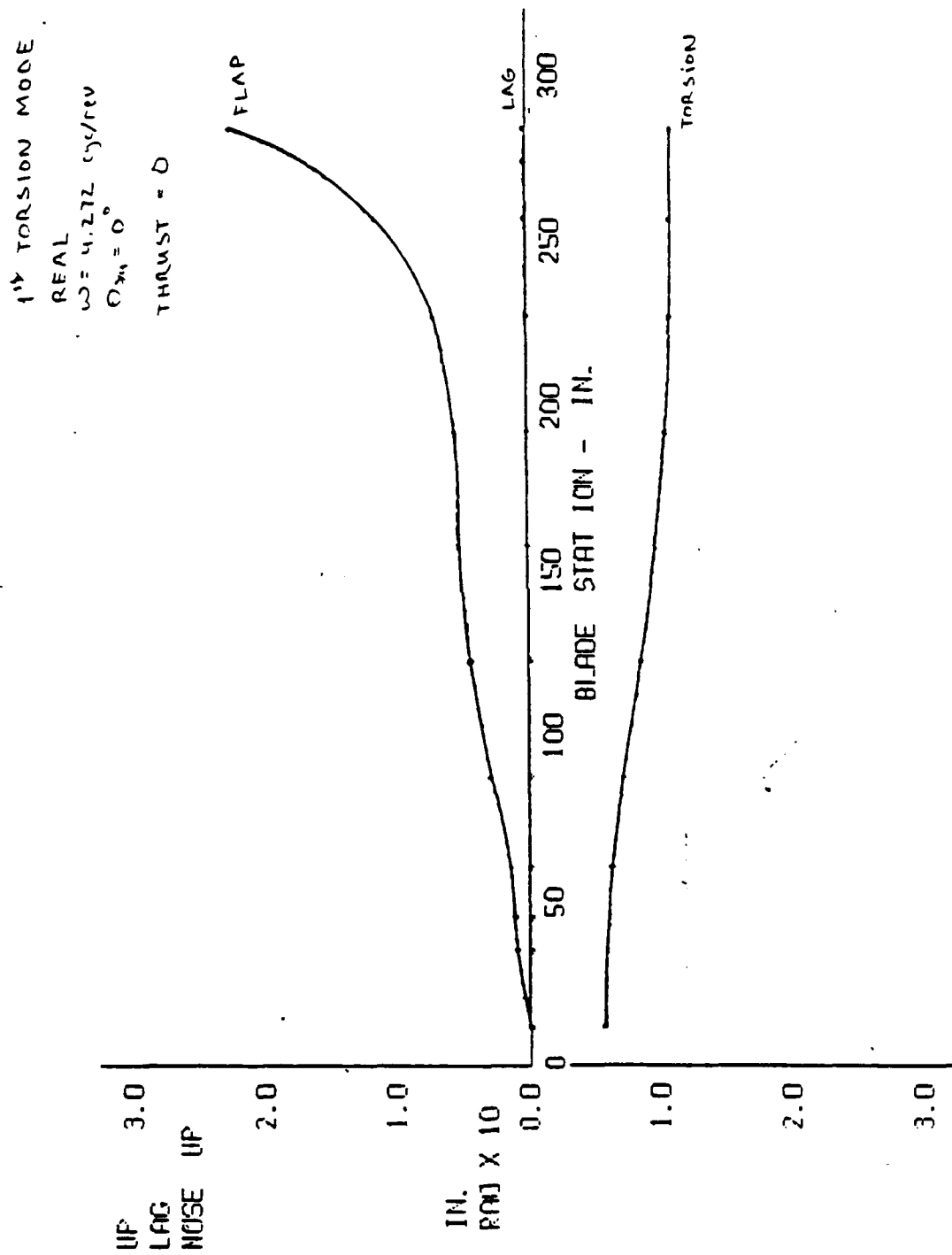


Figure D-1e. CMRB mode shapes.

1st TORSION MODE
 IMAGINARY
 $\omega = 4.272 \text{ cyc/rev}$
 $GJ/K = D$
 THRUST = 0

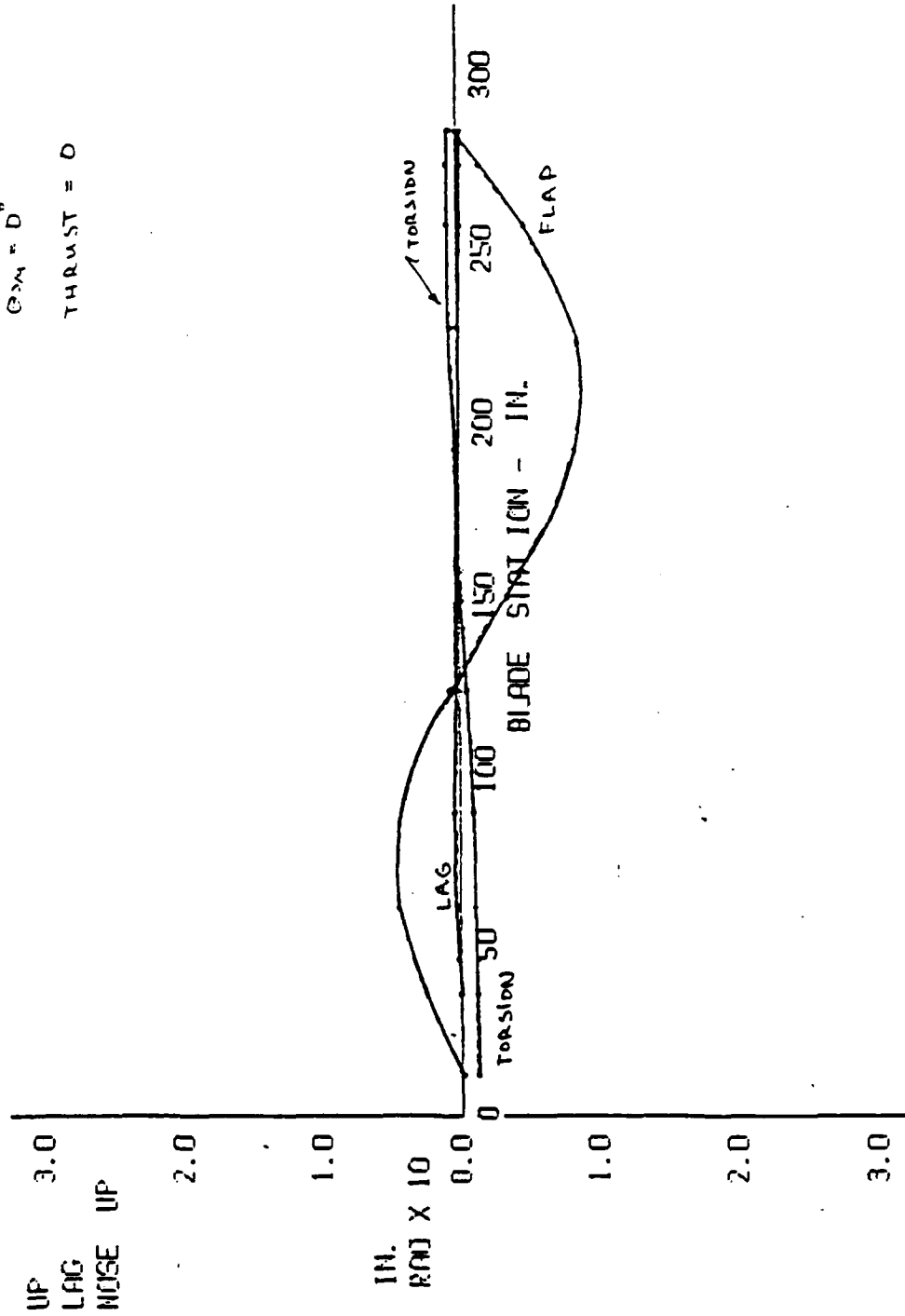


Figure D-1f. CMRB mode shapes.

2nd FLAP BENDING MODE

REAL

$\omega = 4.651 \text{ cyc/rev}$

$\phi_{21} = 0^\circ$

THRUST = 0

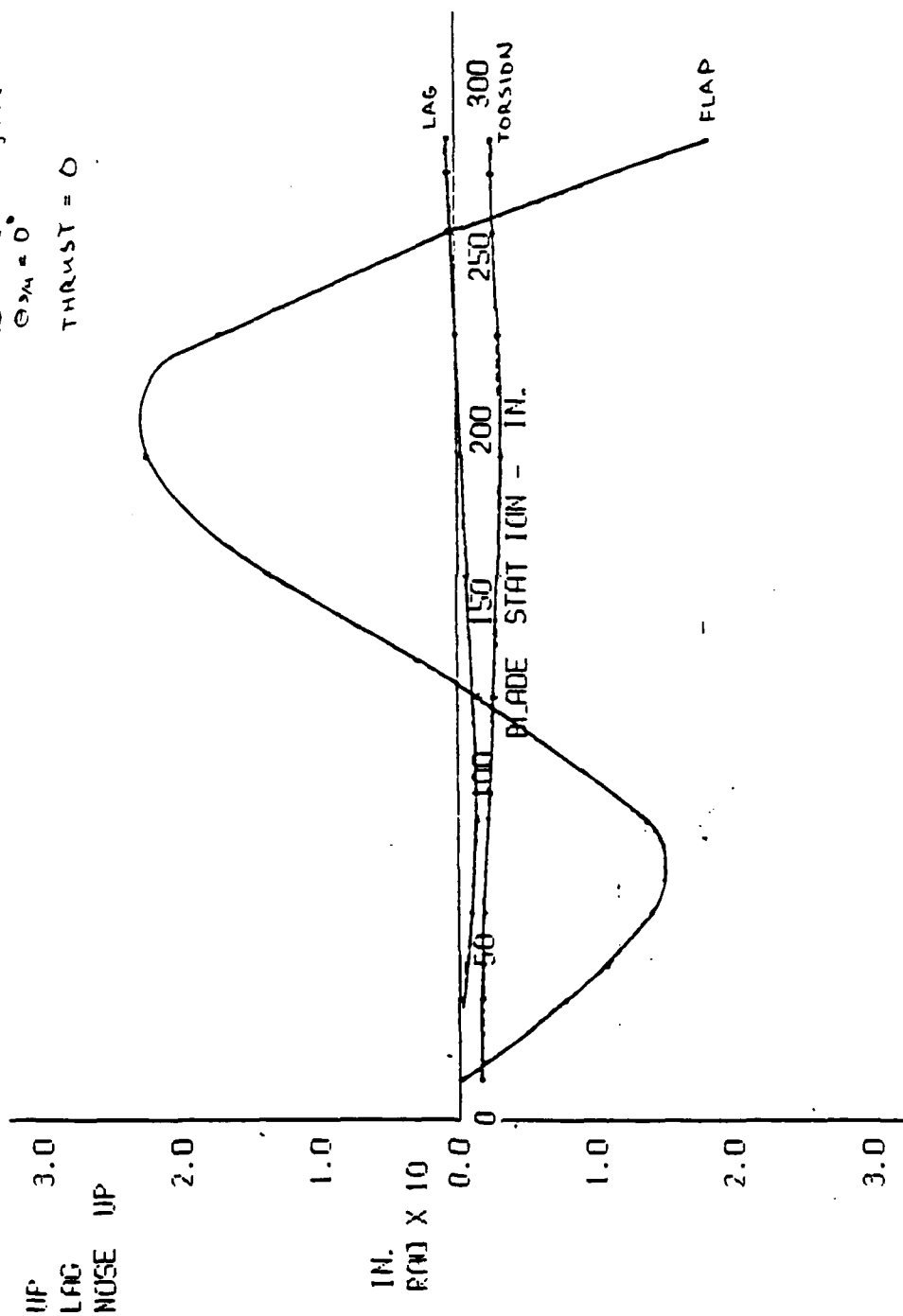


Figure D-1g. CMRB mode shapes.

2nd FLAP BENDING MODE
 IMAGINARY
 $\omega = 11.651 \text{ 1/rad}$
 $\theta_{2M} = 0^\circ$
 THRUST = 0

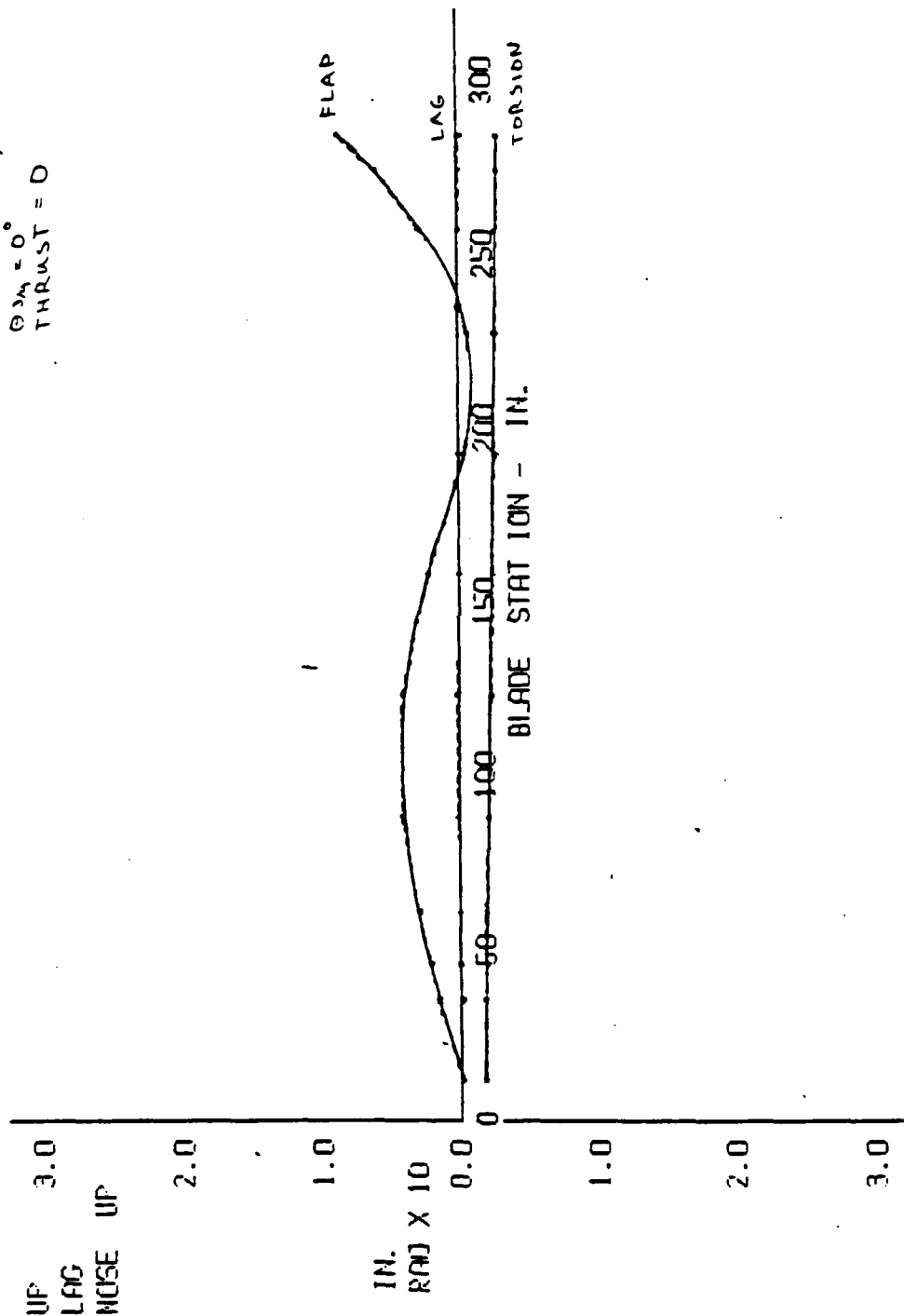


Figure D-1h. CMRB mode shapes.

1st CHORDWISE BENDING MODE

REAL

$\omega = 6.568$ cyc/rev

$\phi_{\text{in}} = 0^\circ$

THRUST = 0

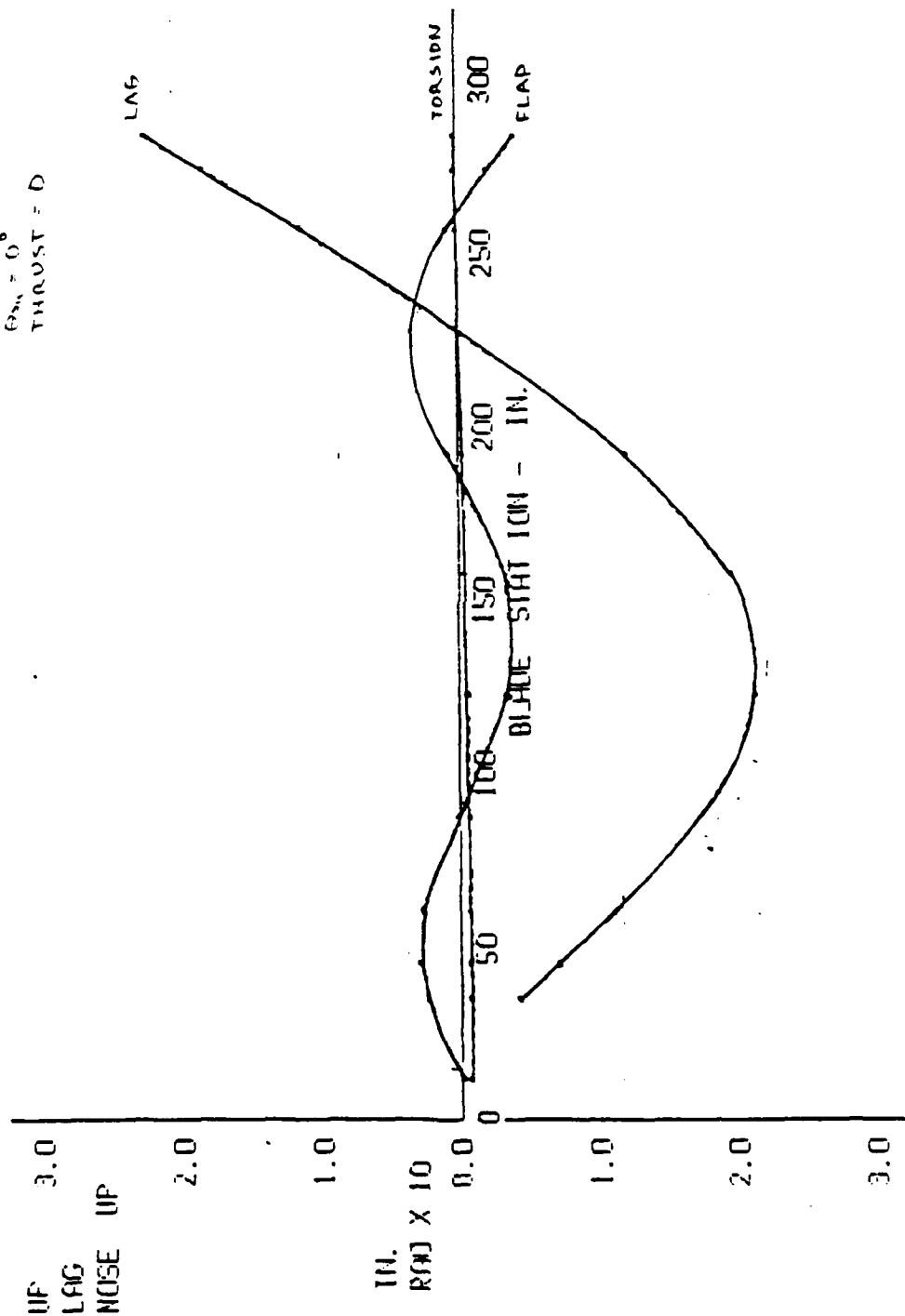


Figure D-1i. CMRB mode shapes.

1st CIRCUMFERENCE BENDING MODE
 IMAGINARY
 $\omega = 1.568 \text{ CY/REV}$
 $\beta_{1/4} = 0^\circ$
 THRUST = 0

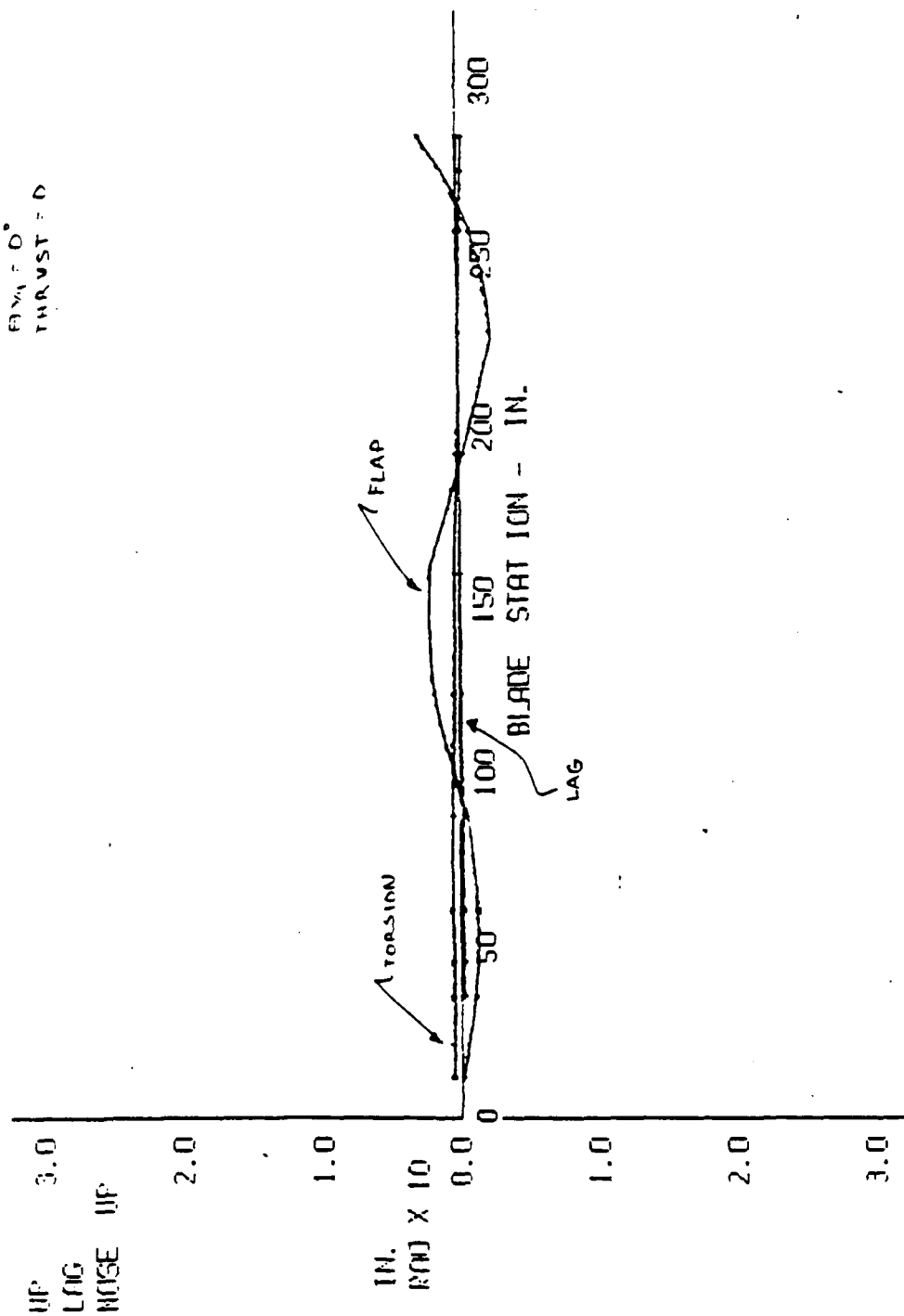


Figure D-1j. CMRB mode shapes.

3rd FLAPWISE BENDING MODE

REAL

$\omega = 7.112$

$\beta_{11} = 0^\circ$

THRUST = 0

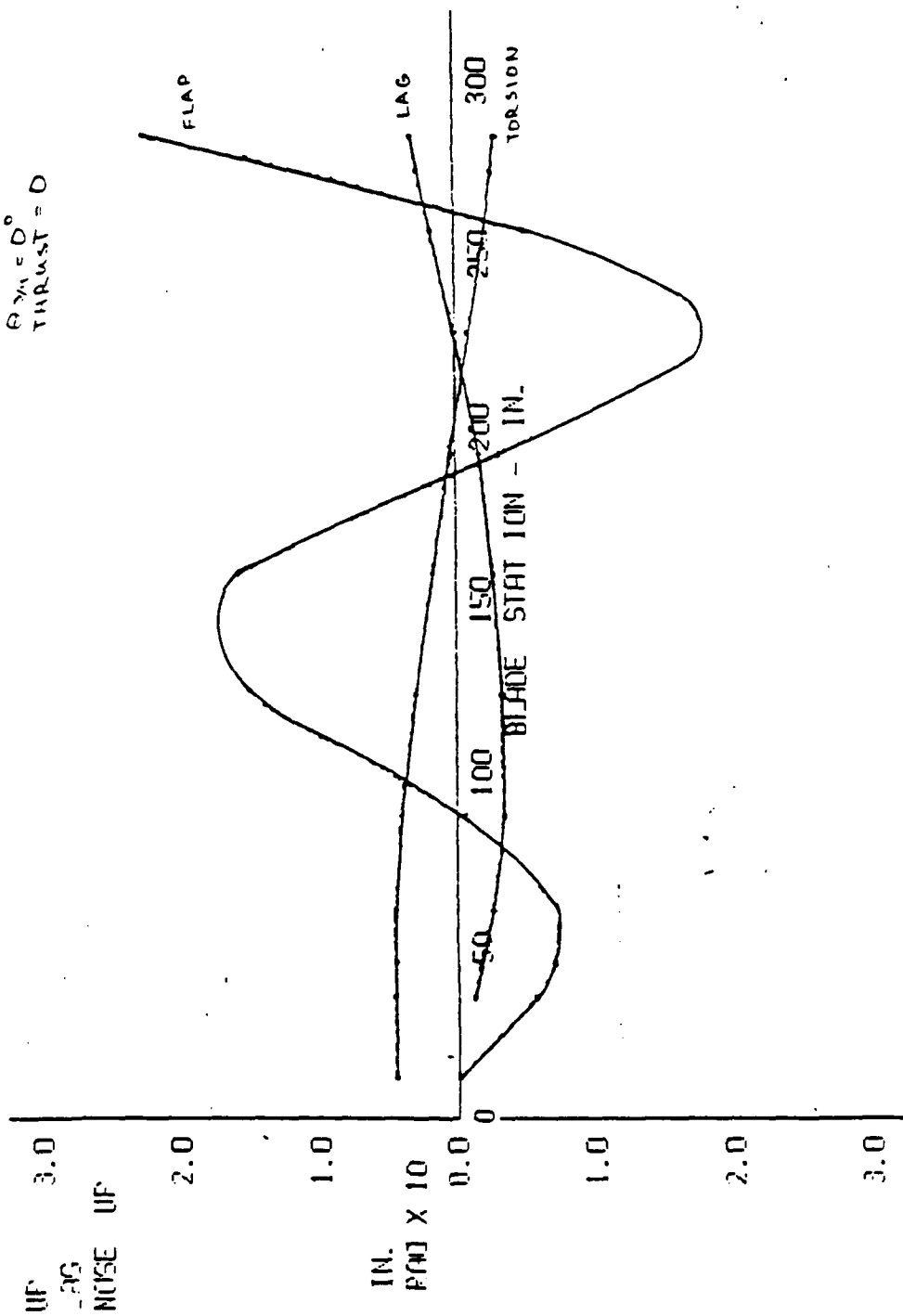


Figure D-1k. CMRB mode shapes.

3rd FLAPWISE BENDING MODE
 IMAGINARY
 $\omega = 7.112$
 $\theta_M = 0^\circ$
 THRUST = 0

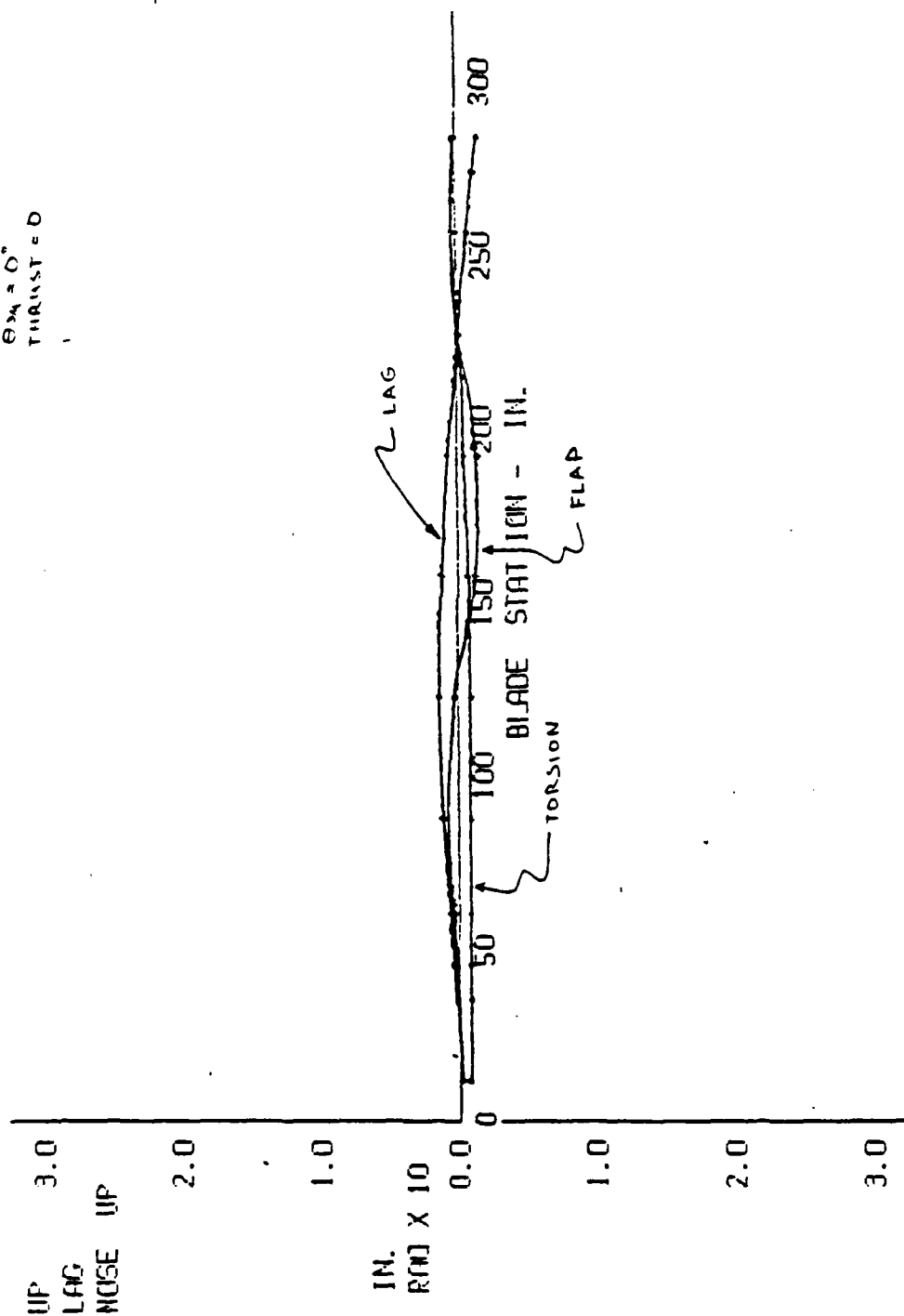


Figure D-11. CMRB mode shapes.

2nd TORSION MODE

REAL

$\omega = 8.443 \text{ rad/sec}$

$\theta_{\text{in}} = 0^\circ$

THRUST = 0

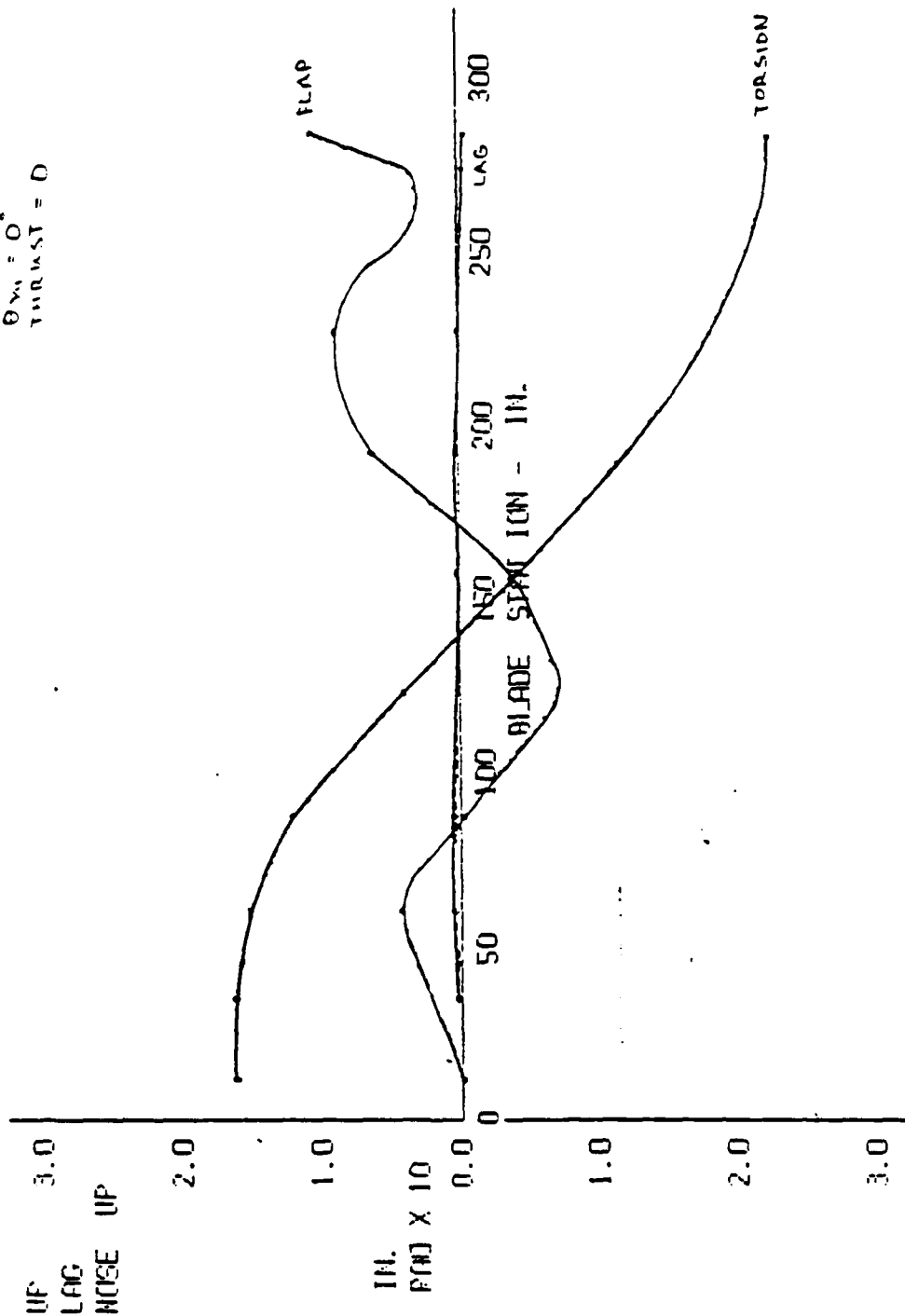


Figure D-1m. CMRB mode shapes.

2nd TORSION MODE
 IMAGINARY
 $\omega = 8.443 \text{ rad/sec}$
 $\theta_{\text{tip}} = 0^\circ$
 THRUST = 0

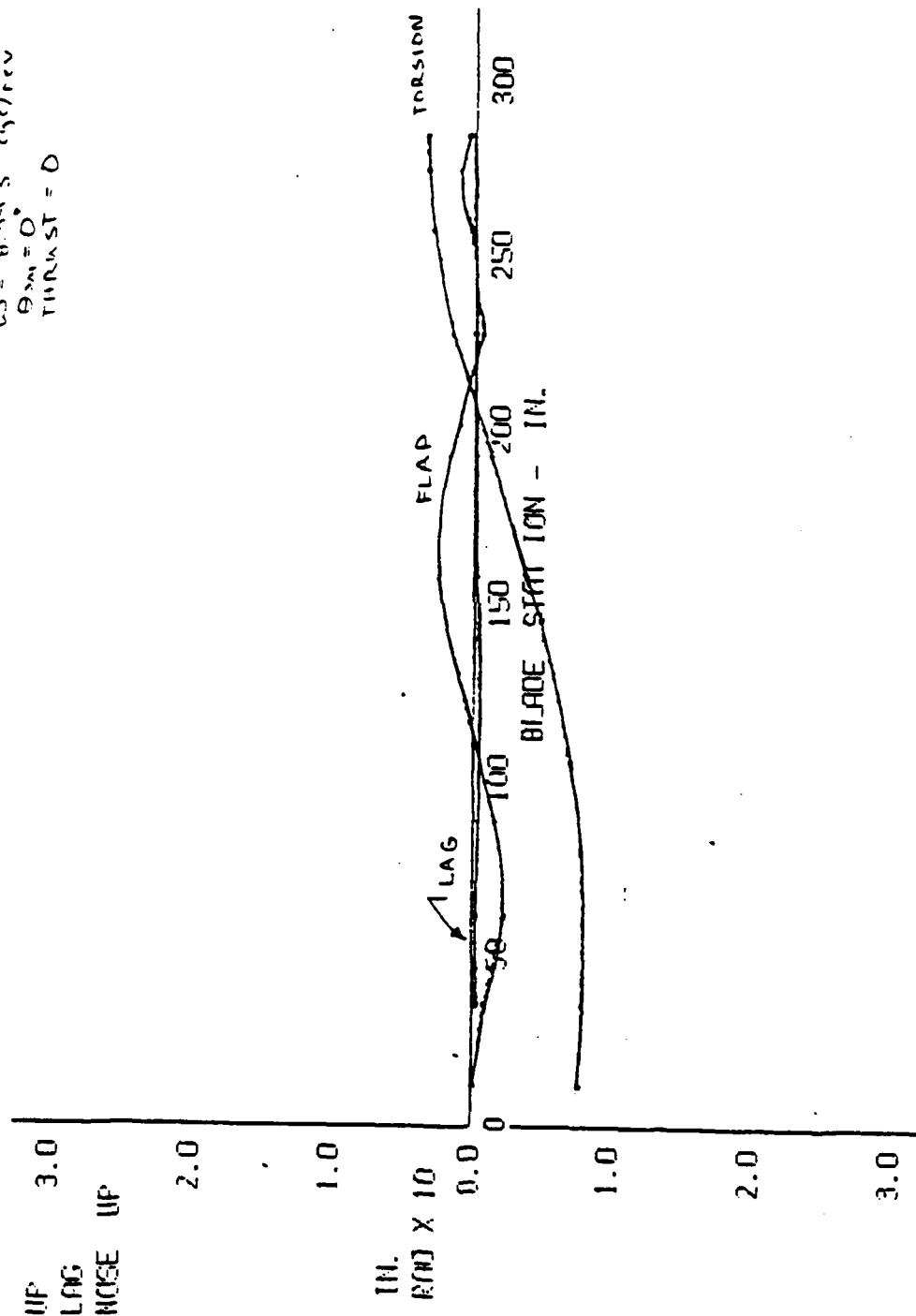


Figure D-1n. CMRB mode shapes.

APPENDIX E

ENGINEERING PROCESS MANUAL FOR FABRICATING THE
COMPOSITE MAIN ROTOR BLADE
FOR THE AH-64A HELICOPTER

*All even pages are missing
and are not available*

30 aug 89

1. SCOPE

1.1 This process bulletin establishes the materials and processes required to fabricate the Model 77 composite main rotor blade (CMRB) PN 7-311412500. It is currently in preliminary form and will be finalized before production begins.

2. APPLICABLE DOCUMENTS

2.1 Government documents. The following documents, of the issue in effect on date of the initiation for bids or request for proposal, form a part of this specification to the extent specified herein. In case of conflict between these documents and this specification, the requirements of this specification shall prevail.

SPECIFICATIONS

Federal

QQ-W-423	Wire, Steel, Corrosion Resisting
RR-W-360	Wire Fabric, Industrial
TT-I-735	Isopropyl Alcohol
TT-M-261	Methyl Ethyl Ketone, Technical
MMM-A-132	Adhesive, Heat Resistant, Airframe Structural, Metal to Metal

Military

MIL-C-9084	Cloth, Glass, Finished, for Resin Laminates
MIL-T-21014	Tungsten Base, High Density Metal (Sintered or Hot Pressed)
MIL-A-21180	Aluminum Alloy Casting, High Strength
MIL-S-22473	Sealing, Locking and Retaining Compounds, Single-Component
MIL-R-60346	Roving, Glass, Fibrous (for Filament Winding Applications)

E-2 not avail.

HMS 16-1164	High Strength Organic Fiber (Kevlar) Reinforcements, Yarn and Fiber
HMS 16-1171	Adhesive for Polyurethane Bonding
HMS 17-1172	Polyurethane, Rain Erosion Resistant Elastomer
HMS 17-1175	Polyurethane Foam, Self-Skinning, Self-Extinguishing, Closed Cell, Rigid
HP 1-17	Heat Treatment of 17-4PH and 15-5PH Precipitation Hardenable Corrosion Resistant Steels
HP 4-35	Anodic Treatment of Aluminum Alloys for Metal-to-Metal Bonding
HP 5-10	Environmental Sealing
HP 6-3	Torquing of Aircraft Bolts, Screws, and Nuts
HP 6-5	Magnetic Particle Inspection
HP 8-5	Identification of Detail Parts and Assemblies
HP 9-20	Etching and Priming of Tungsten Alloys for Adhesive Bonding
HP 9-26	Etch and Prime of Austenitic Corrosion- Resistant Steel for Adhesive Bonding
HP 10-7	Shelf Life
HP 15-42	Fabrication of Reinforced Plastics
HP 15-45	Application of Liquid Locking Com- pound for Sealing and Retaining Metal Fasteners, Bearings, and Bushings
HP 15-67	Fabrication of Composite Parts by Filament Winding Method
HP 16-21	Structural Metal-to-Metal Bonding

E-4 not avail.

E-5

7-311412615	Forward channel mold
7-311412616	Aft channel mold
7-311412617	Trailing edge longo mold
7-311412618	Root end wedge mold
7-311412619	Form block
7-311412620	Root end dam mold
7-311412625	Template (erosion strip buildup)
7-311412629	Index plate, end plate
7-311412630	Tool assembly layout
7-311412632	Template guide setup
7-311412633	End dome detail winding mandrel
7-311412636	Spar broom winding fixture
7-311412638	Spacer - tip core and mold
7-311412639	Skin layup layout
7-311412640	Bushing location fixture
7-311412641	Blade cooling fixture
7-311412642	Root end dam locator
7-311412643	Filler - dummy tube and trailing edge longo
7-311412644	Tip weight locator
7-311412645	Spar wedge template
7-311412646	Template spar cap tip
7-311412647	Staging table



E-6 not avail

Microballoons

Polyurethane erosion strip bonding adhesive and primer (HMS 16-1171)

Polyurethane erosion strip banding adhesive and primer (HMS 17-1172)

Resin and hardeners (HMS 16-1115)

S-glass roving (MIL-R-60346, Type IV, Class 1)

Tungsten (MIL-T-21014)

Urethane foam (HMS 17-1175)

Wire rods, 316 CRES (QQ-W-423)

3.2.2 Shop aids.

Double-back tape

Isopropyl alcohol (TT-I-735)

Metal spacer

Methyl ethyl ketone (MEK) (TT-M-261)

Mold release (Ram 225, or equivalent)

Peel ply (Air Tech, Tool Tech, or equivalent)

Polyethylene, film, 2-mil, embossed

Polyvinyl alcohol

Scrim cloth

Sealant tape

Styrofoam, sheet, 1/2-inch (12.7 mm)

Tedlar film, 1-mil

Teflon plugs

Wax (Trewax, or equivalent)

Wrightlon tube (Vac Pac, 3-mil) (7400 LF, 0.003)

*E-8 not avail.*

3.3.2 Fabrication of reinforced plastic subassemblies. Reinforced plastic subassemblies shall be fabricated in accordance with HP 15-42 and HP 15-67. Colored cotton thread may be used within the fiberglass laminates to indicate the fiber orientation.

3.3.2.1 Fiberglass subassemblies shall be fabricated with a nylon peel ply which shall be removed just prior to the bonding operation. All peel plies shall be marked "Remove Peel Ply" with letters no smaller than 1/4 inch (6.35 mm) in accordance with HP 8-5.

3.3.2.2 Fiberglass may be spliced in the filler area and 60-degree wraps of spar tubes only. Splices shall be overlapped at least 1 inch (25.4 mm).

3.3.2.3 Fiber volume requirements and dry:wet fiber weight ratios are specified below.

3.3.2.3.1 A 50-percent fiber volume and a 0.56 ± 0.03 dry:wet fiber weight ratio are required for Kevlar 49 fabric and rovings.

3.3.2.3.2 A 55-percent fiber volume and a 0.60 ± 0.03 dry:wet fiber weight ratio are required for graphite fabric and rovings.

3.3.2.3.3 Fiber volume and dry:wet fiber weight ratios shall be performed as required by this EPB in accordance with the techniques specified in HP 15-67.

3.3.2.4 Storage of any filament wound or other uncured component awaiting incorporation into a blade shall be done at low temperatures, in accordance with the guidelines set forth in HP 15-67.

3.3.2.5 HMS 16-1164 (Kevlar) yarns and fabrics shall be dried out prior to impregnation in accordance with HP 15-67.

3.3.3 Fabrication records. The following information is required to be recorded in the individual planning for each blade fabricated (including individual components).

3.3.3.1 Fabrication, start and completion time.

3.3.3.2 Lot, batch, or any other applicable identification numbers for all materials used.

3.3.3.3 Resin mixing, dates and times.



E-10 not avail.

3.3.4.4 Leading edge balance weight rods. The 316 CRES stainless steel balance rods shall be processed as follows.

3.3.4.4.1 The required number and lengths are as specified in 3.3.6.1.1.

3.3.4.4.2 Etch and prime the cut rods in accordance with HP 9-26.

3.3.4.4.3 Identify in accordance with HP 8-5 and seal in a polyethylene bag until ready for use.

3.3.4.5 Tungsten leading edge balance weight. The tungsten balance weight shall be prepared as follows.

3.3.4.5.1 Etch and prime in accordance with HP 9-20.

3.3.4.5.2 Identify in accordance with HP 8-5 and seal in a polyethylene bag until ready for use.

3.3.4.6 Backing strips. The 301 CRES stainless steel backing strips shall be processed as follows.

3.3.4.6.1 Etch and prime in accordance with HP 9-26.

3.3.4.6.2 Identify in accordance with HP 8-5 and seal in a polyethylene bag until ready for further use.

3.3.4.7 Aluminum wire mesh (7-311412547). The 5056 aluminum lightning screen (RR-W-360, Type I, Class 2) shall be processed as follows.

3.3.4.7.1 Clean using MEK (TT-M-261) spray, repeated as required to remove any visible contamination.

3.3.4.7.2 Identify in accordance with HP 8-5 and seal in a polyethylene bag until ready for further use.

3.3.5 Curing. The minimal acceptable cure cycle is dependent on the adhesive and resin system used. The most frequently used acceptable cure cycles are as follows. When any deviation from these is used it must be with the consent of the HHI Materials Processes and Standards Department, as indicated by the signature of the cognizant MP&S engineer on the applicable shop planning.

E-12 not avail.

3.3.6.2 Voids greater than 0.125 inch (3.175 mm) in depth shall be repaired as follows:

WARNING

Fire hazard; solvent is dangerous when exposed to heat or flame; use only with plenty of ventilation away from smoke and flames. Flashpoint 22°F (-5.5°C).

3.3.6.2.1 Solvent wipe area with TT-M-261 MEK.

3.3.6.2.2 Scuff sand the area with 180 - 320 grit paper to remove any gloss from the resin surface. Solvent clean as in 3.6.3.2.1.

3.3.6.2.3 Mix and apply HMS 16-1068, Class 3 adhesive in accordance with HP 16-25, filling voids flush with the surrounding surfaces.

3.3.7 Secondary bonding operations.

3.3.7.1 Film adhesive bonding operations shall use HMS 16-1111, Class 3 adhesive in accordance with HP 16-30.

3.3.7.2 Paste adhesive bonding operation shall use HMS 16-1068, Class 3, adhesive in accordance with HP 16-25.

3.3.7.3 Electrical connections shall be sealed using HMS 16-1147, Class 2 adhesive in accordance with HP 5-10.

3.3.7.4 The 7-3114152516-11 erosion strip shall be bonded in accordance with EPB 16-139.

3.3.8 Finish (paint). Finish in accordance with EPB 4-230.

3.3.9 Weight and balance. Weight and balance procedures shall be in accordance with EPB 30-164. Install weight retention fitting doors and secure fasteners using MIL-S-22473, Grade C in accordance with HP 15-45. Torque fasteners to 25-35 inch-pounds (2.8-4.0 N·m) in accordance with HP 6-3.

4. QUALITY ASSURANCE

4.1 Provisions of the NDE plan apply.

E-14 not avail

6. NOTES

6.1 Intended use. This process is intended for use in the fabrication of the composite main rotor blades for the Model 77 helicopter.

7. APPROVED VENDORS

Not applicable

E-16 not avail

APPENDIX F

NONDESTRUCTIVE EVALUATION PLAN
OF THE
COMPOSITE MAIN ROTOR BLADE
FOR THE AH-64A HELICOPTER

NONDESTRUCTIVE EVALUATION PLAN

This nondestructive evaluation (NDE) and nondamaging testing (NDT) plan is proposed for the production CMRB to assure structural quality by:

- Detecting critical flaws
- Measuring structural integrity
- Evaluating consistency of fabrication

It will be reevaluated after the first block of production blades is completed, and modified if necessary. This proposed plan anticipates the potential for the occasional occurrence of flaws, defects, and fabrication errors that can degrade the structural quality, it establishes the optimal NDT equipment and procedures for evaluating these possible defects, and it quantifies the tolerance limits that are acceptable for defects and manufacturing inaccuracies.

Table F-1 lists defects, flaws, and fabrication errors that were experienced in the CMRB MM and T prototypes manufactured to date. The list is an anticipatory forecast for the production blade, and will be updated upon completion of the blade preproduction program. At that time, a better categorization can be made with respect to defect types, likelihood of occurrence, size, location, probability of growth rates, and better analysis of the structural criticality of the various defects. The tentative consequences of the flaws described in the rightmost column of Table F-1 will be upgraded after a more substantive data base is accumulated. A part of the work yet to be done will be the establishment of a set of structural criteria that provide "test/don't test" guidelines; i. e. ,

- "Search, inspect, test, and NDE flaws, defects and error that each individually degrade the strength, modulus, fatigue resistance of the MRB by more than 5 percent of its initial or unflawed value."

Table F-2 lists potential techniques and associated instrumentation for evaluating the CMRB. Table F-3 indicates the present evaluation of the success of these techniques.

TABLE F-1. POTENTIAL PRODUCTION FLAWS THAT
MAY OCCUR IN THE CMRB

Type of Defect	Consequences When Defect Exceeds Tolerance Levels
Interlaminar delamination	Delamination grows with cycling, causing local buckling.
Disbonded, debonded honeycomb/interface	Flutter and loss of blade stiffness and rigidity.
Porosity	Degradation of shear strength of epoxy matrix
Void	Local weakening of strength and modulus.
Resin rich, filament-poor area	Tensile strength and modulus decrease with decreasing fiber volume ratio.
Resin starved area	Compressive strength and shear strength decrease with increasing unwetted filament-to-resin ratio.
Spartube rib buckle	Loss of bending stiffness and torsional rigidity.
Thick bond lines	Shear rigidity of bondline is inversely proportional to its thickness.
Tip or leading edge mislocation	Blade won't track, or cannot be balanced easily.
Root end bushing misfit, splits, voids, cracks, separations	Potential for premature root end blade fracture in fatigue.
Foreign objects, inclusions	Some degradation of blade durability from inclusions.

TABLE F-1. POTENTIAL PRODUCTION FLAWS THAT
MAY OCCUR IN THE CMRB (CONT)

Type of Defect	Consequences When Defect Exceeds Tolerance Levels
Filled honeycomb cells	Excessive material in the cells bleed from surrounding skin to point of resin starvation.
Misoriented plies, waviness	Localized weakening of stiffness and strength, lowered fatigue resistance.
Reworked area	Reintroduction of stress concentrators and fatigue nucleation.
Overlap, underlap, gap	Local loss of stiffness, rigidity, and fatigue resistance.
Internal dent, damage	Local loss of strength and fatigue resistance.
Inhomogeneous cure	Degradation of strength and stiffness over wide area.
Mislocation of root-end bushing	Reduction of bushing wall and/or flange thickness during final machining, with accompanying reduction in strength.

TABLE F-2. INSPECTION NDE METHODS AH-64A CMRB

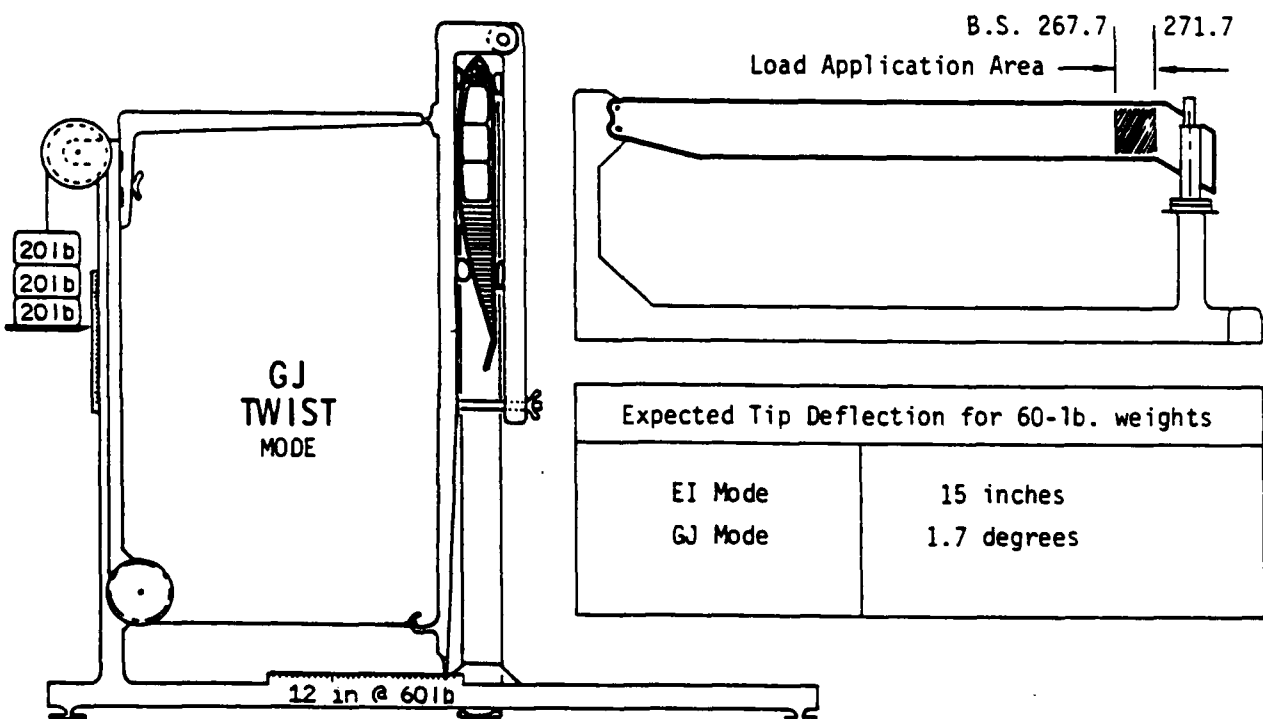
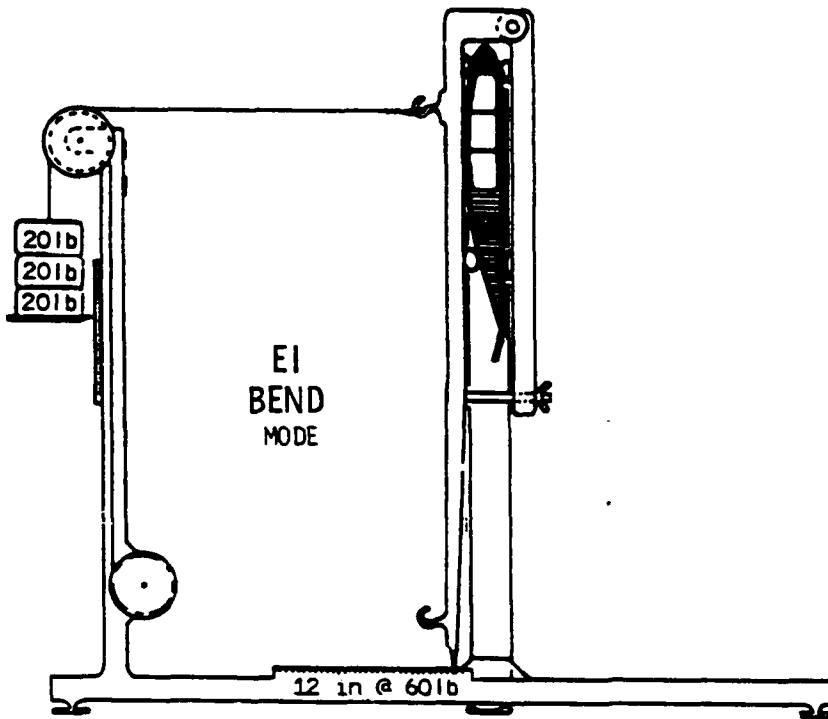
Technique	Instrument/ Equipment	Inspection/Test Frequency ^(a)
<ul style="list-style-type: none"> • Visual detection <ul style="list-style-type: none"> - Normal illumination - High intensity light 	Inspector S150 Xenon Lamp	Every blade Every blade
<ul style="list-style-type: none"> • Audible detection <ul style="list-style-type: none"> - Manual Tapping - Sonic Brush 	Inspector NASA Sonic Brush	Every blade Every blade
<ul style="list-style-type: none"> • Ultrasonic scanning <ul style="list-style-type: none"> - Pulse/echo attenuation - Pulse/echo impedance - Ultrasonic pulse, acoustic echo 	Mark II Harmonic Bond Tester: EPB-15-138. Bondascope 2100 206 AU	Every blade in lot 1 Every second blade in lot 1 Every third blade in lot 1
<ul style="list-style-type: none"> • X-ray radiography <ul style="list-style-type: none"> - Microfocused, video-taped - Conventional, negative film to scale 	Magnaflux NDT 9/6 Cedtech	Every blade in lot 1 Questionable blades from microfocus X-ray.
<ul style="list-style-type: none"> • Impulse/modal response signature 	PCB K291 A05 tapper	Every blade
<ul style="list-style-type: none"> • Structural quality measurement, rigidity, frequencies and hysteresis 	See Figure F-1	Every second blade or TBD

(a) NDT techniques and the frequency of inspection will be recommended after the 20th blade is produced.

TABLE F-3. NDT/DEFECT MATRIX

	Delaminations	Disbond	Porosities	Voids	Resin-rich	Resin-poor	Rib geometry	Thick bond	Weight mislocation	Bushing loose	Foreign objects	Filled cells	Ply misorientation	Rework	Overlaps, gaps	Dents, damage	Miscure	Bushing mislocation
Visual																		
Normal	•	•			•	•		•					•	•				•
High intensity	•	•	•	•			•	•	•	•	•	•	•	•	•			
Audible																		
Tapping	•	•		•				•			•							
Sonic brush	•	•		•				•			•							
Ultrasonic																		
Attenuation	•	•	•	•	•	•		•								•	•	
Impedance	•	•	•	•	•	•		•	•	•	•	•				•	•	
Acoustic echo	•	•	•	•	•	•		•			•	•		•	•	•	•	
X-ray																		
Microfocus	•	•	•	•	•	•	•	•	•	•	•	•	•	•	•	•		
Conventional	•	•		•	•	•	•	•	•	•	•		•	•				
Pulse response	•	•	•		•	•	•	•	•			•					•	
Structural quality	•	•	•		•	•		•	•	•		•		•		•		

Dot size indicates likelihood of detection



FIXTURE FOR MEASURING ROTOR BLADE STIFFNESS

Figure F-1. Fixture for measuring rotor blade stiffness.

A tentative level of acceptable quality is defined by the following flaws, defects, or irregularities. Those that fall within these tolerances will be considered acceptable (minor) manufacturing errors. Figures F-2 through F-15 illustrate these flaws and their tolerances. Those that exceed these tolerances will be submitted to the Material Review Board and treated as unacceptable until disposed of by the Board.

- Skins shall be wrinkle-free over 80 percent of the surface area. No single wrinkle shall exceed 4.0 square inches in extent. Wrinkle pits perpendicular to the surface shall not exceed 0.06 inch in depth. Overriding folds in the plane of the skin shall not exceed 0.15 inch. No two wrinkles shall be closer than 10.0 inches nor shall there be more than five distinctly separate wrinkles in a blade.
- Longos shall be free of waviness over 99 percent of their volume in the lug area and 80 percent over the remainder of the blade. No single wave shall have an aspect ratio smaller than 20.
- Spartube sidewalls shall not deviate from vertical straightness by more than 0.05 inch, and from spanwise straightness by more than 0.50 inch.
- Interlaminar Resin overthickness shall be less than 0.010 inch in the bushing area and less than 0.030 in the longo straight sections.
- Bushings shall adhere to longos and fillers. No single disbond shall exceed 0.06 square inch in area. No more than 3 disbonds 0.06 square inch in size, shall occur per bushing.
- Filler cracks shall not extend more than 1 inch in the spanwise direction, nor more than 0.1 inch in chordwise direction.
- Outer Skins shall adhere to spar caps, and inner skins shall adhere to longos over 95 percent of their interfaces. No single delamination or disbond shall exceed 1.0 inch on an axis, nor shall disbonds be within less than 4.0 inches of each other.
- Fiber/matrix ratios shall rely on in-process control.
- Filament alignment shall be within ± 3 degrees of the correct orientation for all fibers.

- Honeycomb core shall adhere to the skins over a minimum of 90 percent of cell edges. No cell edge disbond will extend beyond 10 cells, nor shall disbonded cell sets be closer than 4 inches.
- Leading edge weights shall be bonded over at least 90 percent of their surfaces, and shall be positioned within ± 0.05 inch of their intended chordwise position and within ± 0.2 inch of their intended spanwise position.
- Tip weights shall be bonded over at least 90 percent of their surfaces.
- Torsional rigidity shall be within ± 6 percent of the moving cumulative average of tested blades.
- The root end bushing shall be located within drawing tolerance.

All production CMRB inspection and NDE Planning Packages shall be jointly reviewed and approved by Quality Engineering, Materials, Processes, and Specifications (MP&S) and cognizant Design/Technical Engineering and shall be in conformance with the instructions in Quality Assurance Production Plan for the CMRB.

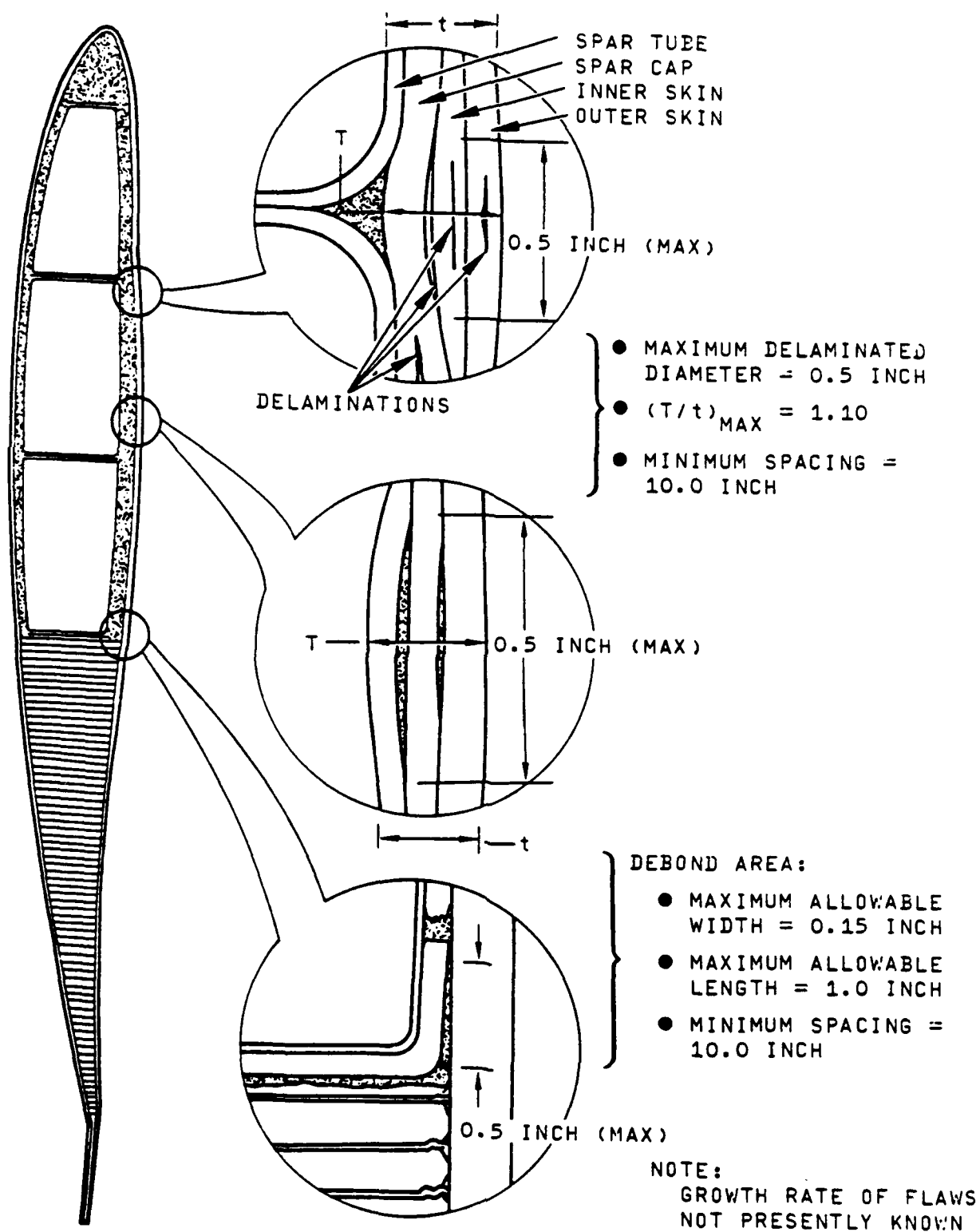
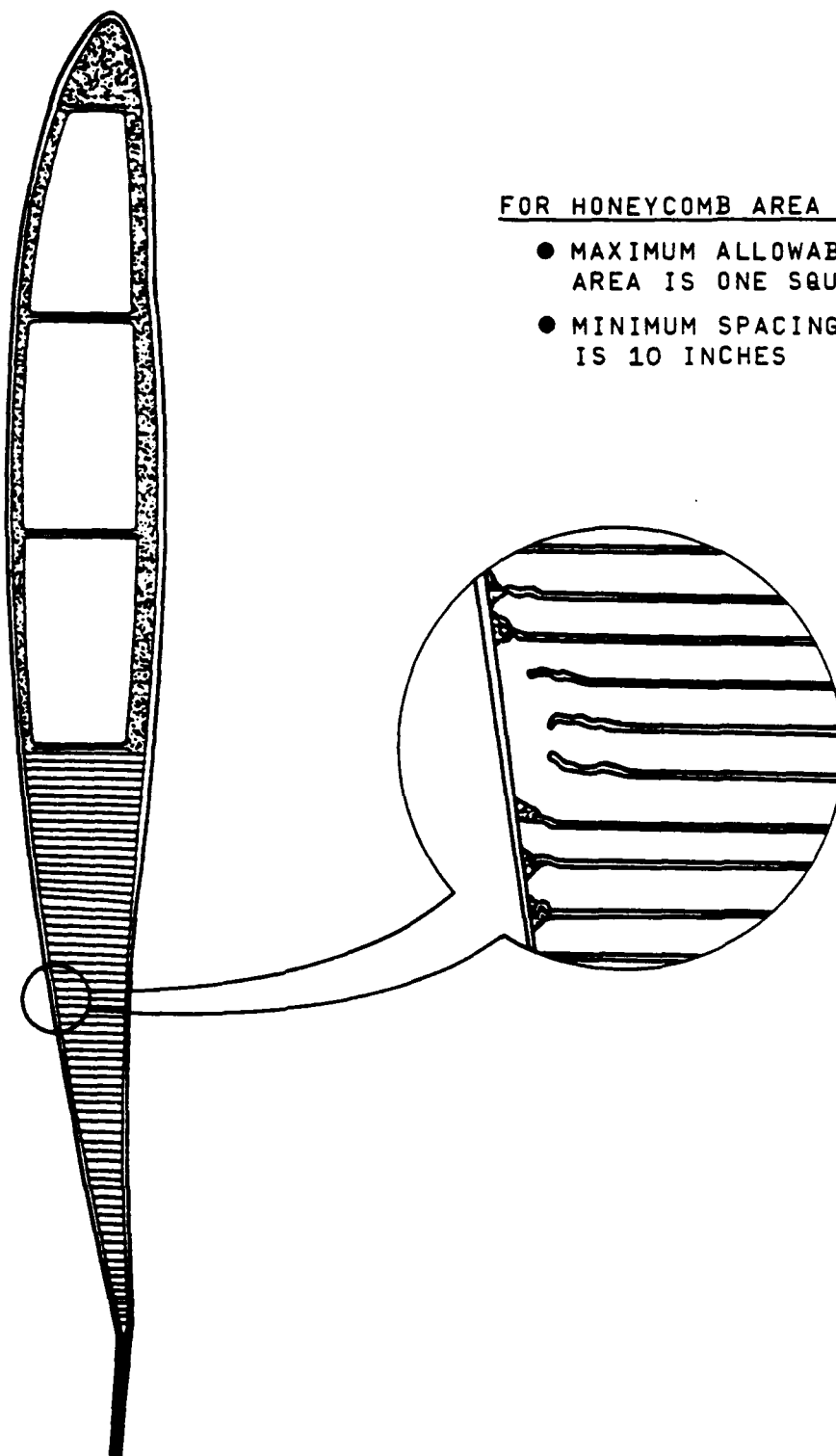


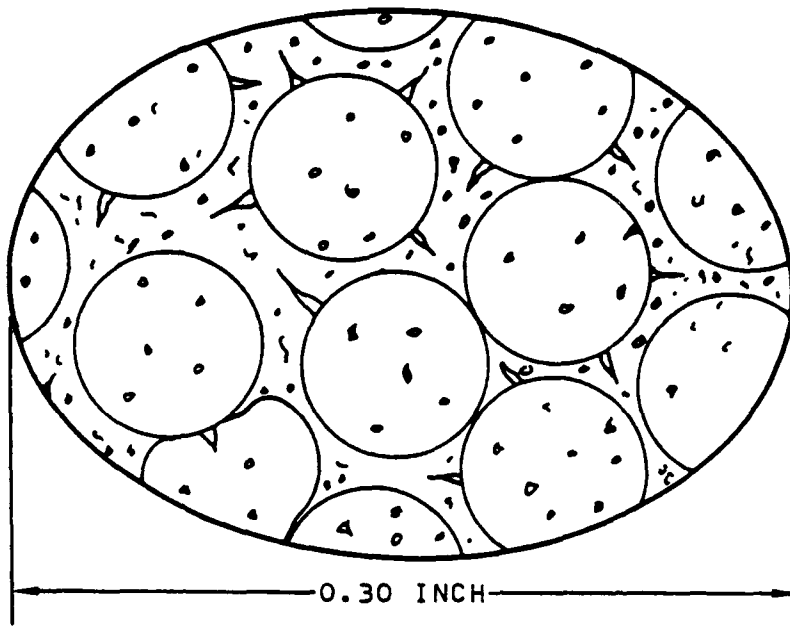
Figure F-2. Potential delamination.



FOR HONEYCOMB AREA ONLY

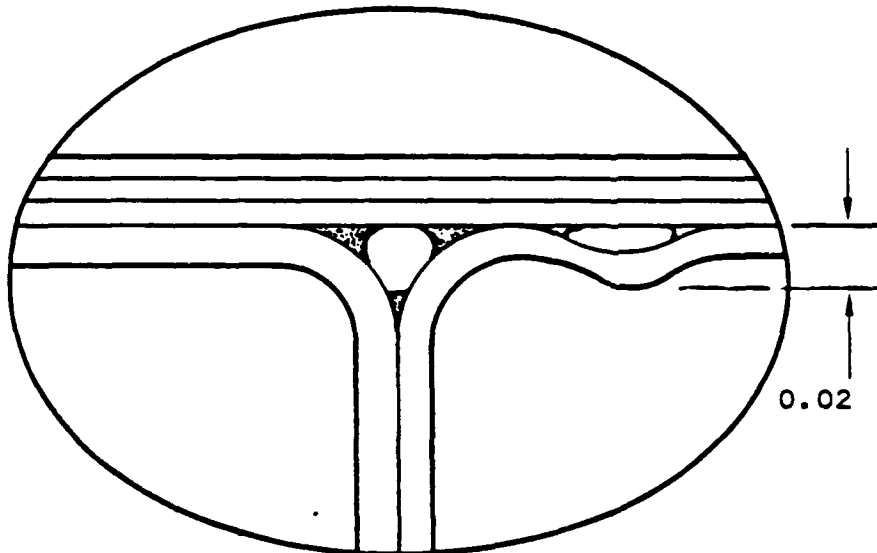
- MAXIMUM ALLOWABLE UNBONDED AREA IS ONE SQUARE INCH
- MINIMUM SPACING FOR FLAWS IS 10 INCHES

Figure F-3. Disbonded honeycomb.



- MAXIMUM ALLOWABLE POROSITY DIAMETER IS 0.30 INCH
- MINIMUM SPACING FOR FLAWS IS 5 INCHES

Figure F-4. Porosities.



- MAXIMUM VOID LENGTH IS 0.5 INCH
- MINIMUM SPACING FOR FLAWS IS 5 INCHES

0.02 INCH (MAXIMUM)

Figure F-5. Voids

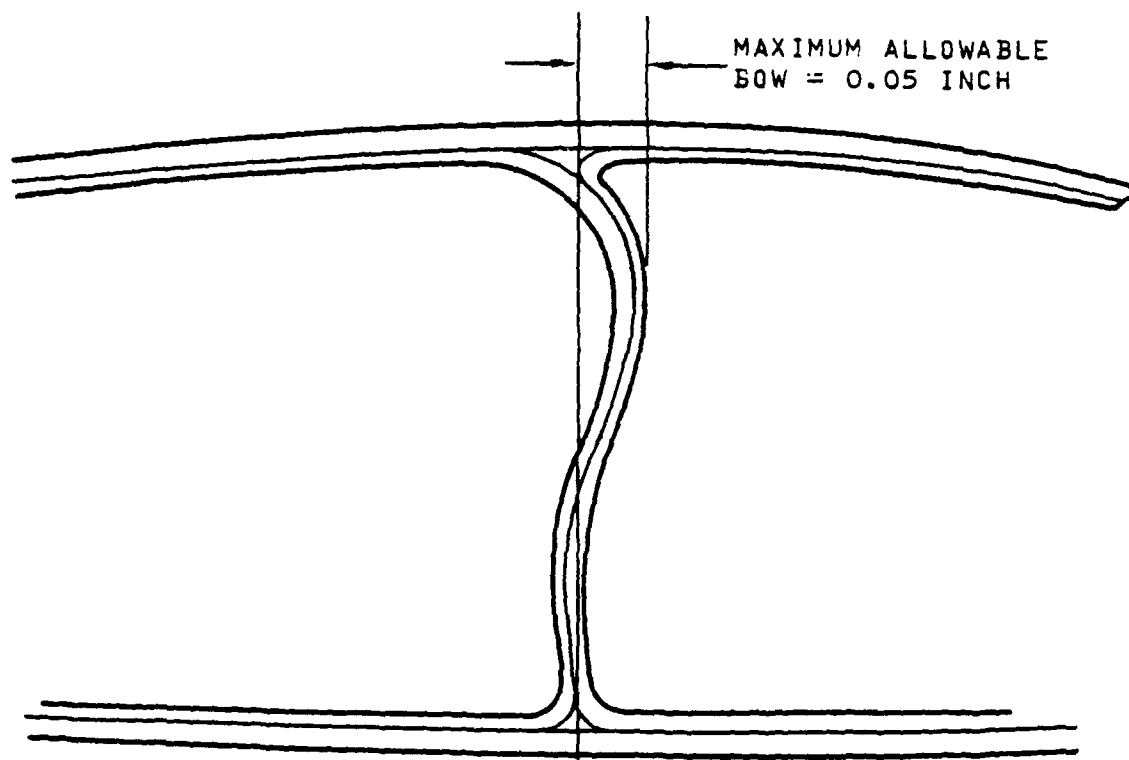


Figure F-6. Spartube rib defect.

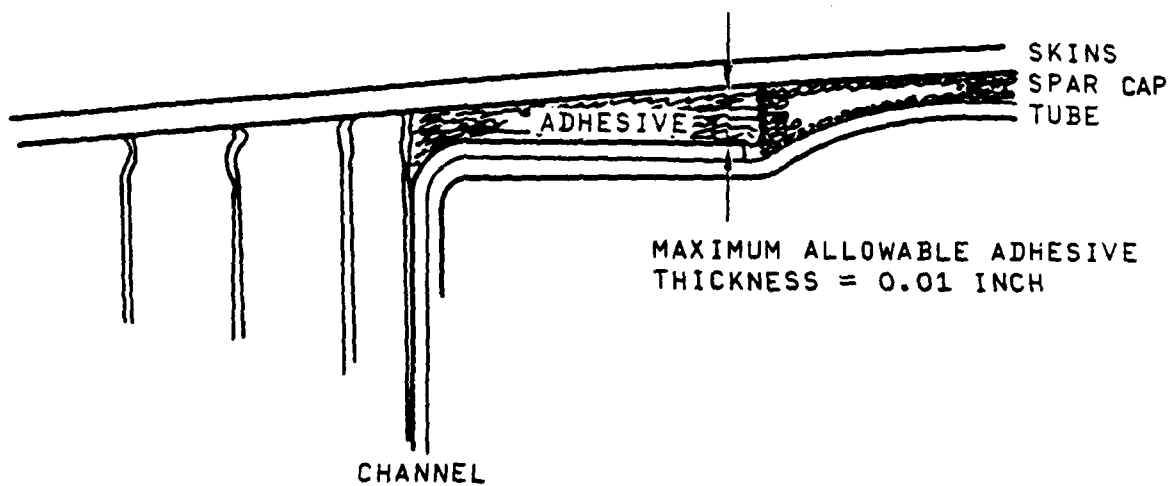


Figure F-7. Thick bondline, irregular adhesive thickness.

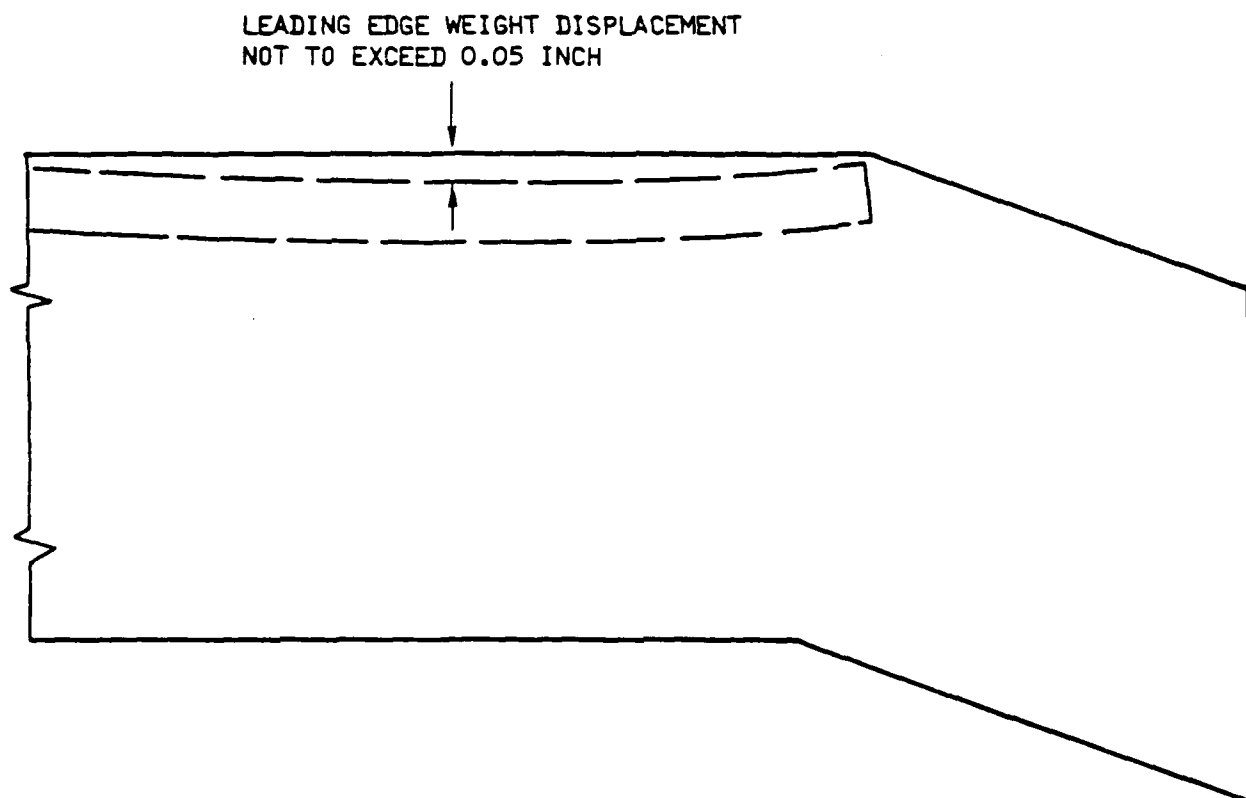


Figure F-8. Leading edge weight location tolerance.

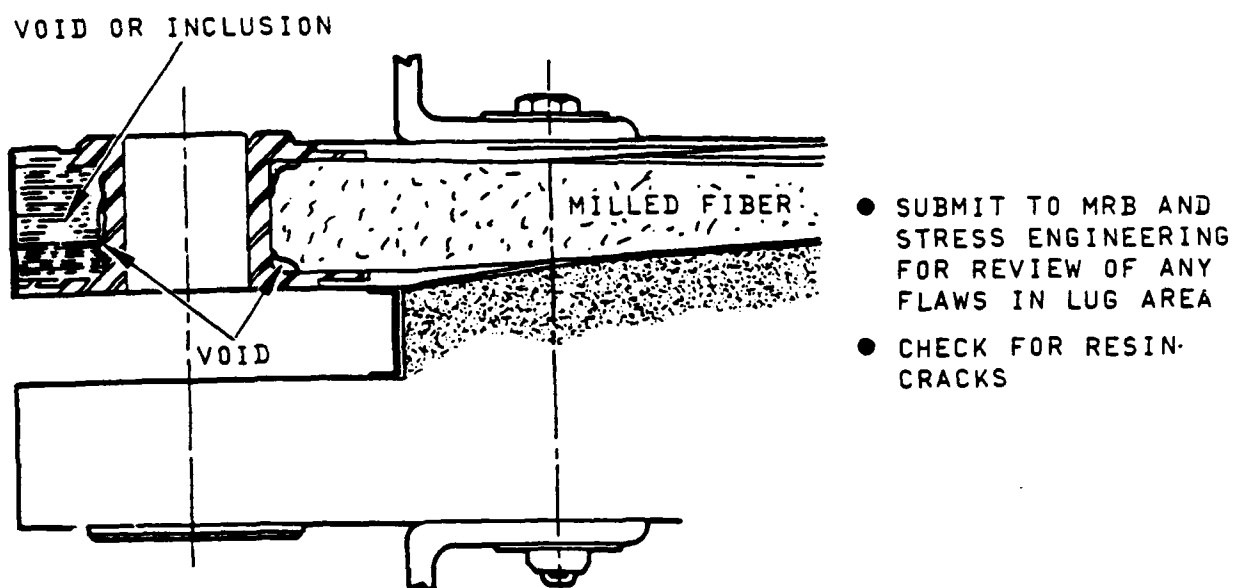


Figure F-9. Root end lug area.

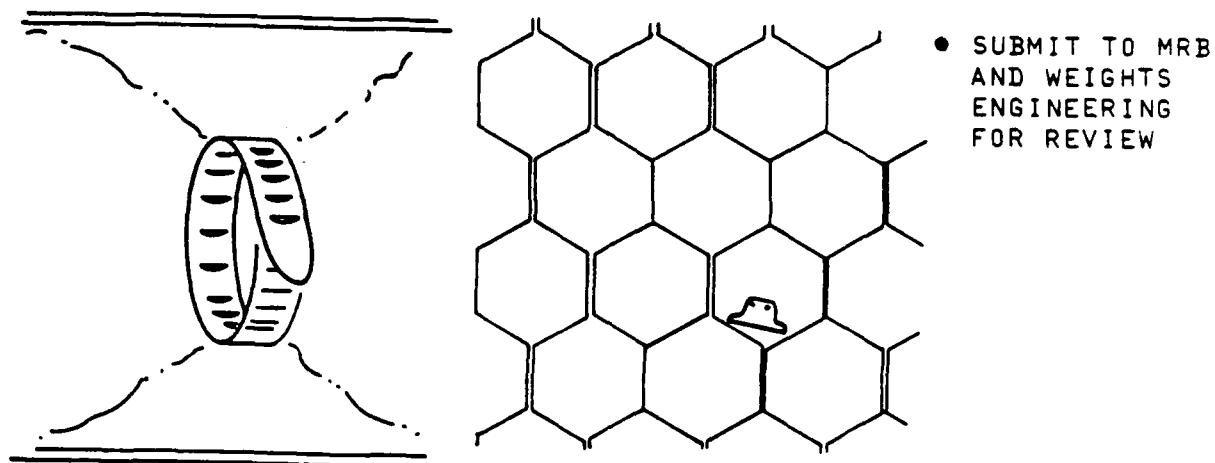


Figure F-10. Foreign objects x-rayed in blade.

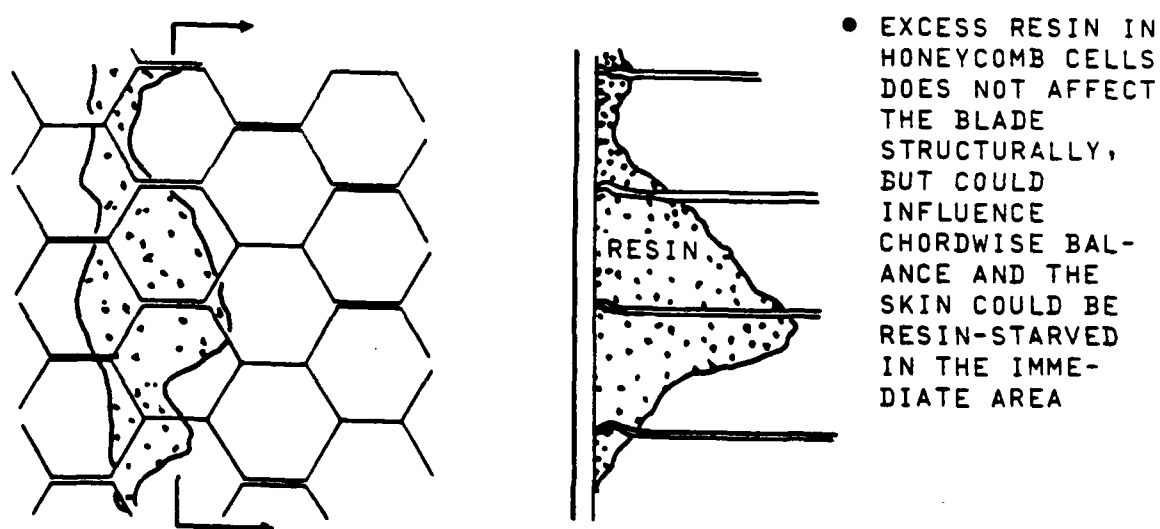
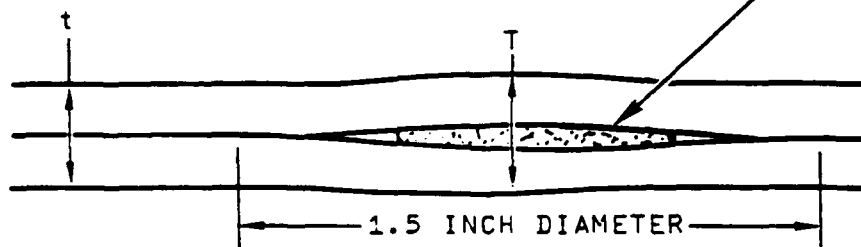
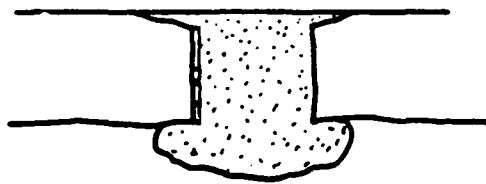


Figure F-11. Honeycomb core cells partially filled with resin.

HYPODERMICALLY REFILLED DELAMINATION

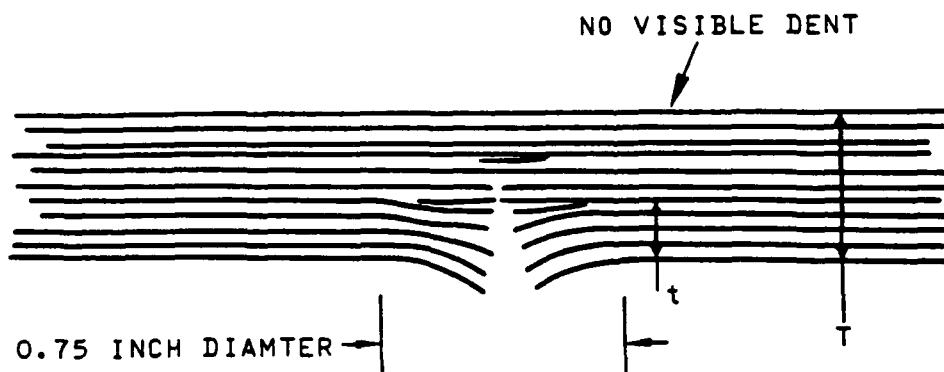


- $\frac{T}{t} \leq 1.10$
- FILL WITH RESIN
- MINIMUM FLAW SPACING IS 10 INCHES



- MIS-DRILLED HOLE UP TO 0.125 INCH DIAMETER BETWEEN B.S. 47 AND 268 MAY BE FILLED WITH RESIN

Figure 12. Reworked areas.



- $\left(\frac{t}{T}\right) \leq 0.1$
- MAXIMUM ALLOWABLE DIAMETER IS 0.75 INCH
- MINIMUM FLAW SPACING IS 5 INCHES

Figure F-13. Dent from tool drop or hammering.

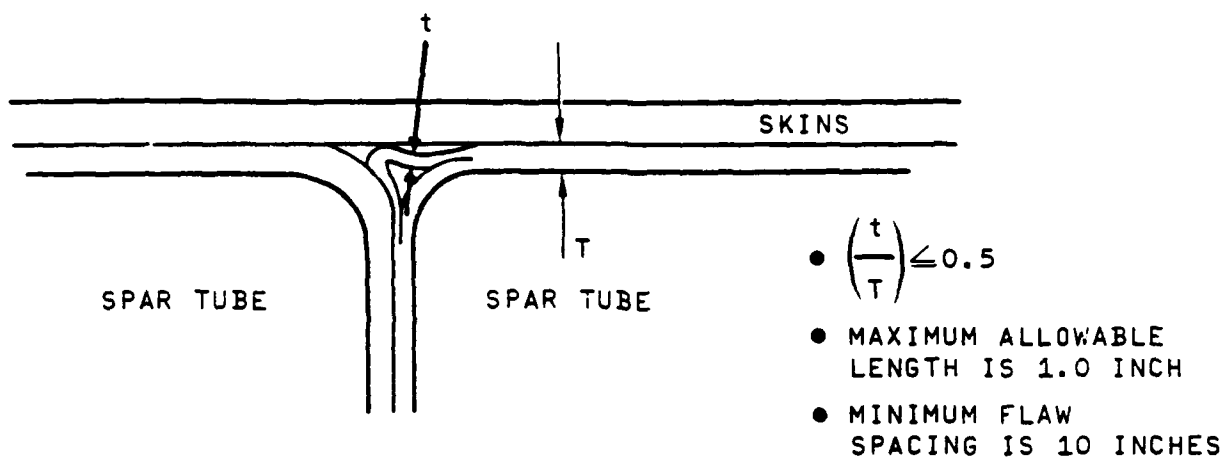


Figure F-14. Overlap, underlap, and gaps.

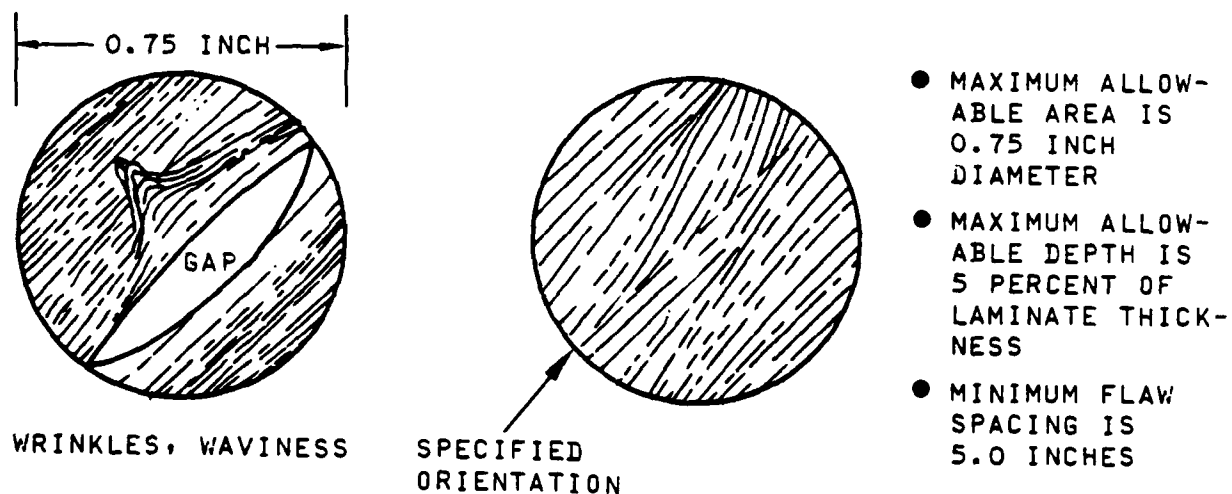


Figure F-15. Improper fly laydown.

APPENDIX G

FAILURE MODES, EFFECTS, AND CRITICALITY
ANALYSIS OF THE COMPOSITE
MAIN ROTOR BLADE FOR
THE AH-64A HELICOPTER

FAILURE MODES, EFFECTS AND CRITICALITY ANALYSIS (FMECA)

SUBSYSTEM: ROTOR GROUP - MAIN ROTOR WBS NO 711 PREPARED BY: J. JONES REV: A DATE 12-15-91 SHEET 1 OF 2

7-111417 SUB-MAIN (THRU BLADE ASSEMBLY)

REF NO (1)	ITEM NOMENCLATURE & FUNCTION (2)	FAILURE MODE/S (3)	METHOD OF DETECTION (4)	FAILURE EFFECT		TOTAL UNSCHEDULED MAINT ACTS (5)	Q Y V (6)	I L M E (7)	MODE L (8)	COMMENTS/COMPENSATING PROVISIONS (12)
				SUBSYSTEM (5)	AIR VEHICLE (6)	UMA (1000 HR) SOURCE (9)				
7-111417-576	CLOSURE ASSEMBLY - IN TROAND Provides good high speed advancing blade tip aerodynamic performance by the location of the aft portion of the swept tip.	(a) Cracked or broken skin (b) Debonding of the skin from the Kevlar/Kevlarcomb core. (c) Structural failure (complete).	Visual Inspection, NDI Visual Inspection, NDI Visual Inspection, system response.	Slight degradation of blade performance. Same as above. Blade becomes unstable.	Possibility of slight vibration. Same as above. Possibility of abort due to vibration.	.005 162 1 1				-45 S Deformation of the outboard aft closure may cause a change in blade tip path resulting in an out of track condition. -45 S Same as above. -106 S Partial loss of the closure would result in rotor imbalance and/or out-of-track condition. Vibration would vary, depending on the flight envelope.

NOTE:

Source 1 - (100)A, B and C series Helicopter Rotor Blade Inflation and wrap rate data analysis (OSAMRRI, technical report 71-58).

Source 2 - Reliability and Maintainability Analysis for Model 410 main rotor blade (BB-75).

Source 3 - Engineering judgement.

FORM 1170 JUL 71 (10-71)



FAILURE MODES, EFFECTS AND CRITICALITY ANALYSIS (FMECA)

SUBSYSTEM: ROTOR GROUP - MAIN ROTOR WBS NO 711 SHEET 7 OF 22
 PREPARED BY: J. JONES REV A DATE 12-10-81

7-311412500-1AAB CHUB BLADE ASSEMBLY

REF NO. (1)	ITEM NOMENCLATURE & FUNCTION (2)	FAILURE MODES (3)	METHOD OF DETECTION (4)	FAILURE EFFECT		TOTAL UNSCHEDULED MAINT ACTS (7)	Q Y	T I M E	M O D U L E	COMMENTS/COMPENSATING PROVISIONS (12)
				SUBSYSTEM (5)	AIR VEHICLE (6)	UMA 1000 HR				
7-31141	CLOSURE, INWARD Exposes the blade root area 2511-15 and portions of the blade leading and trailing edges. Fabricated from REVLAR and bonded to blade.	(a) Cracked or broken (b) Inboarded	Visual Inspection, NDI Visual Inspection, NDI	Slight to negligible degradation of blade performance Degradation of blade performance dependent upon extent of delam- ing.	None None	0.012 0.012	1 1	1 1	50 50	In process control limits the possibility of delamination.

FORM 1700-1 (10/77)



FAILURE MODES, EFFECTS AND CRITICALITY ANALYSIS (FMECA)

SHEET 3 OF 22

REV A DATE 11/15/11

PREPARED BY J. JONES

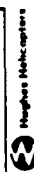
WBS NO 711

7-111612500-1A01 CHIR BLADE ASSEMBLY

SUBSYSTEM ROTOR LUBRIC-MAIN ROTOR

7-111612500-1A01 CHIR BLADE ASSEMBLY

REF NO (1)	ITEM NOMENCLATURE & FUNCTION (2)	FAILURE MODE/S (3)	METHOD OF DETECTION (4)	FAILURE EFFECT		TOTAL UNRECORDED MAINT ACINS (7)		Q V V (8)	T I M E (9)	O P E (10)	COM-ACINS/COMPENSATING PROVISIONS (12)
				SUBSYSTEM (5)	AIR VEHICLE (6)	UMA 1000 HR	SOURCE				
P-11161 2517 and 1	ROTOR BLADE ASSY When opened, allows access to the adjustable tuning system balance weights for installation, removal or adjustment. Fabricated from 6061-T6 aluminum alloy and secured by 4 screws.	(a) Cracked	Visual Inspection	None	None	.0012	1	2	1		
		(b) Bent or Loose.	Visual Inspection	Degraded blade performance due to lack of aerodynamic stability.	Possibility of a out-of-track condition.					.70 S	
										.30 S	



FORM 1170-01-1 (10/77)

FAILURE MODES, EFFECTS AND CRITICALITY ANALYSIS (FMECA)

SHEET 4 OF 22
DATE 12 JUL 81

PREPARED BY J. JONES REV A

WBS NO. 711

SUBSYSTEM ROTOR GROUP-MAIN ROTOR

7-331412500-MAIN UPR BLADE ASSEMBLY

REF NO (1)	ITEM Nomenclature & Function (2)	FAILURE MODE/S (3)	METHOD OF DETECTION (4)	FAILURE EFFECT		TOTAL UNSCHEDULED MAINT ACTS (7)	QTY (8)	T (9)	F (10)	M (11)	COMMENTS/COMPENSATING PROVISIONS (12)
				SUBSYSTEM (5)	AIR VEHICLE (6)	UWA 1000 HR (7)					
7-331412514 -1 thru -13	WEIGHT, ADJUSTABLE - BLADE ASSEMBLY, SHIPT TIP, MAIN ROTOR, AND COMPOSITE BLADES Allow effective tuning of the blade in both the spanwise and chordwise directions. The tuning alloy weights, A/R for the No. 1 spar tube and A/R for the No. 3 spar tube, are secured by a bolt, nut and washer.	(a) Structural failure (crack, bolt or washer).	Sound of loose objects during rotor coast down and/or blade movement.	Reg. High blade	Too slight to notice.	001 16.7	A/R 1				
		(b) Mucked loose (bolt or nut).	Same as above.	None	None						

FORM 1300-1 (10/71)

62 Hughes Helicopters

FAILURE MODES, EFFECTS AND CRITICALITY ANALYSIS (FMECA)

SUBSYSTEM: ROTOR CRIMP MAIN ROTOR WBS NO 711 PREPARED BY J. JONES REV A DATE 12-15-81 SHEET 01 72

7-111412500-1 AOH CRMP BLADE ASSY

REF NO (1)	ITEM NOMENCLATURE & FUNCTION (2)	FAILURE MODES (3)	METHOD OF DETECTION (4)	FAILURE EFFECT		TOTAL UNSCHEDULED MAINT ACTS (5)		Q Y (9)	T I M E (10)	M O D E (11)			COMMENTS/COMPENSATING PROVISIONS (12)
				SUBSYSTEM (5)	AIR VEHICLE (6)	UMA 1000 HR (7)	SOURCE (8)			(11B)	(11C)	(11D)	
7-11141 7516-11	FRONT CRIMP BLADE ASSY SHEET TIP MAIN ROTOR, AOH COMPOSITE BLADES Provides erosion protection of the blade. Consists of thermo plastic elastomer (Extens) 9.5 inch wide, bonded along the leading edge of the blade.	(a) Torn, shedded, eroded. (b) Debanded/pooling.	Visual Inspection Visual Inspection	Degraded erosion protection. Degraded erosion protection.	None Possible slight vibration.	16.2	1	1	1				

FORM 15100-1 (11-81)



FAILURE MODES, EFFECTS AND CRITICALITY ANALYSIS (FMECA)

SUBSYSTEM ROTOR GROUP MAIN ROTOR WBS NO 711 J. JONES REV A DATE 17 JUL 81 SHEET 6 OF 22

7-11141-2500 MAIN PROP BLADE ASSY BY

REF NO. (1)	ITEM NOMENCLATURE & FUNCTION (2)	FAILURE MODES (3)	METHOD OF DETECTION (4)	FAILURE EFFECT		TOTAL UNSCHEDULED MAINTAINANCE (7)	QTY (8)	T/F (9)	MOD (10)	COMMENTS/COMPENSATING PROVISIONS (12)
				SUBSYSTEM (5)	AIR VEHICLE (6)	UMA 1000 HR (7)				
7-11141-2500	BUSHING, ATTACH, SUPT TIP MAIN ROTOR, AND COMPOSITE BLADE Four metallic bushings are permanently attached at the clevis to resist the high radial load exerted by the expandable bushings.	(a) Fractured/cracked.	Visual Inspection	Possible degraded blade retention	None	0.10	1A7	4	1	Failure due to excessive fatigue failure test. Spec from NCHL carried the full G.F. load
		(b) Galled or scored	Visual Inspection	Difficulty in removing or installing blade attaching pin.	None					

FORM 1210-01-1 (10/71)

63 Hughes Helicopters

FAILURE MODES, EFFECTS AND CRITICALITY ANALYSIS (FMECA)

SHEET 8 OF 22

PREPARED BY J. JONES REV A DATE 12 12-81

SUBSYSTEM MOTOR GROUP-MAIN MOTOR

WBS NO 711

7-111412500 144N CTRB BLADE ASSPNRY

REF NO (1)	ITEM (2)	FAILURE MODES (3)	METHOD OF DETECTION (4)	FAILURE EFFECT		TOTAL UNDESIRABLE MAINT ACTION (7)		C (10)	D (11)	COMMENTS/COMPLAINTS PROVISIONS (12)
				SUBSYSTEM (5)	AIR VEHICLE (6)	UNQA 1000 HR (8)	SOURCE (9)			
7-31141 2511 7511	SPAR TUBE There are 1 spar tubes, each serving as an alternate load path in case of ballistic damage and also providing a small amount of structural stiffness. Indefinitely lived from Revlar 4N.	(a) Cracked (one) (b) Separated/bonding voids. (one)	MTI technique MTI technique.	Degraded performance Same as above (a).	None None	.003 .003	142 142	1 1	5 5	Other spar tubes serve as alternate load paths. Same as above (a). In-process inspection will detect depending if redundancy is provided by design.

7-111412500 007 1/10/77

63 Hughes Helicopters

FAILURE MODES, EFFECTS AND CRITICALITY ANALYSIS (FMECA)

SHEET: 9 OF 22
REV: A DATE: 12-15-81

PREPARED BY: J. JUMIS

WORK NO. 711

SUBSYSTEM: BLUON GROUP MAIN BLUON

J-111412500-1, AMI 0200 Blade Assembly

REF NO. (1)	ITEM DESCRIPTION & FUNCTION (2)	FAILURE MODE/S (3)	METHOD OF DETECTION (4)	FAILURE EFFECT		TOTAL UNDESIRABLE MAINT ACTION (10)	I	D	O	C	COMMENTS/COMPARATIONS PROVISIONS (12)
				SUBSYSTEM (5)	AIR VEHICLE (6)	UNSA (100) IN (100) IN					
J-111412500-1	CORE ASSEMBLY, AP1 The core assembly makes up the AP1, portion of the blade (airfoil) and adds to the chordwise and torsional stiffness. Assembly consists of a graphite fabric channel, P/M J-111412513, a Bomec Honeycomb Core, P/M J-111412512 and graphite trailing edge longer, P/M J-111412516	a) Channel, P/M J-111412513 1. Delaminated 2. Bonding voids b) Core, P/M J-111412512 1. Separation of splice joints c) Trailing edge longer, P/M J-111412516 1. Bonding voids 2. Cracked	Visual inspection N.D.I. Same as above N.D.I. Visual inspection N.D.I. Visual inspection	Possibility of slight degradation of blade performance Same as above None Same as a) 1 above Same as a) 1 above	Possibility of slight vibration Same as above None Possibility of vibration due to airfoil deformation Same as above	0.11 (100) IN	1 (100) IN	1 (100) IN	1 (100) IN	1 (100) IN	AP1 deformation along the channel may cause a cut-off track condition Skin to core bond would eliminate any deformation due to splice separation. Vibration due to blade cut-track depends on amount of airfoil deformation Trailing edge subjected to light loads only

McPherson Manufacturing, Inc.

FAILURE MODES, EFFECTS AND CRITICALITY ANALYSIS (FMECA)

SUBSYSTEM: ROTARY AIRCRAFT-MAIN ROTOR WBS NO 711 SHEET: 10 OF 22 PREPARED BY: J. JONES REV: A DATE: 1-1-71

7-311412500-1AAR-INNER BLADE ASSEMBLY

DEF NO (1)	ITEM NOMENCLATURE & FUNCTION (2)	FAILURE MODES (3)	METHOD OF DETECTION (4)	FAILURE EFFECT		TOTAL DESIGNED MAINTENANCE FACTORS (7)			Y M E (10)	X (11)	COMMENTS/COMPENSATING PROVISIONS (12)
				SUBSYSTEM (5)	AIR VEHICLE (6)	NOI (8)	SOURCE (9)	UN (10)			
7-31141 2537, 49 44, 51, 53	SPAR CAP ASSEMBLY Primary members that provide flapwise stiffness for the blade. Fabricated from Kevlar 49, the assembly consists of an inner skin, spar sub-assemblies, and spar wraps and a graphite inner skin.	(a) Cracked	NDI technique	Degradation of blade performance.	No immediate effect.		.001	142	1	50	A crack, depending on size and location, would decrease the flapwise stiffness, resulting in a out-of-track condition with a change of power
		(b) Delaminated, delaminated	NDI technique	Loss of blade performance.	Possible mission abort					40	

FORM 1700-00-110071

63 Hughes Helicopters

FAILURE MODES, EFFECTS AND CRITICALITY ANALYSIS (FMECA)

SUBSYSTEM: BUTON GROUP-MAIN ROTOR WBS NO: 111 PREPARED BY: J. JONES REV: A DATE: 11 OCT 72 SHEET: 11 OF 22

7-31141/NO 1 AIR CRR BLADE ASSEMBLY

REF NO (1)	ITEM DESCRIPTION & FUNCTION (2)	FAILURE MODES (3)	METHOD OF DETECTION (4)	FAILURE EFFECT		TOTAL UNSCHEDULED MAINT ACTS (7)		P V	I M E	NO OF (11)	COMMENTS/COMPENSATING PROVISIONS (12)
				SUBSYSTEM (5)	AIR VEHICLE (6)	UNMAINT (8)	SOURCE (9)				
7-31141 25M RSQ-11	SEIN, DRIBBLEPS, INWARD Provides skin reinforcement to meet blade torsional requirements. Consists of a lower and upper assembly fabricated from Kovlar 49.	(a) Cracked (b) Delaminated, delaminated.	Nil technique or visual inspection Nil technique or visual inspection	Possible degraded blade performance Loss of blade torsional constraint.	No effect Possibility of vertical vibration.	1 1	1 1	1 1	1 1	1 1	Should be discovered on daily inspection Blade run angle may change more than other blades due to deflection doubler.

FORM 1376-001 (10/71)

63 Hughes Helicopters

FAILURE MODES, EFFECTS AND CRITICALITY ANALYSIS (FMECA)

SHEET 12 OF 22
DATE 12-12-81

PREPARED BY J. JONES REV A

WBS NO 711

SUBSYSTEM: MOTOR GROUP-MAIN MOTOR

7-311A12500-3 AHI CHINA BLADE ASSEMBLY

REF NO. (1)	ITEM DESCRIPTION & FUNCTION (2)	FAILURE MODE/S (3)	METHOD OF DETECTION (4)	FAILURE EFFECT		TOTAL UNDESIR- ABLE ACTING (7)	Q	P	I	O	S	C	COMMENTS/COMPENSATING MEASURES
				SUBSYSTEM (5)	AIR VEHICLE (6)	Q							
2-311A1 2510	ROTOR, IMMERSED CAP Provides cap reinforcement to meet blade structural requirements. Consists of 21 Kevlar 40 fabricated plies.	(a) Cracked (c) Delaminated, delaminated.	NDI technique NDI technique	Degraded blade per- formance. Degrated blade per- formance.	No effect Possibility of vertical vibration.	.013 .02	1 2	1 1	1 1	1 1	1 1	1 1	Blade core angle may differ from angle of other blades.

FORM 13-00 010-1 (10/79)

63 Hughes Helicopters

FAILURE MODES, EFFECTS AND CRITICALITY ANALYSIS (FMECA)

SHEET 11 OF 22
REV A DATE 12-15-81

PREPARED BY J. JONES

WBS NO. 711

SUBSYSTEM ROTOR GROUP MAIN ROTOR

7-311412500-1A00 CHOP BLADE ASSEMBLY

REF NO. (1)	ITEM DESCRIPTION & FUNCTION (2)	FAILURE MODE/S (3)	METHOD OF DETECTION (4)	FAILURE EFFECT		TOTAL UNDESIRABLE MAINT ACTS (7)		V I T I		C O P Y		COMMENTS/REMARKS/PROVISIONS (12)
				SUBSYSTEM (5)	AIR VEHICLE (6)	DATA 1000 HR (8)	SOURCE (9)	(10)	(11)	(12)	(13)	
7-311412500-1A00-1	WING, INBOARD - BLADE ASST. SHEET TIP MAIN ROTOR, AAM COMPOSITE BLADES	(a) Cracked	NPI technique	No effect	No effect	.001	127	1				
7-311412500-1A00-2	Fill the triangular cavity between the inboard longerons and bulkheads to ensure structural integrity of the blade root area. Consists of resin impregnated milled E-glass fibers.	(b) Debonded	NPI technique	Loss of root structural integrity and blade performance degraded.	No effect							

FORM 3170-11-1 (10/71)



SHEET 14 OF 22
REV A DATE 12-15-81

MOTOR GRIP-MAIN MOTOR
 WBS NO 311
 PREPARED BY: J. K. W. S.
 REV: DATE:

7-111412500-MAIN ROTOR BLADE ASSEMBLY												
REF NO (1)	ITEM DESCRIPTION & FUNCTION (2)	FAILURE MODE/S (3)	EVIDENCE OF DETECTION (4)	FAILURE EFFECT		TOTAL UNDESIRABLE HUMAN ACTS (7)	9 Y	1 E	X O	11 S	COMMON RISKS/COMPLICATIONS PROVISIONS (12)	
				SUBSYSTEM (5)	AIR VEHICLE (6)							UNDESIRABLE HUMAN ACTS (7)
7-11141 2541	COMP. ASSEMBLY - COMPOSITE. MAIN ROTOR BLADE SWEPT TIP fills the forward section of the swept tip region to ensure structural integrity. Consists of Kevlar 49, resin impregnated fibers and foam.	(a) Cracked (b) Debonded, delaminated	(a) technique (b) technique	Degraded swept tip structural integrity and blade performance. Loss of swept tip structural integrity and blade performance.	No effect Possibility of vertical vibration.	.001 .001	1 1	1 1	1 1	1 1	(12)	

FAILURE MODES, EFFECTS AND CRITICALITY ANALYSIS (FMECA)

SHEET 15 OF 22
 REV A DATE 12-15-61

PREPARED BY J. JONES

7-31161250C-3140 CWRB BLADE ASSEMBLY

WBS NO. 711

SYSTEM: ROTOR GROUP-MAIN DRIVE

7-31161250C-3A00 CMBR BLADE ASSEMBLY													
REF NO. (1)	ITEM NOMENCLATURE & FUNCTION (2)	FAILURE MODE/S (3)	METHOD OF DETECTION (4)	FAILURE EFFECT		TOTAL UNSCHEDULED MAINT ACTS (5)		PRIORITY (6)	I (7)	O (8)	D (9)	COMMENTS/COMPENSATING PROVISIONS (12)	
				SUBSYSTEM (10)	AIR VEHICLE (11)	TIME 1000 HR (13)	SOURCE (14)						
7-31161 2545	SKIN, OUTER Provides a major portion of the blade torsional stiffness and shear tie for the spar caps and the trailing edge longerons. Consists of one continuous piece of 0.062 inch thick Revalor 49.	(a) Cracked (b) Delaminated, debonded.	Visual inspection NDI, visual inspection	Degraded blade performance. Loss of blade performance.	No immediate effect. Possibility of vibration.	.041	162	1	1		40	S Should be found on daily inspection and repaired as required.	
											45	S Change in air foil may cause an out-of-track condition. In-process control limits delamination possibilities.	

62 Hughes Helicopters

FORM 1320 REV 11/67

FAILURE MODES, EFFECTS AND CRITICALITY ANALYSIS (FMECA)

SHEET 16 OF 22
REV A DATE 12-15-81

PREPARED BY J. JONES

WBS NO 711

SUBSYSTEM: BUTIR GROUP MAIN BUTIR

7-311A1750R-TAN OVER BLADE ASSEMBLY

REF NO (1)	ITEM DESCRIPTION & FUNCTION (2)	FAILURE MODES (3)	METHOD OF DETECTION (4)	FAILURE EFFECT		TOTAL CRITICALITY RATING (5)		COMMENTS/COMPENSATING PROVISIONS (12)
				SUBSYSTEM (5)	AIR VEHICLE (6)	WHA (100 IN) (7)	BOUNCE (10) (8)	
7-311A1 25A2-9 -11, -13 15, 19, 21, 23, and 25	LIGHTNING SCREEN BLADE ASSY SUPPORT TIP MAIN BUTIR AAM (COMPOSITE BLADES) Shield all metallic components in the blade, provide lightning protection of the blades and provide a continuous electrical path into the hub (the shield in conductively bonded to the blade root bushings). Uninsulate of 200 x 200 (all) with 2 all wire dia, 50% aluminum.	(a) Cracked, discontinuities. (b) Bonding voids.	MTI technique MTI technique	Possible loss of some lightning shield protection.	No effect.	.001 142 R	1	Change in stress due to voids, may cause an out-of-track. In-process control limits the possibility of bonding voids.

FORM 1310 REV 11/67/75

Hughes Helicopters

FAILURE MODES, EFFECTS AND CRITICALITY ANALYSIS (FMECA)

SUBSYSTEM ROTOR GROUP-MAIN ROTOR WBS NO 711 SHEET 12 OF 22 PREPARED BY J. JONES REV A DATE 12-15-81

7-111A1250 - MAIN OMBR BLADE ASSEMBLY

7-311412500 - MAIN CHAIN BLADE ASSEMBLY														
REF NO (1)	ITEM NO (2)	FAILURE MODE/S (3)	METHOD OF DETECTION (4)	FAILURE EFFECT		TOTAL UNDESIRABLE MAINT ACTS (5)		P (6)	Q (7)	R (8)	S (9)	T (10)	U (11)	V (12)
				SUBSYSTEM (13)	AIR VEHICLE (14)	WAS 1000 HRS (15)	SOURCE (16)							
7-31141 2540	WEIGHT, FORWARD TIP-MADE ASSEMBLY, SHORT TIP MAIN BLADE, AIR COMPOSITE BLADE Located in the outboard end of the No. 1 spar tube, provision for effective tuning of the blade in the spanwise and chordwise direction. Fabricated from 17-4PH CRES & integrally wound into the spar	(a) Damaged threads	Found during inspection or balance adjustment.	None	None	.001	142	1	1					
		(b) Bending voids	NDT technique	No effect	None									

SHEET 18 OF 22

PREPARED BY: _____
 DATE: _____
 REV: _____
 DATE: _____

7-111412500-1 ALL OTHER READY ASSEMBLY

U.S. NO 711

CONCLUSIONS

REF NO. (1)	ITEM		FAILURE MODES (2)	MODE OF DETECTION (4)	FAILURE EFFECT		TOTAL UNSCHEDULED MAINT ACTS (7)	V	I F E	O	M O D E L	COMMENTS/COMPENSATING PROVISIONS
	DESCRIPTION & FUNCTION (3)	SUBSYSTEM (5)			AIR VEHICLE (6)							
2-31161 2540	WEIGHT, AFT TIP-BLADE ASST. CURVE TIP MAIN ROTOR, AIN TURNSHIP BLADE located in the outboard end of the No. 3 spar tube, provides for effective tuning of the blade in the spanwise and chordwise direction. Fabricated from AlMg-T6 Alon 6 integrally wound into the spar		(a) Damaged threads (b) Bending voids	Found during inspection of balance adjustment.	None None	None As effect	16.2	1	1	100	111	

(b)(7) - DISCLOSE

Mitsubishi Motors

FAILURE MODES, EFFECTS AND CRITICALITY ANALYSIS (FMECA)

SHEET 19 OF 22
REV A DATE 12-15-81
J. DOWNS

PREPARED BY

7-311412500-1A41 THER BLADE ASSEMBLY

W.B.S. NO. 711

SUBSYSTEM: ROTOR GROUP-MAIN ROTOR

REF NO. (1)	ITEM DESCRIPTION & FUNCTION (2)	FAILURE MODES (3)	METHOD OF DETECTION (4)	FAILURE EFFECT (5)		TOTAL UNDESIRABLE MAINT ACTS (6)		P (7)	V (8)	I (9)	D (10)	S (11)	COMMENTS/REMARKS/PROVIDORS (12)
				SUBSYSTEM (5a)	AIR VEHICLE (5b)	UMA (6a)	SOURCE (6b)						
7-31141 2553	BACKING STRIP- BLADE ASSEMBLY, SHEET TIP MAIN ROTOR, A41 COMPOSITE BLADES Stainless steel backing strip for the thermoplastic elastomer erosion strip. (Estate)	(a) Cracked (b) Bonding voids (c) Errored/peened	NDI technique and/or inspection when replacing strip. NDI technique Visual	No effect No effect Degraded performance.	None Possibility of slight vibration.	.075	147	2	1				In-process control limits the possibility of bonding voids.



FORM 1370 REV 11/87

FAILURE MODES, EFFECTS AND CRITICALITY ANALYSIS (FMECA)

SUBSYSTEM: BUTTUP (MAIN ROTOR) WBS NO. 711 SHEET: 20 OF 22 PREPARED BY: J. JONES REV: A DATE: 12-11-81

7-311417-000, AAM POWER BLADE ASSEMBLY

DEF NO (1)	ITEM NO/DESCRIPTION & FUNCTION (2)	FAILURE MODE/S (3)	METHOD OF DETECTION (4)	FAILURE EFFECT		TOTAL UNDESIRABLE MAINT ACTIONS (5)		C	I	D	S	COMMENTS/COMPENSATING PROVISIONS (12)
				SUBSYSTEM (6)	AIR VEHICLE (8)	UNDA 1000 HR (7)	SOURCE (9)					
7-31141 2554	BACKING STRIP-BLADE ASSEMBLY SHEET TIP MAIN ROTOR, AAM COMPOSITE BLADES Stainless steel backing strip for the tip thermo plastic elastomer erosion strip. (Eslane)	(a) Cracked (b) Bonding voids (c) Eroded/peened	NDI technique and/or inspection when replacing strip. NDI technique Visual	No effect No effect Degraded performance.	None None Possibility of slight vibration.	.025 .162 1	1 1 1					In-process control limits the possibility of bonding voids.

FORM 1210 REV 118/71



PREPARED BY: J. LINGS SHEET: 21 OF 22 DATE: 12-15-61

ROUTING SLIP

W. 22. NO. 7. 11.

PREPARED BY: J. Lums

NEW A DATE: 17-15-01

7-111412510-J AAM CHRS Blade Assembly

ITEM		FAILURE MODE/S (2)	METHOD OF DETECTION (4)	FAILURE EFFECT		TOTAL UNDESIRABLE MAINT. ACTION (7)	V (6)	I (9)	D (10)	R (11)	COMMENTS/CONSIDERATIONS PROVIDED
REF NO. (1)	DESCRIPTION & FUNCTION (3)			SUBSYSTEM (5)	AIR VEHICLE (8)						
J-311412 561 and 5	HINER-181M TAR Fabricated from .016 sheet Al. Ally 2024-T1. The hanger is located on the top side and the -3 is located on the bottom of the trailing edge from Sta. 175.50 to Sta. 266.00. The rth tab is bent up or down, at various stations so as to aerodynamically change the blade airfoil making it compatible with the other blades.	a) Cracked b) Bonding voids	Visual, inspection Visual, inspection	Diminble degradation of blade performance None	None	.015 26.1	16			.45 .15 .40	S M Amount of vibration would depend on size and location of crack

1971

CS **Hughes Electronics, Inc.**

RM LEVEL FAILURE MODES, EFFECTS AND CRITICAL ANALYSIS (FMECA)

SUBSYSTEM: MAIN MOTOR RM: CDRN PREPARED BY: I. JONES SHEET: 22 OF: 22
 S/N: 100 RM: 2-31412500-3 RM P/N: 2-31412500-3 REV: DATE: 12-15-81

ITEM PART NO. DESCRIPTION	FAILURE MODES (2)	DETECT (3)	FAILURE EFFECT		ITEM FAILURE RATE (4)	Y T F M E C O D E	COMMENTS/REMARKS (5)
			RU (5)	SUBSYSTEM (6)	FAILURE RATE (4)		
BLADE DE-ICING: Electro thermally heating elements of the de-icer are bonded to the leading edge of the blade. The de-icer is divided internally into four cordless heating zones along the leading edge of the blade. Each zone is heated sequentially to melt the bond between the ice and the blade surface to allow centrifugal and aerodynamic forces to sweep the loosened ice away. The de-icer mat extends over 4.2 percent of the top surface chord length and 26 percent of the lower surface chord from the blade leading edge.	(a) De-icer blanket 15-200-23 P/N 7-311412546 1. Blanket element cracked. 2. Bonding voids. 3. Open in electrical wiring from connector to blanket.	ND) technique ND) technique Pre-test-to-test and/or with system on, rotor stable, check blade for heat rise.	Possibility of degraded de-icing in that zone. No effect on de-icing. Loss of de-icing capability for that blade.	Possibility of vibration. No effect on de-icing. Possibility of mission abort due to imbalanced rotor.	.045 24.3	1	Amount of vibration, due to rotor imbalance will depend on amount of ice build-up. In-process control limits the possibility of voids.
	(b) Receptacle-electrical connection for blade de-icing. 15-20025 P/N 103121-R-81814W 1. Open/shorted pin 2. Bent pin/cracked receptacle (c) Receptacle - restraint receptacle to the connector bracket arm. 15-200-25 P/N 103121-15A10A 1. Cracked/loose	Pre-test-to-test Pre-test-to-test Visual inspection	Loss of de-icing capability in that blade. Same as above None	Same as above (a). Same as above None	1.3 S 0.1 M 0.1 M 0.1 M 0.1 S	1	Blade short would depend on vibration on the result of ice build-up on that blade. Same as above (a).
	(d) Connector bracket arm 15-200-26 P/N 1-311412517 1. Cracked/bent 2. Fractured	Visual Visual	None None, but may result in a secondary failure, such as a loose connector and/or broken wire.	None No effect	0.05 S 0.1 S	1	

62 Hughes Helicopters

APPENDIX H
STRESS ANALYSIS

The static and fatigue stress analyses for the CMRB show that it is satisfactory, structurally, for the mission of the AH-64A. For the undamaged blade, the analysis shows that there will be no failure at ultimate load (1.5 x limit load), and negligible permanent set under limit loads. Table H-1 summarizes the minimum margins of safety for critical regions of the blade. Positive margins are shown throughout. This finding was verified by the laboratory tests.

TABLE H-1. MINIMUM STATIC MARGINS OF SAFETY

Blade Station	Item	Load Condition	Type of Stress	Margin of Safety
39	Attach Lugs	RPM = 289 V = 180 Kts $M_z = 3.5$	Tension in Kevlar Windings	0.40
191.7	Constant Section	RPM = 289 V = 180 Kts $M_z = 3.5$	Compression in Kevlar spar longos in the constant section	0.06
87	Constant Section	RPM = 289 V = 180 Kts $M_z = 3.5$	Shear due to torsion in $\pm 45^\circ$ layers of the constant section	0.05
89	Constant Section	RPM = 0 Max Torque V = 0 Kts $n_z = 1.0$	Compression in Kevlar spar longos after the T. E. longos have buckled	High
270	Blade Tip	RPM = 376 $V_f = 150$ Kts $n_z = 3.5$	Tension load applied to tip weight housings and blade tip	High

The fatigue life of the CMRB has been substantiated by a combination of analysis and component fatigue tests. In using the test data, the endurance limit is reduced for scatter effects according to Table H-2. The life for the various sections of the CMRB are presented in Table H-3. That the CMRB has an adequate static margin of safety and a fatigue life in excess of 4500 hours has been verified by laboratory test of full-scale specimens.

TABLE H-2. L-N CURVE SCATTER REDUCTION FACTORS

Number of Fatigue Test Specimens	Percent of Mean L-N Curve Used
1	50%
2	65%
3	75%
4 or more	Statistical analysis (M-3 σ)

TABLE H-3. FATIGUE ANALYSIS - SUMMARY OF COMPONENT LIVES

Blade Station	Item	Condition	Life
39	Root Lugs	Weighted Fatigue	4,500 hours
		Ground-Air-Ground	100,000 hours
39	Root Close-Out	Weighted Fatigue	Infinite
55	Root Doubler	Weighted Fatigue	4,500 hours
84	Constant Section	Weighted Fatigue	4,500 hours
160	Constant Section	Weighted Fatigue	4,500 hours
192	Constant Section	Weighted Fatigue	4,500 hours
270	Tip Components	Gag	Infinite

Ballistic survivability calculations show that the CMRB can fly a minimum of 30 minutes after being damaged by a 23mm HEI-T projectile. Figure H-1 summarizes the results of the survivability analysis.

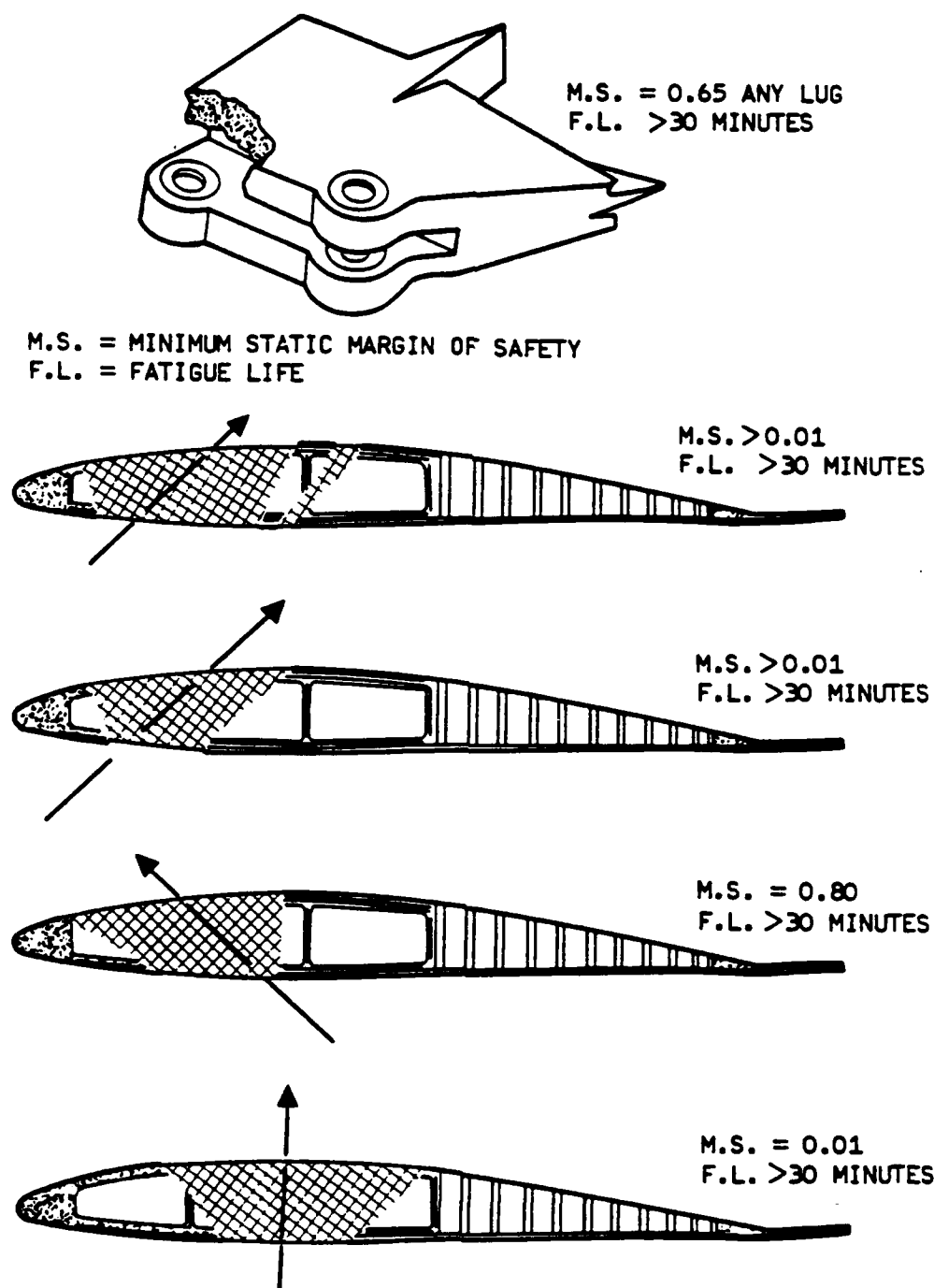


Figure H-1. Ballistic survivability summary - 23mm HEI-T threat.

APPENDIX I
MASS PROPERTIES

The mass properties of the CMRB are summarized in Tables I-1 and I-2. The figures show the distribution of weight, chordwise center of gravity, and pitching inertia along the span of the blade. Table I-1, the rotor blade group (shipset of four blades) weight chart specified by Reference I-1, shows a CMRB group weight of 603.2 pounds - a 24.6-pound reduction from the metal blade group. Table I-2 documents the CMRB center of gravity characteristics for three zones along the blade span that were required for blade dynamic analysis. The polar moment of inertia of each CMRB is 993 slug-feet-squared as compared with 1017 slug-feet-squared for the metal blade. This is anticipated to have a negligible effect on autorotation performance.

I-1 Military Standard - Weight and Balance Data Reporting Forms for Aircraft (including Rotorcraft), MIL-STD-1347A Part II, 30 September 1977.

TABLE I-1. AH-64A ROTOR/BLADE GROUP WEIGHT

		Metal		CMRB			
1.							
2.							
3.							
4.							
5.							
6.							
7.							
8.	Spar/Tube-Front	87.1		143.6			
9.	Spar/Tube-Intermed.	64.3		14.4			
10.	Spar/Tube-Rear	65.1		19.6			
11.	Interspar-Cover			107.2			
12.							
13.							
14.							
15.	Interspar Adhesive	11.5		-			
16.							
17.							
18.							
19.							
20.	Leading Edge-Cover	94.6		16.4			
21.							
22.							
23.							
24.	L.E. De-Ice Blanket	13.9		6.8			
25.							
26.							
27.							
28.	Trailing Edge-Member	-		20.0			
29.	Trailing Edge Cover	25.5		-			

TABLE I-1. AH-64A ROTOR/BLADE GROUP WEIGHT (CONT)

		Metal		CMRB			
30.							
31.	Trailing Edge Ribs	0.9		-			
32.	Trailing Edge-Core	8.1		6.8			
33.							
34.							
35.	Trailing Edge-Adhes	12.1		5.2			
36.							
37.							
38.							
39.							
40.	Tips	33.9		16.0			
41.							
42.							
43.							
44.							
45.	Balance Weights-Tip	14.7		12.8			
46.	Bal. Wts. -Lead. Edge	95.1		152.8			
47.							
48.							
49.	Trim Tab	11.0		2.0			
50.							
51.	Root End-Fittings	73.1		57.6			
52.	Root End-Fasteners	10.5		3.6			
53.	Exterior Finish	6.3		5.2			
54.	Static Discharge	0.1		0.8			
55.	M/R Mfg. Allowance	-		12.4			
56.	Column Totals	627.8		603.2			
57.							

TABLE I-2. CENTER OF GRAVITY CHARACTERISTICS

	Center of Gravity				
	Weight (lb)	BS (in.)	Chord (in.)	% Chord	Dynamic Criteria % Chord
CMRB	Root (BS 37 to 82)	55.34	5.78	27.5	≤27.6
	Mid (BS 82 to 244)	162.95	5.37	25.6	≤26.5
	Tip (BS 244 to 288)	<u>33.62</u>	<u>5.25</u>	<u>25.0</u>	<u>≤25.0</u>
	Total	147.30	5.46	26.0	26.4
	(Shipset: 589.20 lb)* (Spanwise moment = 23,500 lb-in)				

*603.2 lb in Table I-1 includes manufacturing allowance.

APPENDIX J

AEROELASTICITY AND MECHANICAL STABILITY

The stability of the CMRB and support structure was investigated by a linear eigenvalue analysis and by a nonlinear transient analysis described in Reference 8. The eigenvalue analysis couples an eleven-cell single blade to a simple model of the hub flexibility and fuselage rigid body degrees of freedom. The rotor support flexibility and fuselage rigid body degrees of freedom are necessarily isotropic for this linear analysis. Coupling terms are included to relate blade pitch changes to hub motion. This idealization of the system is adequate to represent the advancing and regressive cyclic modes of the system, the most important of which is the advancing whirl mode. The nonlinear transient analysis allows the anisotropic properties of the rotor system to be represented and includes all four blades, lateral and longitudinal control stiffnesses, hub constraints, fuselage free-body modes, and two fuselage bending modes. Each blade is represented by five degrees of freedom: two flap modes, two torsion modes, and one lead-lag mode.

Cyclic and collective resonance diagrams, including the influence of aerodynamic forces, are presented in Figures J-1 and J-2, respectively, and show good separation between natural frequencies and forcing functions for all modes except for the second torsion mode and the 7Ω line. However, this mode is very well damped and was impossible to excite during the whirlstand test, and is considered to be acceptable for the CMRB. Figure J-3 shows modal damping ratios as a function of rotor speed for a series of forward speeds, and Tables J-1 through J-3 show the corresponding natural frequencies. Forward speed is accounted for by applying aerodynamic forces corresponding to the 90-degree azimuth position (advancing blade).

Figure J-4 shows the whirl mode damping for the severe condition obtained from the linear eigenvalue analysis. The most critical condition ($\theta_{3/4} = 6$ degrees, $N_Z = 3.5$) has a stability boundary above 130 percent N_R .

Advancing lag mode stability boundaries are presented in Figure J-5 and show a low boundary for the case of high load factors at low collective pitch settings (cyclic pullup in autorotation). However, in comparing this figure with Figure B-7 of Reference J-1, the CMRB is shown to have an improvement in the advancing lag mode stability boundaries over that of the metal

J-1 Silverthorn, L. J.; Childers, H. M., and Neff, J. R., Preliminary Aeroelasticity and Mechanical Stability Report YAH-64 Advanced Attack Helicopter, Hughes Helicopters, Inc. Report No. 77-X-8001, June 1976.

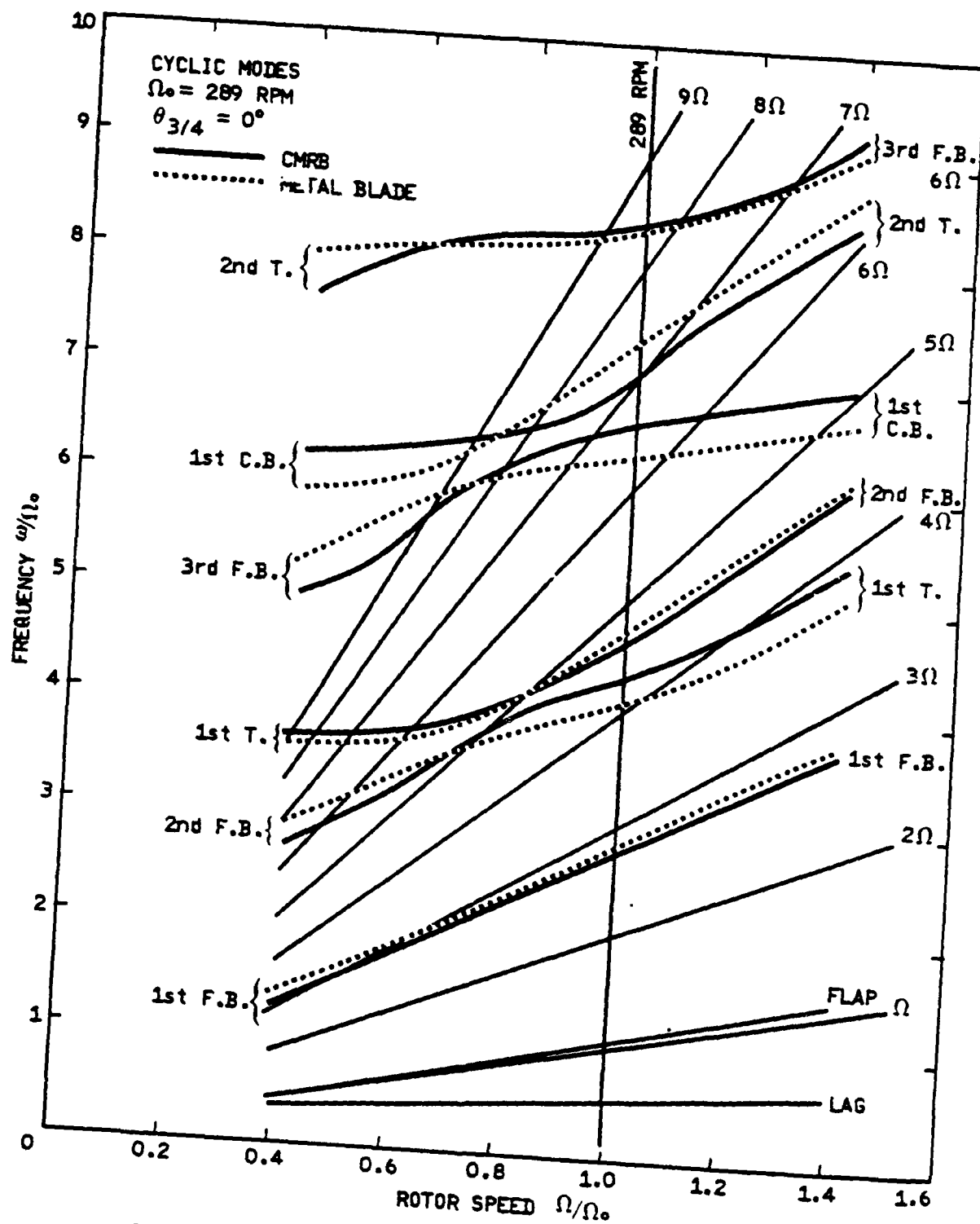


Figure J-1. CMRB cyclic resonance diagram.

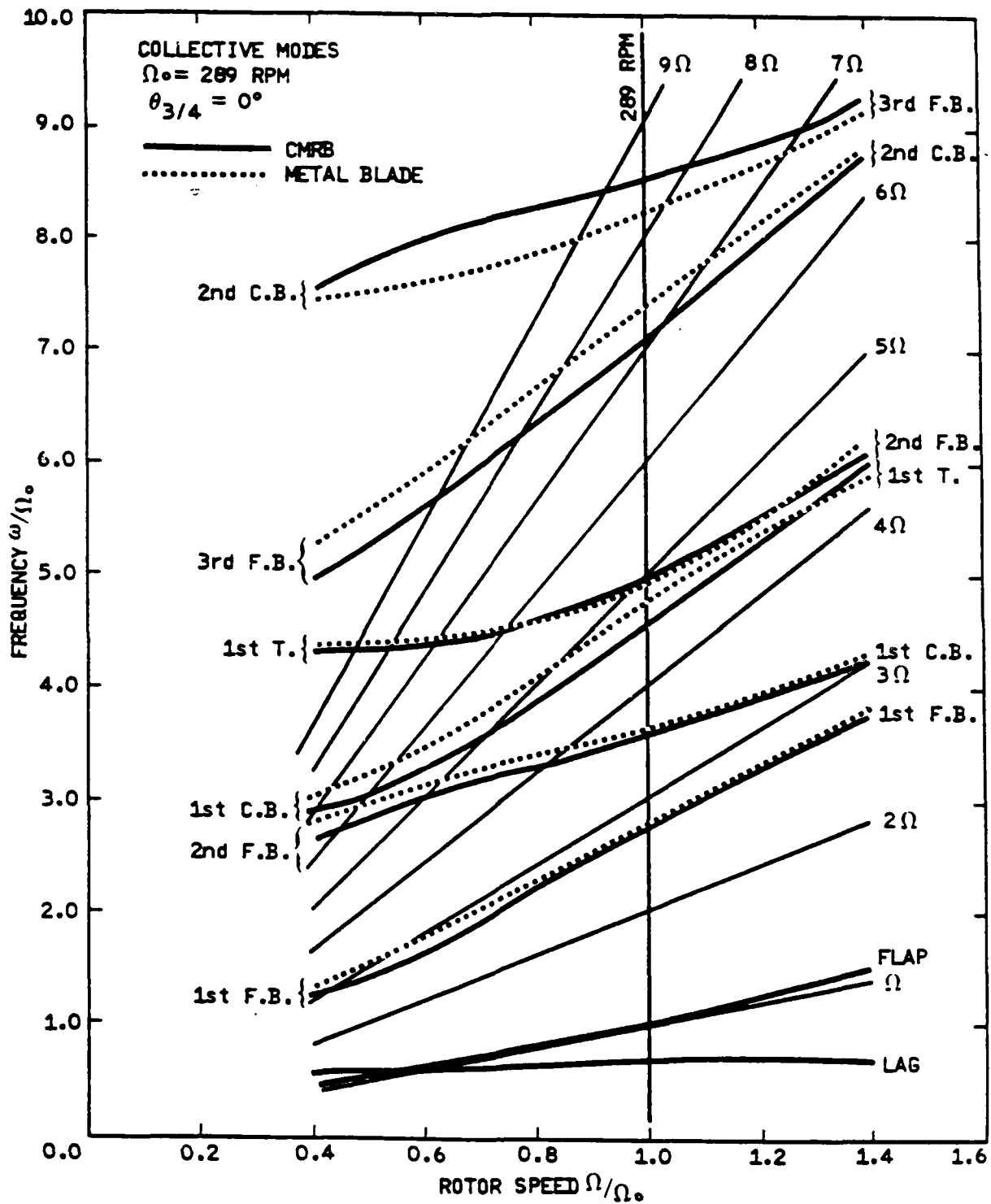


Figure J-2. CMRB collective resonance diagram.

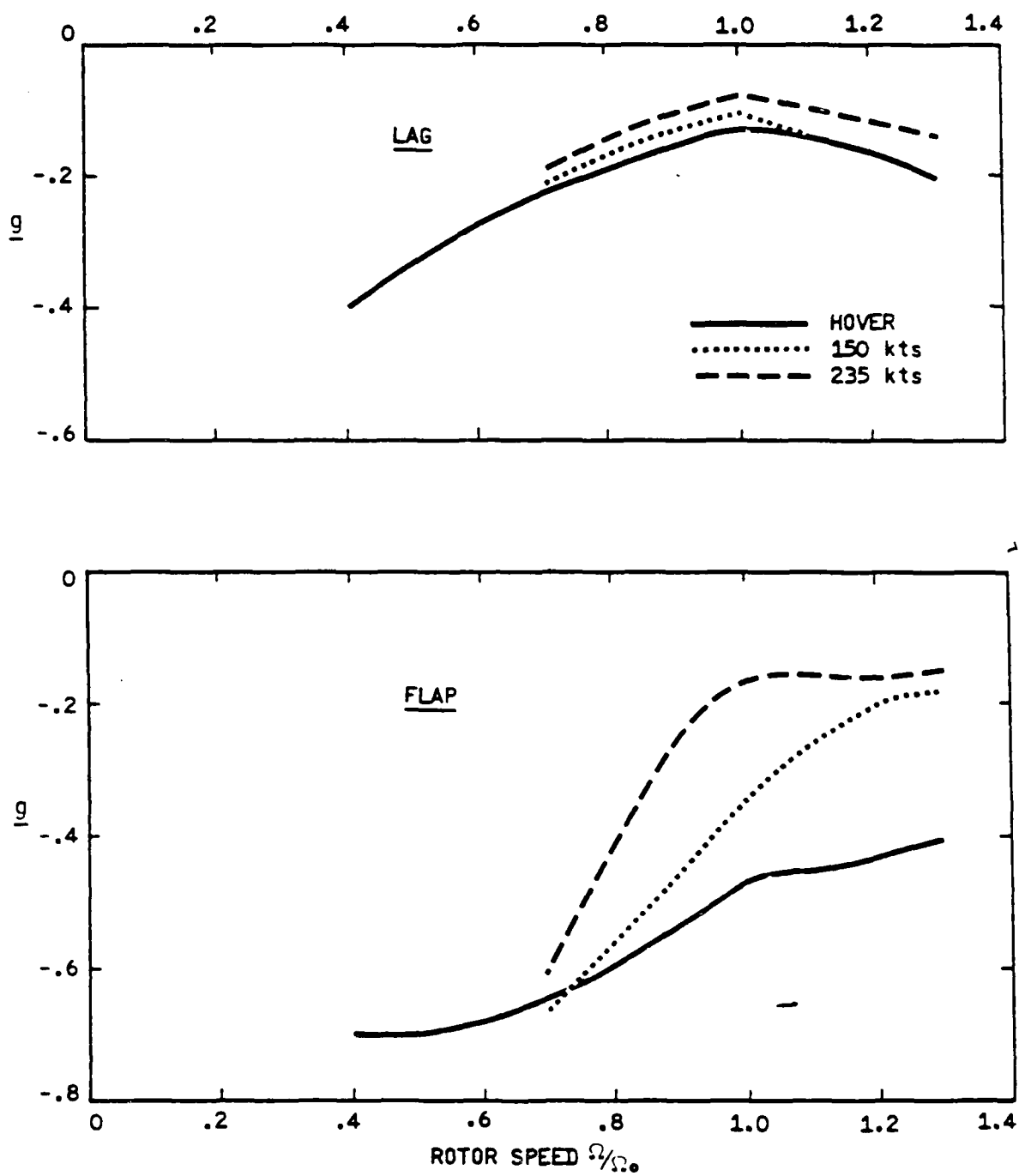


Figure J-3. CMRB modal damping versus rotor speed (sheet 1 of 4).

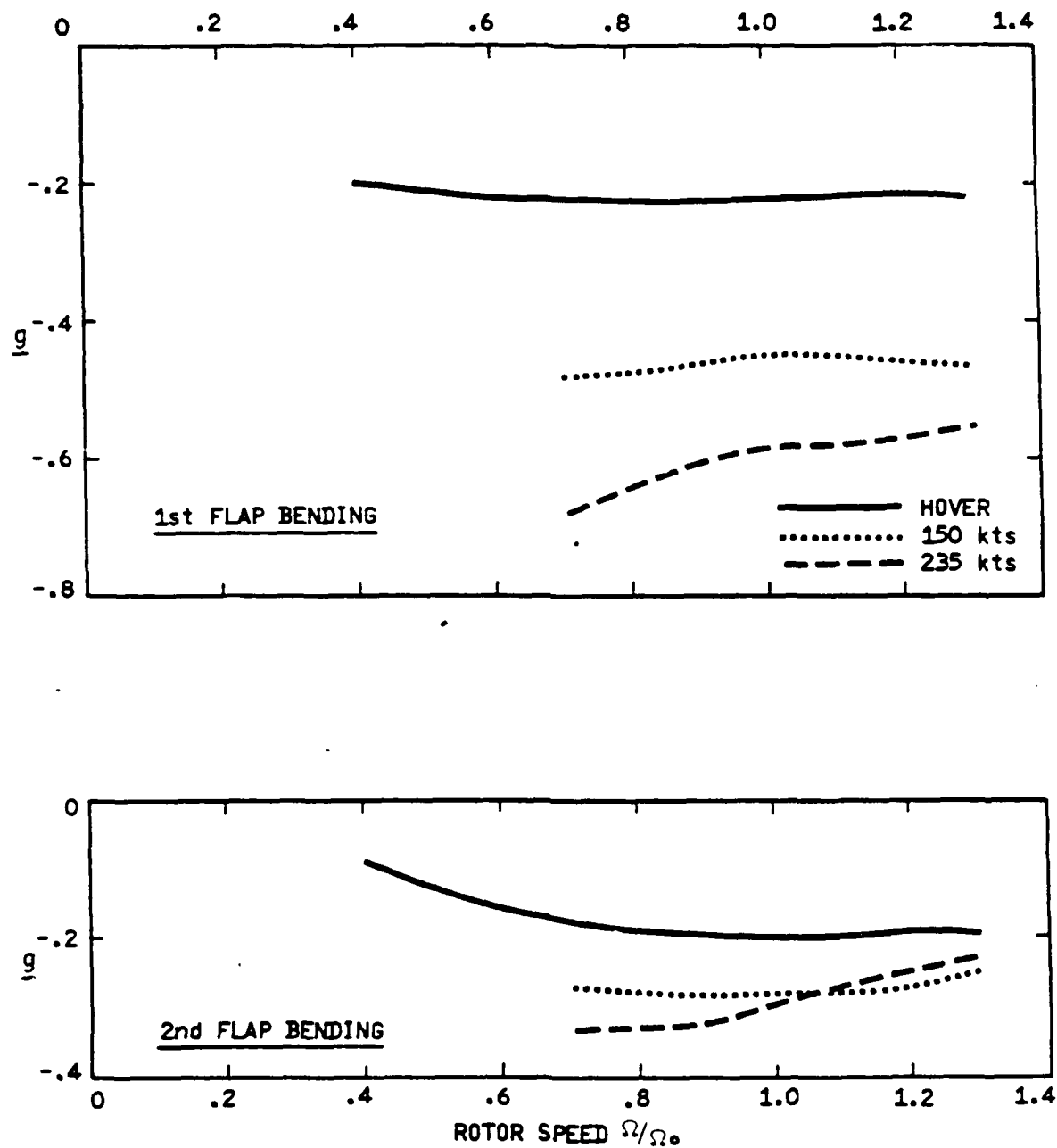


Figure J-3. CMRB modal damping versus rotor speed (Sheet 2 of 4).

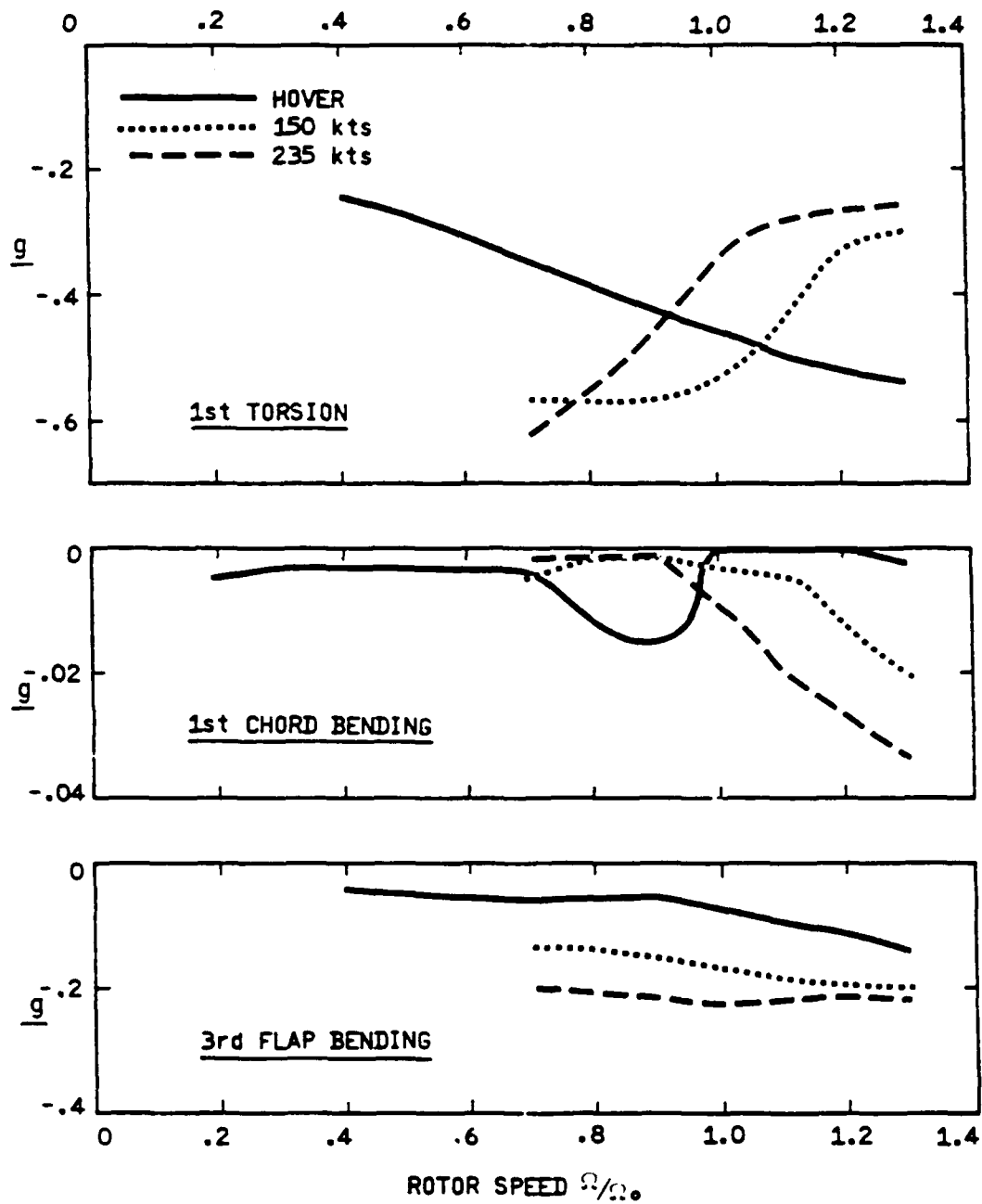


Figure J-3. CMRB modal damping versus rotor speed (Sheet 3 of 4).

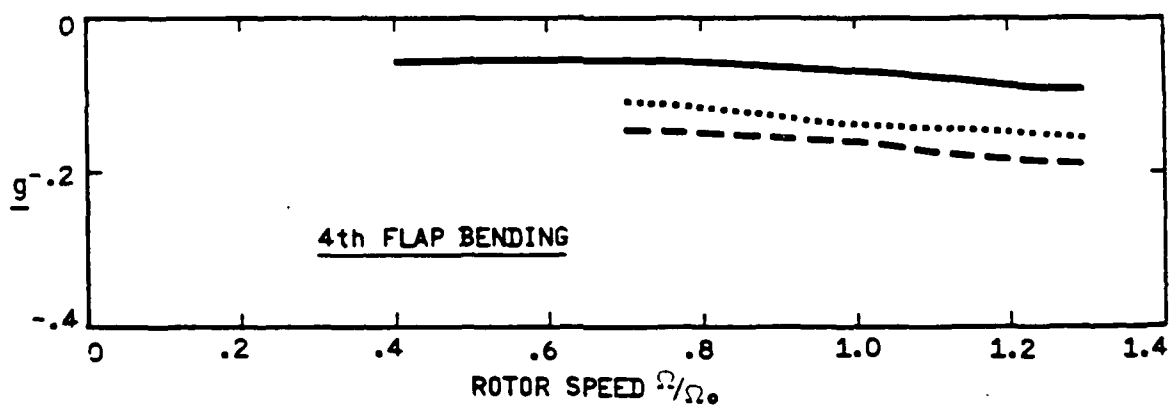
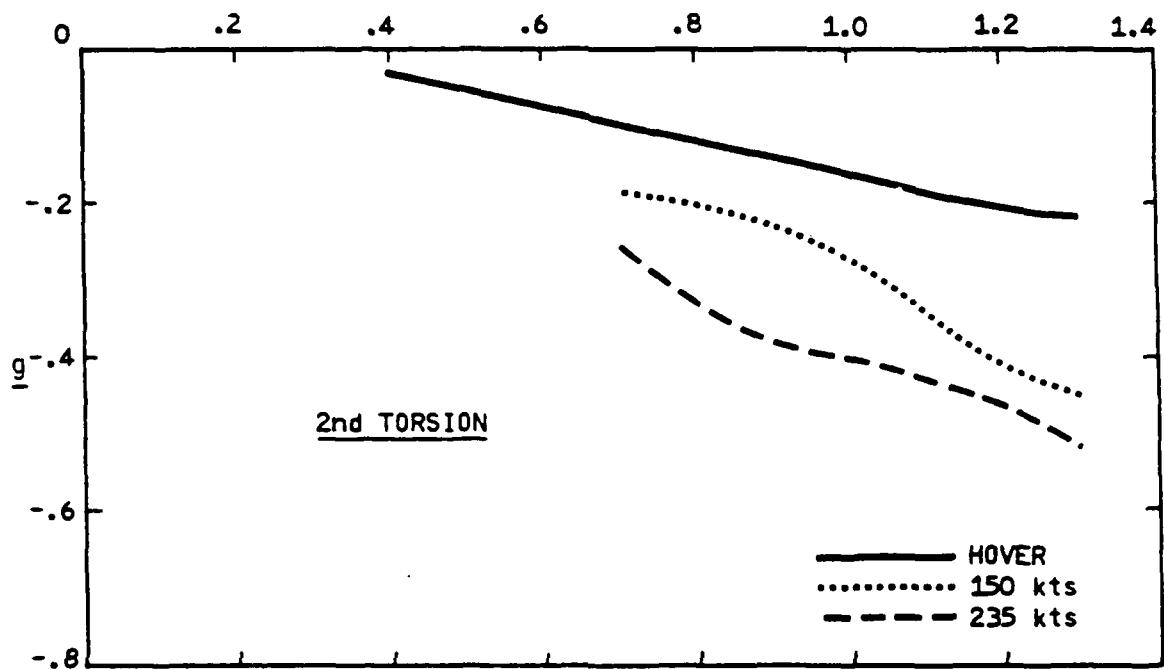


Figure J-3. CMRB modal damping versus rotor speed (Sheet 4 of 4).

TABLE J-1. CMRB DAMPED NATURAL FREQUENCIES,
3.5 g, $\theta_{3/4} = 12^\circ$, HOVER

Root No	Frequency (cyc/rev)						
	116 rpm	202 rpm	260 rpm	289 rpm	318 rpm	347 rpm	376 rpm
1	0.667	0.500	0.450	0.432	0.431	0.426	0.421
2	1.189	1.194	1.214	1.221	1.191	1.174	1.166
3	3.163	2.830	2.767	2.749	2.740	2.735	2.724
4	6.731	5.028	4.470	4.256	4.107	3.985	3.849
5	9.001	5.447	4.771	4.654	4.566	4.489	4.424
6	12.24	8.256	6.953	6.388	5.942	5.568	5.256
7	15.23	9.061	7.525	7.121	6.809	6.534	6.250
8	19.12	12.06	9.561	8.733	8.015	7.458	7.049
9	20.98	12.46	10.65	10.06	9.593	9.217	8.907

TABLE J-2. CMRB DAMPED NATURAL FREQUENCIES,
3.5 g, $\theta_{3/4} = 12^\circ$, $V = 150$ KNOTS

Root No	Frequency (cyc/rev)					
	202 rpm	260 rpm	289 rpm	318 rpm	347 rpm	376 rpm
1	0.484	0.430	0.412	0.409	0.412	0.417
2	1.254	1.299	1.304	1.260	1.213	1.172
3	2.876	2.782	2.736	2.711	2.684	2.657
4	5.008	4.575	4.450	4.428	4.381	4.303
5	6.596	5.796	5.618	5.568	5.435	5.168
6	8.404	7.055	6.455	6.017	5.645	5.328
7	8.923	7.415	7.042	6.775	6.612	6.436
8	12.44	9.926	9.188	8.809	8.868	8.664
9	12.50	10.73	10.13	9.641	9.248	8.928

TABLE J-3. CMRB DAMPED NATURAL FREQUENCIES,
3.5 g, $\theta_{3/4} = 12^\circ$ V = 235 KNOTS

Root No	Frequency (cyc/rev)					
	202 rpm	260 rpm	289 rpm	318 rpm	347 rpm	376 rpm
1	0.497	0.434	0.421	0.428	0.435	0.434
2	1.266	1.287	1.262	1.201	1.151	1.124
3	2.881	2.755	2.702	2.661	2.629	2.603
4	5.017	4.691	4.592	4.476	4.389	4.328
5	7.537	6.990	6.492	6.049	5.668	5.345
6	8.467	7.110	6.706	6.261	5.875	5.554
7	8.850	7.387	7.090	6.853	6.634	6.460
8	12.53	10.74	10.13	9.648	9.269	8.936
9	12.74	10.87	10.93	-	10.42	10.07

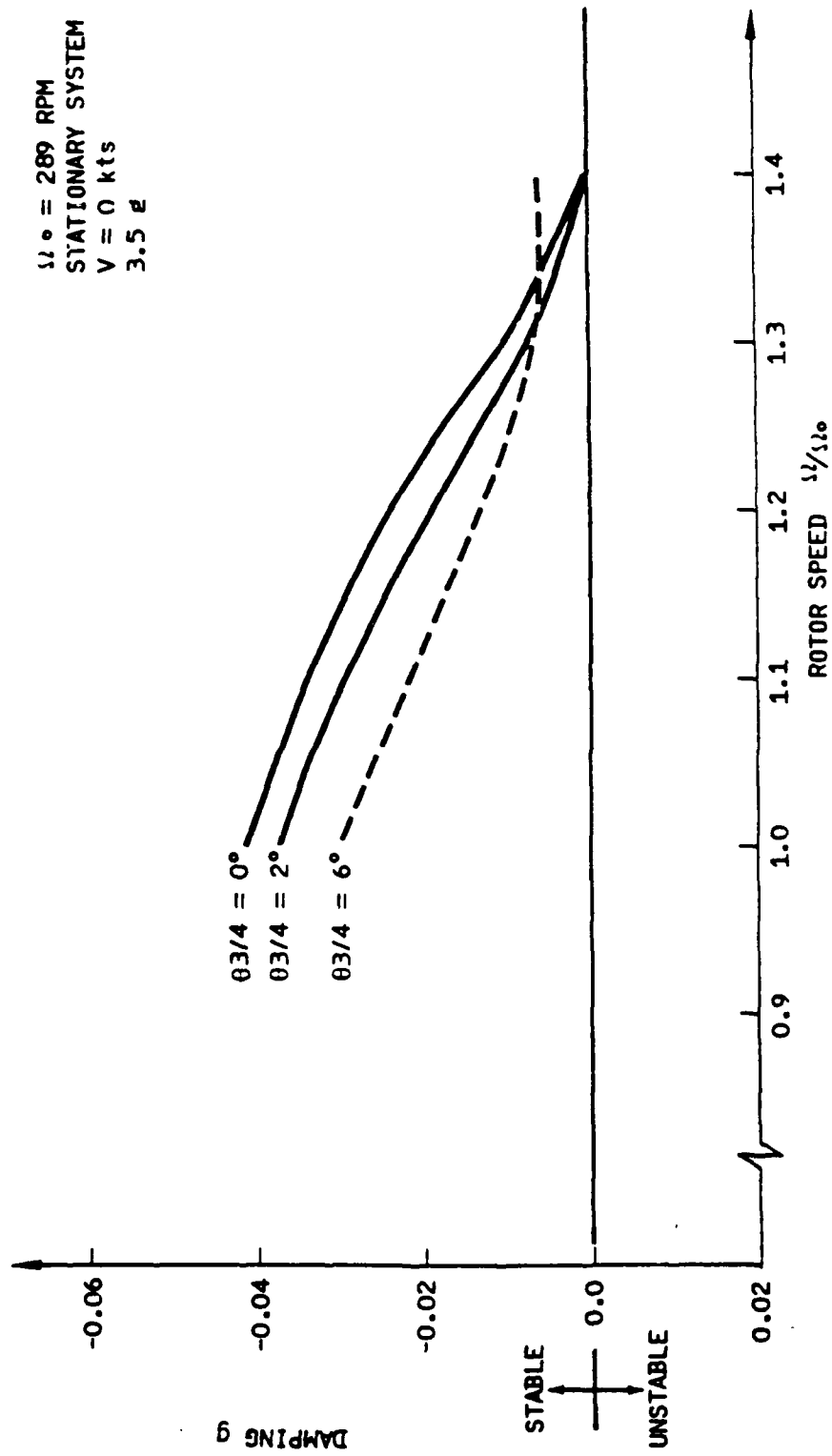


Figure J-4. Advancing whirl mode damping.

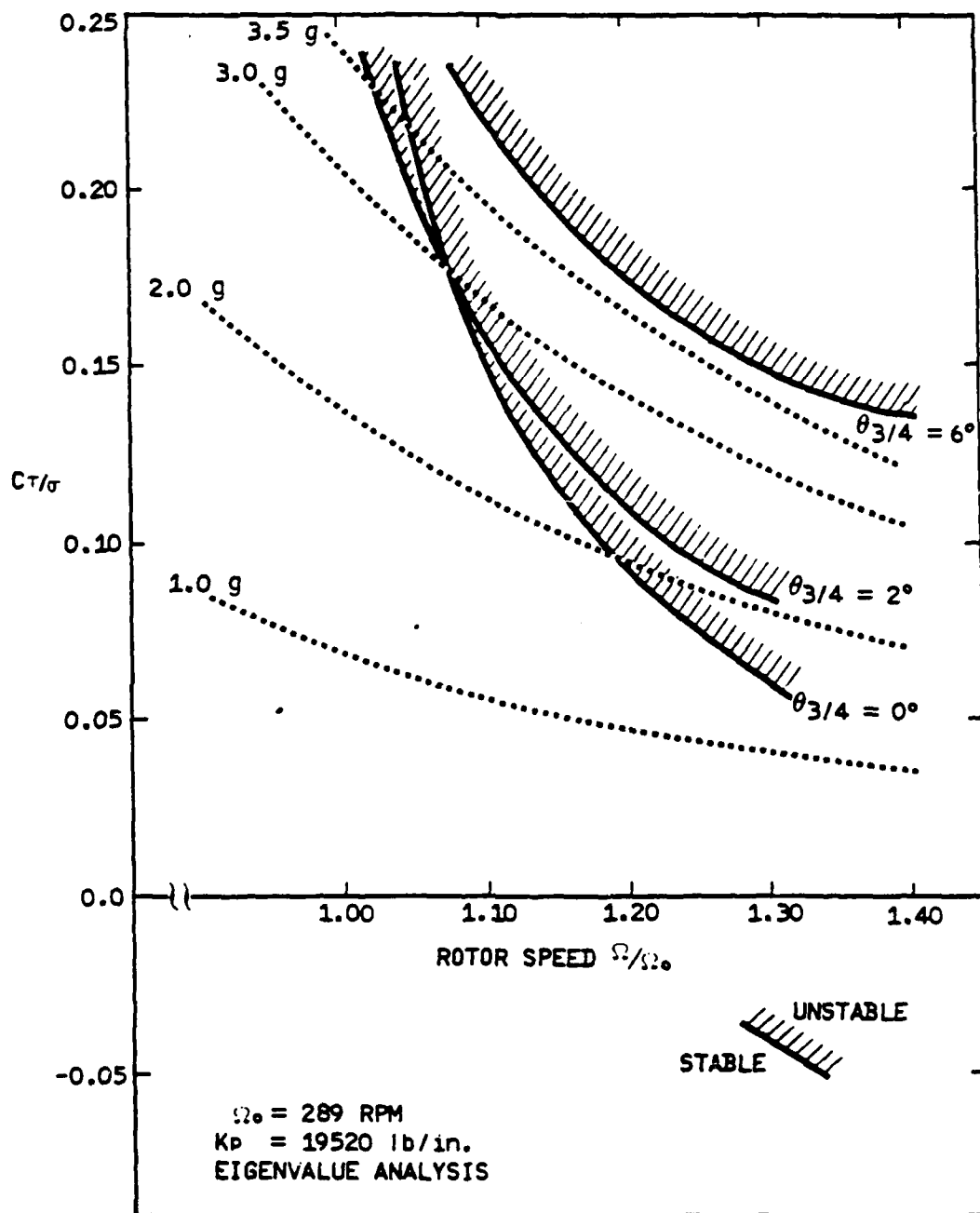


Figure J-5. CMRB advancing lag mode stability boundaries.

blade. Reference J-1 shows that the linear eigenvalue analysis is conservative compared to the four blade transient analysis.

A transient analysis was run for the most severe advancing lag mode case ($\theta_{3/4} = 0$ degree, $N_z = 3.5g$, 376 rpm). An initial chordwise excitation was applied to one of the blades and the decay of the mast bending response was measured to calculate damping. The results shown in Figure J-6 indicate that the condition is stable with a modal damping of $g = -0.033$. It is, therefore, concluded that the advancing lag mode stability boundary is greater than 130 percent N_R .

For the mechanical instability (ground resonance) analysis of the AH-64A with the composite main rotor blades, the most important parameter is the blade first moment about the lag hinge. As shown in Table J-4, both the blade weight and first moment are less for the CMRB than for the metal main rotor blade. Since the lead-lag dampers and airframe are unchanged for the CMRB, the reduced blade first moment will give increased ground resonance stability margins. Therefore, the AH-64A with composite main rotor blades should have at least as good ground resonance stability as that demonstrated with the metal blades.

In summary, the advancing whirl mode stability boundary is above 130 percent N_R for all load factors and collective pitch settings, the advancing lag mode stability boundary is above 130 percent N_R , there are no flutter or divergence limitations within the operating spectrum of N_{DL} (130 percent N_R) and 115 percent of V_{DL} , and mechanical stability margins are similar to those of the AH-64A with the metal blades. With respect to the torsional stability of the main rotor drive system, the only difference in the system with the CMRB installed from that with the metal blade installed is a minor reduction in rotor inertia from 0.829 slug-feet² for the metal blades to 0.783 slug-feet² for the CMRB. Hence, both systems are anticipated to perform similarly.

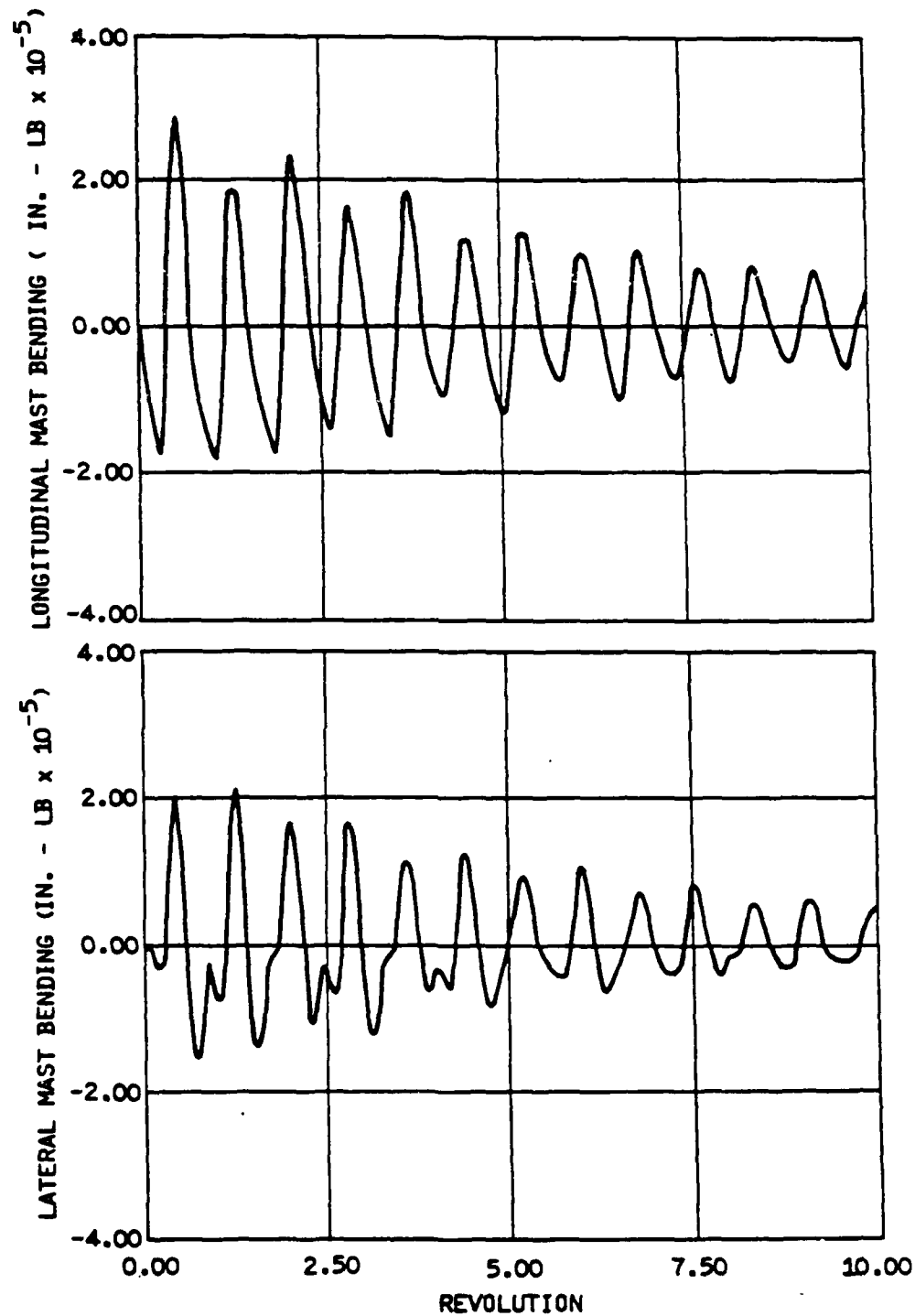


Figure J-6. Main rotor mast bending
 $N_z = 3.5g$, $\theta_{3/4} = 0$ degree,
 376 rpm.

TABLE J-4. MAIN ROTOR BLADE WEIGHT AND MOMENT COMPARISON

	Metal Blade	CMRB	% Change
Weight (lb)	154.3	147.3	-4.5
σ_{ξ}^* (in-lb)	18,980	17,940	-5.5
I_i (slug-ft ²)**	1,017	993	-2.4

* σ_{ξ} = Blade first moment about the lag hinge ($r = 34.5$ inches)

** I_i = Rotor blade polar moment of inertia about rotor shaft

APPENDIX K
RELIABILITY ASSESSMENT

K-2

Reliability assessment of the CMRB is based on a Failure Modes, Effects, and Criticality Analysis (FMECA) that considers degradation of reliability that may occur during subassembly manufacturing processes, final blade assembly manufacturing processes, and in-service operations. The types of defects contributing to reliability degradation, the effects on blade and air vehicle performance (as determined by the FMECA), and compensating provisions wherein these defects can or are being ameliorated are discussed below.

The significant contributors to reliability degradation are hazards induced during air vehicle operation and maintenance, including thermal cycling, shock, vibration, aircraft fluids, rotor downwash (induced airborne particles and foreign object damage), rocket debris, rough handling, impact with terrain objects, maintenance, and contact with work stands and ground vehicles. Design allowables tend to compensate for some of these hazards and the resultant degradation may be readily visible. However, the resultant degradation due to those hazards, but not readily visible, can only be determined by an effect and adequate nondestructive evaluation or nondestructive test technique. Based on results of previous testing and for equivalent material thickness, the order of damage tolerance is as follows. Kevlar is the most damage tolerant, graphite is much less damage tolerant, and fiberglass is intermediate. Sandwich construction has poorer impact resistance than monolithic constructions and tends to suffer reductions in strength due to subsurface damage.

Being made primarily of advanced composite materials, corrosion as a failure mode will be essentially non-existent for the CMRB. Of the metal parts that could be subject to corrosion, the 304 CRES tip weight is passivated, the A356-T6 aluminum aft tip weight and 6061 T4 aluminum adjustable weights are chromic acid anodized, tungsten adjustable weights are etched and primed, 17-4 PH bushings and forward tip weight are passivated, and the 316 CRES balance rods are wiped with MEK prior to being embedded in the epoxy matrix.

Delamination of the Kevlar plies can occur during in-service operations resulting in loss of blade performance and possible excessive vibration. The FMECA has determined that 20 percent of the failure rate is attributed to delamination with resulting reliability degradation. These delaminations can be detected using non-destructive inspection techniques.

While porosity or voids within the elements themselves should not occur because rigid inspection techniques would have discovered them prior to assembly, porosity or voids can occur between any of the blade components

during the temperature-pressure curing process. Porosity or voids contribute approximately 4 percent to the total failure rate of the CMRB, according to the FMECA. The remoteness of their occurrence is based on the nondestructive inspection (NDI) and/or nondestructive evaluation (NDE) techniques used on the CMRB after its initial molding, or after in-service repair.

Resin-starved areas result in delamination as well as an upset of the fiber / resin density ratio. Resin-rich areas result in an upset of the desired fiber / resin density ratio. Both resin-starved or resin-rich areas can contribute to blade imbalance and loss of effective blade performance. These conditions can only occur during manufacturing, not during in-service operations, and would be discovered during inprocess control. The resin-rich or resin-starved defect is not considered as a failure mode in the FMECA since it would be a failure mechanism (cause) of a delamination failure mode. Unbonded areas defects would be prevalent only during the final manufacturing phase. Debonding can occur during the final manufacturing process as well as in-service operations. Reliability degradation caused by debonding results in degraded blade performance and excessive blade vibration thus affecting air vehicle performance. Debonding represents about 20 percent of the failure rate as determined by the FMECA. Bond line consistency will prevent debonding during in-service operations.

Rain erosion and ultraviolet (UV) radiation contribute greatly to environmental degradation of CMRB reliability. Sand and dust can be classified as FOD-induced erosion, as in maintenance-induced damage due to tool marks or tool drops. A leading edge erosion strip tends to protect against erosion. All trimmed edges are capped to prevent water absorption. The blade is painted with an epoxy primer and a urethane top coat to preclude degradation of the Kevlar and epoxy from UV radiation.

Three areas of the blade that are candidates for repair are the leading edge, the multitubular spar area, and the aft portion of the blade. The root end region is considered to be not repairable. The thermoplastic elastomer (Estane) leading edge erosion material may be repaired on the helicopter by:

- Repair local pitting
 - Cut away and repair local area
 - Remove entirely, and bond on new Estane strip
- } use kit furnished by manufacturer

The repair technique for the multitubular spar area is anticipated to include trimming away damaged material, scarfing the blade skin around the hole, emplacing spar tube repair segments, applying a 0-degree longo/ ± 45 -degree composite skin patch, bonding the patch in place with heat and pressure, and sanding and painting the area. The repair technique for the aft portion of the blade will be to trim away the damaged skin and underlying honeycomb. A small repair area will be filled with glass milled fiber/epoxy paste - a piece of honeycomb will be cut to fit and bonded into larger damaged areas. The procedure for patching and the skill required will be similar to that for the spar area. Tip weight adjustment may be required to compensate for the location and weight of the repair patches.

HHI plans to estimate the damage that can be safely repaired and then define the skin, longo, and spar repair materials and adhesives that are necessary to perform the repair. HHI plans to select one CMRB, make a repair to it in each of the two zones, and subject the blade to a midspan fatigue test to evaluate the effectiveness of the repair during the full qualification effort.

A failure reporting system based on the Army-developed RAM/LOG (Reliability Availability Maintainability/Logistics) data collection methodology (AMSAV-L form 1249, 1250, 1252, 1266) will be instituted with the beginning of flight test. These forms will be used to record all failures that occur during the test program. Then a qualitative reliability assessment will be made based on the data that results. This assessment will then be evaluated against the comparative reliability value of the metal blade that is currently used on the AH-64A flight vehicles.

APPENDIX L
MAINTAINABILITY ASSESSMENT

The Maintainability Engineering Analysis (MEA) for the CMRB addressed all the failure modes and effects data that are reported in the Reliability Assessment section as representing unscheduled maintenance items. The scheduled maintenance part of this MEA includes both daily and phased inspection. Phased inspection includes routine preparatory cleaning and selected preventive maintenance tasks. This MEA for Aviation Unit Maintenance (AVUM), Aviation Intermediate Maintenance (AVIM), and Depot Maintenance (DEPOT) predicts maintenance man-hours per flight hour as listed in Table L-1.

The repair limits and maintenance organization levels that are listed in Table L-2 are based on design criteria and stress evaluations. The repair level is considered to be very conservative inasmuch as many of the minor damage listings could be downgraded to the next lower maintenance level from AVIM to AVUM. In fact, because of the slow damage propagation rates of the CMRB, many repairs could receive temporary AVUM repairs and be operated for an additional 10 hours, or until a scheduled preventative maintenance check.

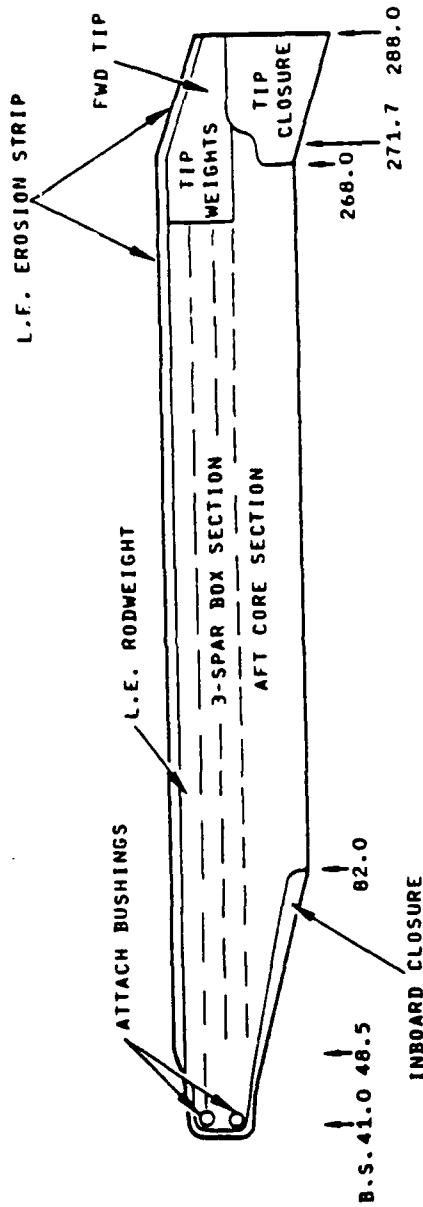
The repair procedures that are outlined in Table L-3 address the major and minor damage listed in Table L-2. While HHI's Maintainability Engineers consider these repair procedures to be within the current State-of-the-Art, it is realized that the aerospace industry is putting increased emphasis on composite structures and their repair causing the current state-of-the-art to change significantly.

As new technology becomes available, it will be incorporated into the repair procedure. During the CMRB production program it is planned to further refine the depot level repair procedures.

TABLE L-1. MAINTENANCE MAN-HOURS/FLIGHT HOUR

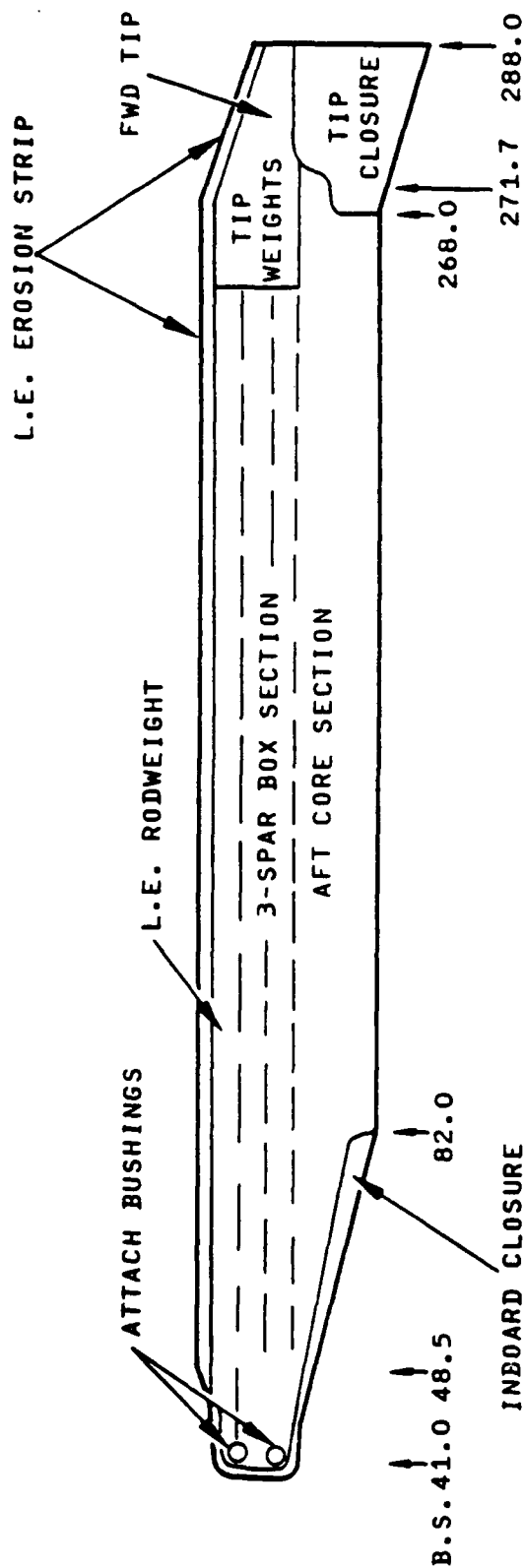
Level	Scheduled	Unscheduled	Total
AVUM	0.00898	0.0200	0.02898
AVIM	0.01473	0.0125	0.02723
DEPOT	0.00697	—	0.00697
	<u>0.03068</u>	<u>0.0325</u>	<u>0.06318</u>

TABLE L-2. CMRB DAMAGE LIMITS AND MAINTENANCE LEVELS



Repair Area	Minor Damage	Limit	Repair Level	Major Damage	Limit	Repair Level
L.F. Erosion Strip	Cuts, nicks, missing	4 in	AVUM	More than 4 in	None	AVIM
L. Edge Back Strip	Cuts, nicks	4 in	AVUM	More than 4 in	34 in	AVIM
L. Edge Rod Weight	Cut thru	4 Rods	AVIM	4 in to . in	7 in	AVIM
L. Edge Debonding	Crack - 3 in	4 in	AVIM	More than 4 in	-	DEPOT
Attach Bushings	Scratches	None	AVUM	Loose/cracked	-	DEPOT
BS 37.5 to 48	Nicks, finish	None	AVUM	Cracks/Debond	TBD	DEPOT
Inboard Closure	Debond/Delam	6 in	AVIM	Replace	None	AVIM
Spar Box 1, 2, 3: BS 49 to 271	Debond/Delam/Hole	1 in	AVIM	Cracks	1 Spar/1.5 in	AVIM
Aft Core Section	Debond/Delam	1 in	AVIM	Holes/Damage	4 in x 10 in long	AVIM
Trail Edge	Debond/Delam	6 in	AVUM	24 in - 48 in	60 in	AVIM
Hinge Tab	Cracked	1 Section 11.3 in	AVIM	To 8 Sections	None	AVIM
Tip Weight Area	None	-	-	Loose Stationary	-	DEPOT
Tip Weight Area	Loose Adj Wgts	-	AVUM	-	-	-
Forward Tip	Erosion	Minor	AVIM	Major	-	AVIM
Forward Tip	Hole/Delam	4 sq in	AVIM	Remove & Replace	-	DEPOT
Tip Closure	Hole/Delam	12.25 sq in	AVIM	Remove & Replace	-	DEPOT

TABLE L-3. CMRB REPAIR PROCEDURES



Area	Damage	Repair
L.E. Polyurethane Erosion Strip	Minor cuts, nicks, 4 inches of strip missing.	Clean area, remove loose/frayed strip material. Fill with material from repair kit. Clean adhesive from area where erosion strip was removed, radius corners, prepare patch from like material, fit with minimum E. Dist. Bond in place and fill gaps from kit material.
	Major - More than 4 inches of strip missing.	Remove loose or damaged erosion strip material. Clean adhesive, repair any backstrip damage. Prepare and fit, bond in place, heat if required. Fill edge gaps with kit material.

TABLE L-3. CMRB REPAIR PROCEDURES (CONT)

Area	Damage	Repair
L.E. Backstrip	Minor - cuts, nicks	Sand nicks and fill with epoxy. Cure, sand to fair with adjacent material. Patch with erosion strip kit.
	Major backstrip eroded through or missing.	Sand with 320 WD paper. Fair to undamaged material. Lay in repair cloth. Epoxy, cure, sand smooth, and fair. Prepare erosion strip to overlap, repair ends 3 inches and bond in place. Fill butt end with kit material.
L.E. Rodweight	Minor - 4 rods cut through (TR)*	Remove erosion strip 4 inches past damage, remove backstrip 1 inch past damage, radius damage, fill with epoxy material EA 960 filler, cure and blend. Cover area with backstrip Kevlar 49 material and bond using adhesive
	Major - Same procedure	EA 934NA cure, blend, and install erosion strip using adhesive A1503B1A1343B Estane cement and accelerator, fill edge gaps with kit material.
L.E. Edge	Minor - 3 inch crack. (TR)*	Clean air dry fill crack with EA 934NA and use.
	Major	Depot specialized repair scrap potential 80 percent.

*(TR) designates temporary repair - permanent repair may be delayed up to 10 flight hours.

TABLE L-3. CMRB REPAIR PROCEDURES (CONT)

Area	Damage	Repair
Attach Bushings	Minor scratches	Polish and measure for limits using inside measuring micrometer.
	Major fretted, cracked loose	Depot - specialized repair part.
	Minor - scratches, nicks	Blend and refinish.
	Major - cracks delamination	Depot specialized repair scrap rate 85 percent
Inboard Closure	Minor - debonded/delam	Rebond using EA 934NA. Standard practices apply. Remove with router. Bond repair part in place with EA 934NA, fill and blend, refinish
	Major - TE crushed	Drill hole to accommodate hypo needle and fill void with EA 934NA. Apply pressure to surface to squeeze out excess adhesive. Apply pressure and heat as required. Accomplish flush plug patch using EA 934NA. Standard practices apply.
Spar Box No. 1, 2, 3 STA 49 to 271	Minor - debond/delam 1 inch hole	
	Major cracked outer cover, doubler 1.5 inch limit/spar only	Rout damage only. Apply patch of Kevlar 49 with EA 934NA (Maintain filament direction), cover damage only may be expanded to 2.5 inches (No spar, no doubler damage).

TABLE L-3. CMRB REPAIR PROCEDURES (CONT)

Area	Damage	Repair
Aft Core Section	Minor - one face sheet debonded 6 inches	Rout out debonded face sheet as required until bonded core/sheet is established. Prepare Kevlar sheet stock, fit and clean. Apply EA 934NA to both sheet and core contact surface. Install. Apply pressure and heat if required, blend surface. Remove finish to allow for 3 inch doubler patch overlap. Doubler patch of same materials and adhesive. Apply lightning mesh with 0.5 inch overlap. Apply doubler over top, apply poly sheet to insulate pressure pad, apply pressure pads, apply heat if required - cure - remove heat, pressure pads, poly sheet - blend as required and refinish.
Aft Core Section	Major - holes through or damage to core and both face sheets.	Rout out damage from both face plates, rout out damaged core, cut replacement core. Clamp flush face plate and doubler in place. Install core (dry) and rout contour. Fit top plate, check contours, and cut lightning mesh, disassemble, and clean. Apply EA 934NA to all contact surfaces and assemble. Apply filler, poly sheet, and pressure pads, remove poly sheet. Blend as required and refinish. Direction filaments apply.

TABLE L-3. CMRB REPAIR PROCEDURES (CONT)

Area	Damage	Repair
Trailing Edge	<p>Minor - delamination (TR)*</p> <p>Major - delamination extended 60 inches, crushed trail edge</p>	<p>Air clean, inject EA 934NA. Apply poly sheet. Apply clamp blocks and clamp, cure, remove clamps, blocks, and sheet. Sand to blend and refinish.</p> <p>Same as above. Rout out damage, scarf repair longo 5-to-1 at both ends. Scarf longo at undamaged ends. Apply adhesive and install. Fabricate core and face sheets. Fabricate doublers, cut lightning mesh. Assemble dry for fit check. Apply adhesive EA 932NA to all contact surfaces. Assemble, apply poly sheet, apply pressure and heat if required. Cure - remove heat, remove pressure and poly sheet. Apply filler EA 960F, cure, sand to blend, and refinish.</p>
Hinge Tab	<p>Minor crack or damaged to 11.3 inches</p>	<p>The hinge tab is a repair part and is provided in section lengths of 11.3 inches. Repair applies to both major and minor.</p>

*(TR) designates temporary repair - permanent repair may be delayed up to 10 flight hours.

TABLE L-3. CMRB REPAIR PROCEDURES (CONT)

Area	Damage	Repair
	Major - 8 sections or 90 inch replacement	Rout damaged tab sections to remove, being careful not to remove material from trailing edge. Clean surface and bond repair in place, block, and clamp. Heat if required. Remove clamps and blocks, clean, and blend overrun. Bend tab using special tool to original setting and refinish.
Tip Weight Area	Major - loose stationary weights	Depot action only.
Tip Weight	Minor - loose adjustment weights	Tighten mounting and adjusting bolts.
Forward Tip	Minor - erosion	Fill pits with EA 960F, sand smooth with 320 WD, and refinish.
Forward Tip	Major - delamination	Air clean - apply EA 934NA and pressure bond cure - remove pressure pads, clean and refinish.
	Hole to 40 sq in	Rout out damage, fill void with foam, patch with Kevlar 49 and EA 934NH, fair with EA 960F, and blend - refinish.
Aft Tip Closure	Minor - delamination Hole to 12.25 sq in (TR)*	Same as repair No. 9.

*(TR) designates temporary repair - permanent repair may be delayed up to 10 flight hours.

Because of its high safety factor and slow damage propagation rate, the CMRB is able to withstand minor damage while remaining serviceable. However, a temporary repair that is essentially cosmetic will keep out dirt and moisture and retain the necessary aerodynamic shape until it is convenient to make a permanent repair. Repair man-hours for those items listed as minor are estimated to require 1.6 to 2.4 man-hours plus cure time of 2 hours at ambient temperature of 77°F, or 30 minutes with supplemental heat. Major damage repairs at the AVIM level are estimated to require an average of 7 man-hours. In addition, the cure times given above must be added.

Depot level repairs were not estimated and will require specific engineering for custom repair designs.

APPENDIX M

REFERENCES

- I-1. Military Standard - Weight and Balance Data Reporting Forms for Aircraft (Including Rotorcraft), MIL-STD-1347A Part II, 30 September 1977.
- J-1. Silverthorn, L. J. , Childers, H. M. , and Neff, J. R. , Preliminary Aeroelasticity and Mechanical Stability Report YAH-64 Advanced Attack Helicopter, Hughes Helicopters, Inc. Report No. 77-X-8001, June 1976.

APPENDIX N

DRAWING LIST FOR THE COMPOSITE
MAIN ROTOR BLADE FOR THE
AH-64A HELICOPTER

N-2

Drawing Number	Revision	Title
7-311412500	R	Blade
7-311412508	D	Blade Ordinates
7-311412509	A	Lines Definition
7-311412511	M	Closure, Inboard
7-311412512	E	Door
7-311412514	D	Weight
7-311412515	C	Bolt
7-311412516	E	Erosion Strip
7-311412517	F	Bracket Assembly
7-311412530	G	Weight Assembly
7-311412531	C	Spar Tube No. 1
7-311412532	B	Spar Tube No. 2
7-311412533	C	Spar Tube No. 3
7-311412536	J	Longo, T. E.
7-311412537	L	Cap Assembly
7-311412538	H	Doubler Assembly, Skin
7-311412539	E	Doubler, Cap
7-311412541	F	Wedge, Inboard
7-311412542	K	Wedge, Spar Cap
7-311412543	H	Core Assembly, Tip
7-311412545	D	Skin
7-311412546	G	De-icer Blanket
7-311412547	E	Lightning Screen
7-311412548	J	Weight, Forward, Tip
7-311412549	K	Weight, Aft, Tip
7-311412550	B	Tip Weight, Leading Edge

Drawing Number	Revision	Title
7-311412551	-	Rod
7-311412553	A	Backing Strip
7-311412554	-	Backing Strip, Tip
7-311412556	C	Bracket Assembly
7-300412557	G	Root End Dam
7-311412559	A	Cap, Leading Edge
7-311412561	E	Hinge, Trim Tab
7-311412563	G	Plate, Face
7-311412567	F	Plate Clevis
7-311412568	B	Bushing
7-311412569	C	Inner Skin
7-311412570	A	Absorber Assembly
7-311412572	D	Core, Aft
7-311412573	D	Channel
7-311412574	G	Core Assembly, Aft
7-311412575	B	Filler Doubler
7-311412576	C	Closure, Outboard
7-311412577	-	Strip, Fairing
7-311412581	B	Target Set